Plastic cracking of concrete and the effect of depth

by

Lourens Steyl

Thesis presented in fulfilment of the requirements for the degree of Master of Engineering in the Faculty of Science at Stellenbosch University

Promotor: Dr Riaan Combrinck
Faculty of Engineering
Department of Civil Engineering

December 2016

Declaration

By submitting this thesis electronically, I declare that the entirety of the work contained therein is my own, original work, that I am the sole author thereof (save to the extent explicitly otherwise stated), that reproduction and publication thereof by Stellenbosch University will not infringe any third party rights and that I have not previously in its entirety or in part submitted it for obtaining any qualification.

December 2016

Signature:

Abstract

Plastic settlement and shrinkage cracking dominate cracking in the early life of conventional concrete. The mechanisms responsible for these cracking types include differential settlement and restrained shrinkage. The driving force behind differential settlement and restrained shrinkage is settlement and capillary pressure build-up (shrinkage). These plastic cracks are largely a problem for slab-like elements with large exposed surfaces, where the cracks act as pathways for degrading agents to penetrate the concrete. These premature detrimental defects can decrease the service life of the structure. Plastic cracks can be prevented by using effective construction techniques and/or applying the correct finishing operations and curing techniques at the appropriate time. Nevertheless, these cracks still occur due to ignorance towards effective construction techniques as well as towards concrete mix designs, and due to the lack of knowledge of the interaction between these cracking types. This is especially true as a result of the limited test methods that exist to isolate plastic shrinkage from plastic settlement cracking.

The study aims to isolate and understand plastic shrinkage cracking as well as describing the interaction between settlement cracking and shrinkage cracking. This was done by designing a mould capable of inducing a single isolated plastic shrinkage crack, or settlement induced plastic shrinkage crack. Finally, the framework for a plastic cracking risk model is introduced, which can aid engineers and contractors in appropriate cracking risk estimations.

The test results aided in the understanding of both cracking types for different mixes and climates, as well as identifying and describing their cracking mechanisms. Three dominant cracking phases in plastic concrete were identified along with three distinct cracking types. The three cracking types are plastic settlement cracking, plastic settlement induced plastic shrinkage cracking, and pure plastic shrinkage cracking. Phase 1 starts once the concrete is placed, and ends once the capillary pressure starts to rise. Pure settlement cracking occurs only in this phase and can be accompanied by the start of settlement induced plastic shrinkage cracking. Phase 2 starts once the capillary pressure starts to rise, and ends once settlement reaches its maximum. Pure plastic shrinkage cracking can start in this phase, as well as further widening of a settlement induced plastic shrinkage crack. Phase 3 starts once the settlement stops, and ends once the concrete hardens and reaches the final setting time. This end of Phase 3 is characterised by the stabilisation of plastic cracking. Furthermore, the investigation of the effect of depth and finishing operations on plastic cracking, proved invaluable in describing the different cracking phases and their respective mechanisms. For deeper sections the severity of pure plastic shrinkage cracking decreases while increasing the severity of plastic settlement cracking. If these two cracking types interact in deeper sections, the cracking severity drastically increases.

Finally, the plastic cracking model presented, showed great potential in predicting the risk, and especially the interaction risk, between the plastic cracking types. The empiric model makes use of dominant influencing factors of plastic cracking to ultimately calculate the risk estimation. This model should be improved by future studies, which can further estimate the effect of the influencing factors, especially using large scale tests.

Opsomming

Plastiese versakking en krimpkrake oorheers kraakvorming in die vroeë lewe van konvensionele beton. Die meganismes wat verantwoordelik is vir hierdie kraak tipes sluit in differensiële versakking en opgehoude inkrimping. Die dryfkrag agter differensiële versakking en krimpkrake is versakking en die opbou van kapillêre druk. Hierdie plastiese krake is hoofsaaklik 'n probleem by bladagtige elemente met groot blootgestelde oppervlaktes waar die krake optree as deurgange vir afbrekende middele in die beton. Hierdie vroeë nadelige defekte kan die diensleeftyd van die struktuur verminder. Plastiese krake kan voorkom word deur die gebruik van effektiewe konstruksie tegnieke en/of die uitvoering van die korrekte afwerkings metodes en kuurtegnieke op die regte tyd. Nietemin ontstaan hierdie krake steeds as gevolg van onkunde oor effektiewe konstruksietegnieke en betonmengselontwerp sowel as die gebrek aan kennis oor die wisselwerking tussen die verskillende krake. Dit is veral weens die gebrek aan toetsmetodes om plastiese krimpkrake te isoleer van plastiese versakkings krake.

Die studie beoog om plastiese krimpkrake te isoleer en te bestudeer en gevolglik die interaksie tussen versakkings krake en krimpkrake te beskryf. Dit is gedoen deur die ontwerp van 'n vorm wat of ‘n enkele plastiese krimpkraak kon isoleer. Laastens is die raamwerk van ‘n plastiese kraak risiko model bekend gestel wat ingenieurs en kontrakteurs kan help met toepaslike skattings vir kraakrisiko.

Die toetsresultate het gehelp om beide kraak tipes en mengsel eienskappe te verstaan sowel as om kraak meganismes te beskryf. Daar bestaan drie dominante plastiese kraak fases in beton asook drie kraak tipes: Plastiese versakkings krake, versakking geïnduseerde plastiese krimp krake en suiwer plastiese krimp krake. Fase 1 begin sodra die beton geplaas is en dit eindig sodra die kapillêre druk begin styg. Suiwer versakkings krake kom slegs in hierdie fase voor en kan vergesel word deur die begin van versakking geïnduseerde plastiese krimpkrake. Fase 2 begin sodra die kapillêre druk begin styg en dit eindig sodra die versakking ‘n maksimum bereik het. Suiwer plastiese krimpkrake begin in hierdie fase, sowel as by die begin of verdere vergroting van die versakking geïnduseerde plastiese krimpkrake. Fase 3 begin sodra die beton se versakking ophou en dit eindig sodra die beton verhard en die finale set tyd bereik. Die einde van hierdie fase word gekenmerk deur die stabilisering van plastiese krake. Verder was die ondersoek oor die invloed van diepte sowel as oor afwerkings praktyke op plastiese krake, van onskatbare waarde vir die beskrywing van die verskillende kraak fases en hul onderskeie meganismes. Suiwer plastiese krimp krake verklein in dieper beton snitte terwyl plastiese versakkings krake vergroot. Die interaksie tussen die twee kraak tipes lei tot groter krake in dieper beton snitte.

Laastens het die plastiese kraak model wat bekend gestel is, groot potensiaal getoon vir die voorspelling van die kraakrisiko en veral vir die interaksie risiko tussen die verskillende kraak tipes. Die model maak gebruik van dominante faktore wat plastiese krake beïnvloed. Hierdie model kan verbeter word deur toekomstige studies wat die effek van die verskillende invloeds faktore kan bestudeer deur veral grootskaalse toetse te gebruik.

Acknowledgements

I would like to thank the following people for their assistance and whom contributed to this study:

- My supervisor, Dr Riaan Combrinck for his guidance, knowledge and support through the entire study.
- The laboratory staff at the Civil engineering department for all their cooperation during the experimental work.
- My parents for always being there for me and their unconditional love and support through my entire study.
- My friends and especially Renée Crous for the much needed distraction in this time.

Contents

Declaration....i
Summary....ii
Opsomming....iii
Acknowledgements....iv
Contents....v
List of Figures....viii
List of Tables....xi
Notations and acronyms....xii

Chapter 1 : Introduction 1
1.1. Objectives 2
1.2. Research significance 2
1.3. Report outline.... 2
Chapter 2 : Background study on plastic cracking of concrete.... 4
2.1. Introduction to plastic cracking of concrete 4
2.2. Stiffening, setting and hardening of young concrete 5
2.3. Driving forces behind plastic cracking 7
2.4. Plastic settlement 8
2.4.1. The behaviour of plastic settlement cracks 8
2.5. Plastic shrinkage cracking 9
2.5.1. The behaviour of plastic shrinkage cracks 10
2.6. Influence of depth on plastic cracking.... 11
2.7. Influence of finishing operations on plastic cracking.... 11
2.8. Other factors influencing plastic cracking 12
2.8.1. Evaporation 12
2.8.2. External restraint.... 12
2.8.3. Capillary pressure.... 13
2.8.4. Bleeding 15
2.8.5. Setting times 15
2.8.6. Water-cement ratio.... 16
2.8.7. Concrete cover 16
2.8.8. Fines content 16
2.9. Interaction between plastic settlement and shrinkage cracking 16

2.10. Current methods evaluating plastic shrinkage cracking 17
2.11. Concluding summary 18
Chapter 3 : Mould design 20
3.1. Shortcomings of previous methods 20
3.2. Initial mould design considerations 22
3.2.1. Crack length 22
3.2.2. Sample size 23
3.3. Mould design requirements 23
3.4. Mould design 24
3.4.1. Preliminary experimental tests 24
3.4.2. Finite Element Modelling 24
3.4.3. FEA input parameters 25
3.4.4. FEA results 26
3.5. Experimental results 28
3.6. Final mould adjustments 30
3.6.1. Crack length 30
3.6.2. Influence of restraint 31
3.7. Concluding summary 33
Chapter 4 : Experimental framework 34
4.1. Climate chamber 34
4.2. Experimental moulds 34
4.2.1. Plastic cracking 35
4.2.2. Shrinkage and settlement 35
4.2.3. Capillary pressure 36
4.2.4. Setting times 36
4.3. Measuring methods 37
4.3.1. Average crack width 37
4.3.2. Capillary pressure 38
4.3.3. Shrinkage and settlement 39
4.3.4. Setting times 39
4.4. Test procedure 40
4.5. Materials 40
4.6. Mixes and climate conditions 42
4.7. Test program 43
4.8. Concluding summary 44

Chapter 5 : Experimental results and discussion 45
5.1. Plastic shrinkage cracking 45
5.1.1. Crack formation characteristics 45
5.1.2. Setting times 49
5.1.3. Effect of depth 50
5.1.4. Conclusions 55
5.2. Interaction between plastic settlement and shrinkage cracking 56
5.2.1. Effect of depth 60
5.2.2. Conclusions 63
5.3. Summary of cracking types 64
5.4. Finishing operations 66
5.4.1. Conclusions 68
5.5. Concluding summary 68
Chapter 6 : Plastic cracking risk model and prevention guidelines 69
6.1. Introduction 69
6.2. Plastic settlement cracking risk 70
6.3. Plastic shrinkage cracking 71
6.4. Factors influencing plastic settlement and shrinkage cracking 71
6.5. Settlement 72
6.5.1. Restraint 72
6.5.2. Setting time 73
6.5.3. Depth 73
6.5.4. Finishing operations 74
6.5.5. Evaporation 74
6.6. Interaction between plastic settlement and shrinkage cracking 75
6.7. Preventative measures 75
6.8. Practical risk model example 76
6.9. Concluding summary 80
Chapter 7 : Conclusions and recommendations 82
References 87

List of figures

Figure 2.1: Illustration of the different initial stages in the hydration process created by Combrinck, 2016 (Adapted from Powers, 1968; ACI 308R, 2001; Mehta & Monteiro, 2006; Sant et al., 2009 and Domone & Illston, 2010). 6

Figure 2.2: Tensile cracks, shear cracks and water pocket formation due to a rigid inclusion (Combrinck, 2016) 9

Figure 2.3: Typical phenomenological behaviour of plastic shrinkage cracking (Combrinck, 2011; Maritz, 2012 and Boshoff & Combrinck, 2013). 10

Figure 2.4: Plastic shrinkage cracking on a slab section with external restraint as illustrated in plan. 13

Figure 2.5: Capillary pressure build-up in a drying suspension (adapted from Combrinck 2016). 13

Figure 2.6: Forces caused by menisci forming in capillary pores (Combrinck, 2016). 14

Figure 2.7: ASTM C1579 test mould. 17

Figure 2.8: Plastic shrinkage cracking mould used by Combrinck (2016) 18

Figure 2.9: Nordtest method ring test. 18

Figure 3.1: Internal cracks due to restraint located on both sides of the ASTM C1579 mould as seen from the side. 21

Figure 3.2: Initial settlement cracks observed above the central triangle of the ASTM C1579 mould obtained from preliminary experimental tests 21

Figure 3.3: Illustration of cracking and shrinkage observed for a) Normal shrinkage cracking mould with 64 mm bottom triangular insert at centre. b) Modified shrinkage cracking mould with no triangular insert at centre (Combrinck, 2016). 22

Figure 3.4: Preliminary experimental moulds and their respective results. 25

Figure 3.5: Plastic shrinkage cracking mould shape 26

Figure 3.6: Variation in the arc shape of the web arc of the mould with stress contours. 26

Figure 3.7: FEA mould Variation 1 results. 27

Figure 3.8: Variation of the web width of the mould with stress contours. 27

Figure 3.9: FEA mould Variation 2 results. 28

Figure 3.10: Final FEA mould geometry with respective stress distribution 28

Figure 3.11: FEA assumptions experimentally tested 29

Figure 3.12: Experimental wood mould with 200 mm crack length 29

Figure 3.13: Experimental mould with 150 mm crack length. 31

Figure 3.14: Frictionless PVC mould final test results. 31

Figure 3.15: Proposed mould with grooves to increase restraint 32

Figure 3.16: Final proposed mould with triangular prism restraint 32

Figure 3.17: Plastic shrinkage cracking monitored in the final proposed mould. 33

Figure 4.1: Climate chamber used with camera setup. 34
Figure 4.2: Plastic cracking mould. 35
Figure 4.3: Shrinkage and settlement mould. 36
Figure 4.4: capillary pressure moulds. 36
Figure 4.5: Setting time apparatus. 37
Figure 4.6: Plastic cracking mould test setup. 37
Figure 4.7: Average surface crack width measuring example 38
Figure 4.8: Sieve analysis of fine aggregate (Sand). 41
Figure 4.9: Sieve analysis of coarse aggregate. 41
Figure 5.1: Plastic shrinkage cracking results in the 100 mm deep mould with the NB-Mix in Climate E. 46
Figure 5.2: Cracking results for the NB-Mix exposed to Climate E along with digital images of the crack as seen from the side at selected times. 47
Figure 5.3: Plastic shrinkage cracking results for the NB-Mix in Climate M along with a digital image of the final crack width as seen from the side. 48
Figure 5.4: Plastic shrinkage cracking results for the NB-Mix in Climate N along with a digital image of the final crack width as seen from the side. 48
Figure 5.5: Plastic shrinkage cracking results for the HB-Mix in Climate E along with a digital image of the final crack width as seen from the side. 49
Figure 5.6: Results of the average surface crack width for 100, 150 and 200 mm cracking moulds for the NB-Mix at Climate E. 50
Figure 5.7: Plastic shrinkage crack propagation observed from the side for the NB-Mix at Climate E. 51
Figure 5.8: Plastic shrinkage cracking results and mix properties in 200 mm deep mould for the NB-Mix at Climate E. 52
Figure 5.9: Shrinkage results measured in the 200 mm mould over the depth at selected time periods for the NB-Mix at Climate E. 53
Figure 5.10: Results of the NB-Mix in Climate E in the 100 mm deep mould without a steel bar and with 45 mm embedded steel bar with no settlement cracks, along with digital images of the section as seen from the side. 55
Figure 5.11: Interaction results for the NB-Mix at Climate E with and without embedding a steel bar in the 100 mm mould. 56
Figure 5.12: Example of typical tension and shear cracks in Phase 1 obtained from the NB-Mix at Climate 57
Figure 5.13: Interaction results for the HB-Mix in Climate E with and without an embedded steel bar (100 mm mould). 58
Figure 5.14: Side surface cracking results (25 mm steel bar in 100 mm deep mould) for the NB-Mix exposed to the Climate E. 59
Figure 5.15: Average surface crack width results for the HB-Mix and NB-Mix in Climate E with and without a steel bar. 60

Figure 5.16: Crack interaction results for NB-Mix at Climate E with and without an embedded steel bar in the 200 mm deep mould. 61

Figure 5.17: Crack development for the NB-Mix at Climate E with an embedded steel bar at 95 mm as seen from the side. 62

Figure 5.18: Side surface cracking results (25 mm embedded steel bar in 200 mm deep mould) for the NB-Mix exposed to Climate E along with selected digital images. 63

Figure 5.19: Plastic cracking diagram with respective driving forces. 65

Figure 5.20: Effect of finishing operations on pure plastic shrinkage cracking for the NB-Mix at Climate E. 67

Figure 5.21: The effect of finishing operations on plastic settlement cracking for the NB-Mix at Climate E with an embedded steel bar at a depth of 25 mm. 67

Figure 6.1: Plastic settlement cracking risk estimation. 70

Figure 6.2: Plastic shrinkage cracking risk estimation. 71

Figure 6.3: Interaction risk between plastic settlement and shrinkage cracking. 75

Figure 6.4: Example of the settlement cracking model with values. 78

Figure 6.5: Example of the shrinkage cracking model with values. 79

Figure 6.6: Example of the interaction cracking model with values. 80

List of tables

Table 3.1: Crack area for most commonly used moulds. 23
Table 3.2: Crack cross-sectional area of three common mould geometries. 30
Table 4.1: Material properties. 40
Table 4.2: Mixture constituents and properties. 42
Table 4.3: Climate conditions. 42
Table 4.4: Summary of the experimental plan. 44
Table 6.1: Typical bleeding rates after an hour. 72
Table 6.2: Typical restraint types. 73
Table 6.3: Typical initial setting times. 73
Table 6.4: Typical slab depths. 74
Table 6.5: Typical evaporation rates. 74
Table 6.6: Example of settlement cracking influencing factors. 79
Table 6.7: Example of shrinkage cracking model. 80

Notations and acronyms

Notations:

ER	Evaporation rate [kg/m^2/h]
r	Relative humidity [%]
T_a	Air temperature [°C]
T_c	Concrete temperature [°C]
V	Wind velocity [km/h]
σ_t	Surface tension [N/m^2]
P	Capillary pressure [Pa]
R_1	Maximum radius of water meniscus [mm]
R_2	Minimum radius of water meniscus [mm]
$m_{bleedwater}$	Mass of accumulated bleed water [kg]
$A_{container}$	Area of container [m^2]

Acronyms:

ACI	American Concrete Institute
ASTM	American Standard Testing Methods
Climate E	Extreme climate
Climate M	Medium climate
Climate N	Normal climate
CSF	Condensed silica fume
FA	Fly ash
FEA	Finite element analysis
GGBS	Ground granulated blast furnace slag
HB-Mix	High bleeding mix
NB-Mix	Normal bleeding mix
L	Grounded limestone
LVDT	Linear variable differential transformer
SANS	South African National Standards
UN	European Standards

Chapter 1 : Introduction

Cracking of conventional concrete in its plastic state predominantly includes both plastic settlement and shrinkage cracks. The term plastic refers to the state concrete finds itself in. The plastic state of concrete starts once water is added to the constituent materials and it ends once the concrete hardens and gains significant mechanical strength. This is usually between 4 to 8 hours after mixing (Mehta & Monteiro, 2006). Settlement and shrinkage refer to the change in volume in the vertical and horizontal direction. If this change in volume is restrained, stress occurs and the potential for cracking arises.

These plastic cracks are largely a problem for slab-like elements with large exposed surfaces where these cracks can act as pathways for degrading agents to penetrate the concrete, which decreases the service life of the structure (Weyers et al., 1982 and Chengqing, 2003). Insufficient cover depth to underlying rebar, change in concrete cross-sectional depth and environmental conditions characterised by high evaporation rates, are all significant external factors influencing the behaviour of these plastic cracks.

Once the concrete has been placed and consolidated, the denser solid particles in the concrete start to settle. Stresses in the concrete exist if this settlement is non-uniform in the depth of the concrete. This can lead to plastic settlement cracking which is arguably the earliest form of cracking and over the past fifty years, numerous researchers have studied settlement and its effect on plastic settlement cracking (Powers, 1968; Weyers et al., 1982; Sanjuan & Moragues, 1997; Holt, 2000; Kwak et al., 2010 and Combrinck, 2016).

Plastic shrinkage occurs due to the capillary pressure build-up in the concrete matrix. The capillary pressure build-up is caused by high evaporation rates, which cause the pore water to evaporate. Plastic shrinkage and plastic shrinkage cracking have been well researched over the past fifty years (Wittmann, 1975; Kraai, 1985; Kronlof et al., 1995; Shah & Weiss, 2006; Slowik et al., 2008; Boshoff, 2012 and Combrinck, 2016). However, although the basic mechanisms responsible for settlement and shrinkage cracking are known, these plastic cracks are often unpredictable and they remain a problem in slab-like elements. Plastic cracks can be and are mostly prevented by using effective construction techniques and/or applying the correct finishing operations at the appropriate time. Nevertheless, these cracks still occur due to ignorance towards effective construction techniques and concrete mix designs.

The plastic period in terms of the service life of the structure is insignificant with respect to time. Nonetheless, the plastic period can have premature detrimental effects on structural elements, which can drastically reduce the service life. Furthermore, the two cracking types in the plastic period have mostly been isolated (wrongfully) and investigated separately by most research studies that are available in the literature.

Studying and ultimately predicting the interaction between plastic settlement and shrinkage cracking has only recently been suggested (Combrinck, 2016). Isolating plastic shrinkage cracking from settlement cracking proves to be difficult, and no standard test method exists. Lastly, the effect of the cross-sectional depth and finishing operations on plastic cracking are still unknown and requires investigation.

1.1. Objectives

These objectives are set out for this study:

1. Design a mould and propose a standard test method for evaluating plastic shrinkage cracking without the influence of initial plastic settlement cracks.
2. Study the effect of plastic shrinkage cracking without the influence of plastic settlement cracking.
3. Investigate the interaction between plastic settlement and shrinkage cracking.
4. Study the effect of depth on plastic cracking.
5. Determine the effect of surface finishing operations on plastic cracking.
6. Provide a fundamental understanding of the mechanisms which cause plastic settlement and shrinkage cracking and of how these mechanisms interact.
7. Present a framework for a risk model that can predict the risk for the plastic cracking types separately as well as combined.

1.2. Research significance

Plastic cracking of conventional concrete occurs between the placement and consolidation of the concrete which typically range between 4 to 8 hours. Within this initial short period the formation of plastic cracks can decrease the long-term durability, aesthetical value and strength of the concrete structure.

Although the basic driving forces (settlement and shrinkage) causing these cracks are known, little is known on how the mechanisms behind plastic settlement and shrinkage cracks interact. This is ascribed to the absence of a test method evaluating plastic shrinkage cracking without the influence of initial plastic settlement cracks. Applying the correct constructions techniques would eliminate and generally minimise plastic cracking. However, the lack of understanding regarding the interaction between plastic cracking types, the effect of depth and finishing operations together with negligence, create instances where these cracks still form.

There exist many complexities that influence plastic cracking and time-dependent prediction models have only recently been attempted and suggested (Combrinck, 2016). Factors such as cracking interaction, the effect of depth and influence of finishing operations could further aid and improve the understanding of these cracks. These prediction models can act as tools which could ultimately assist engineers in designing and constructing structural elements in such a way that it minimises the risk for plastic cracking.

1.3. Report outline

This report is set out as follows:

- Chapter 2 contains a background study on the properties and cracking of plastic concrete. General properties of concrete and factors influencing both plastic settlement and shrinkage are considered. Lastly, current methods evaluating plastic shrinkage cracking are reviewed.

- Chapter 3 entails the design process behind the development of a new plastic shrinkage cracking mould. Finally, the mould is experimentally tested and verified where after a standard test method is proposed.
- Chapter 4 provides the experimental framework used in this study.
- Chapter 5 presents and discusses the results obtained for each objective. Plastic shrinkage cracking and the interaction between plastic cracking types are discussed first, followed by the effect of depth and finishing operations on plastic cracking.
- Chapter 6 provides a risk model which can assist in the prediction of plastic cracking followed by general guidelines which could minimise plastic cracking.
- Chapter 7 provides conclusions and recommendations on this study.

Chapter 2 : Background study on plastic cracking of concrete

This chapter outlines previous research done and provides an understanding of plastic cracking in concrete. Two cracking types dominate the plastic phase namely, plastic settlement cracking and plastic shrinkage cracking. Before the fundamental behaviour of plastic settlement and shrinkage cracking are discussed, the principal aspects related to the development of early-age concrete are highlighted. Finally, the methods evaluating these plastic cracks are reviewed.

2.1. Introduction to plastic cracking of concrete

Plastic cracking of concrete occurs in concrete where concrete is a composite material and made up from a mixture of sand, cement, stone and water. The sand and stone (classified as either coarse or fine aggregate) are fillers in the concrete matrix and they predominantly add volume to the concrete and they make the concrete dimensionally stable as well. Furthermore, the cost of aggregates compared to cementitious materials is less, thereby reducing the cost of concrete (Illstron & Domone, 2010). Water and cement have a chemical reaction called hydration, and this forms a matrix which binds coarse and fine aggregate particles to form a strong rigid composite known as concrete (Owens, 2009).

Modern-day concrete has evolved and does not invariably consist of aggregate, cement and water as mentioned above. Modern concrete also consists of additions and/or admixtures. Additions, also referred to as supplementary cementitious materials, can be inert or they can have a secondary cementing effect when used in combination with cement. In South Africa pure cement is rare and supplementary cementitious materials such as Ground granulated blast furnace slag (GGBS), Fly ash (FA), Grounded limestone (L) and Condensed silica fume (CSF) are blended with the cement in varying degrees, depending on the application.

Admixtures in powder or liquid form can modify the fresh and/or hardened properties of concrete if added to the concrete mixture. The use of admixtures and additions are not part of the scope of this study and more information can be obtained from these sources (Owens, 2009; Aïtcin & Eberhardt, 2016 and Aïtcin, 2016).

The term plastic refers to a period in the phase, or phase of matter the concrete is in, just after water is added to the constituent materials and before the concrete has hardened or gained significant strength. The end of the plastic phase of concrete can be relatively quantified as a time value using setting times.

Setting times are measured by standardised methods that indicate the current phase in which the concrete finds itself with the use of penetration needles. The end of the plastic phase is characterised around the final setting time (ACI 231R, 2010). For conventional concrete this period usually occurs within eight hours after the mixing. For this study, cracking is considered as plastic, from first consolidation and placement up to the final setting time.

2.2. Stiffening, setting and hardening of young concrete

The term young concrete or early age concrete describes concrete as the first couple of days between placing and consolidating it, which is characterised by significant strength gain. Setting times can be used to determine the phase of concrete before hardening. Setting times do not indicate a sudden change and should not be used or seen as an exact science (Illstron & Domone, 2010). Instead of using initial and final setting as an exact parameter or change in the concrete composition or matrix, the focus is rather given to the particular phases (characteristics etc.) concrete finds itself in.

The different phases concrete passes through before it starts gaining significant mechanical strength, can be characterised by a combination of various aspects. These aspects include the state of matter, setting times, hydration stages, the rate of hydration, volume change, finishing operations, permeability and porosity (Combrinck, 2016). Hammer (2007) characterised three prominent consecutive phases of early age concrete up until final set, which he called the liquid/plastic phase, semi-plastic phase and early hardening/solid phase. Combrinck (2016) compiled Figure 2.1 that combines and illustrates these phases and the various aspects attributed to each phase.

In the stiffening or liquid/plastic phase, no mineral skeleton has formed due to hydration of the cement, and the concrete cannot support its own weight. Settlement occurs mostly in this phase solely due to gravity. Additional settlement can also occur in the setting phase or semi-plastic phase due to capillary pressure build-up as will be discussed in Section 2.8.3.

The permeability of the concrete in the stiffening phase drastically reduces with time. For conventional concrete, this period usually lasts between 2 to 4 hours after mixing (Illstron & Domone, 2010). In the stiffening phase, the concrete is transported, placed, consolidated and finished as presented in Figure 2.1. The end of this phase is just before the concrete loses its fluidity and it gradually starts to set.

In the setting or solidification/semi-plastic phase the stiffness of the concrete matrix starts to develop where after initial settlement ceases. If the evaporation amount exceeds amount of bleed water on the top, capillary pressure starts to build-up. Not only does the capillary pressure build-up induce horizontal shrinkage, but it also has an additional settlement effect. The end of this phase is characterised by a change in the concrete matrix from setting to hardening. In the setting phase, the concrete surface is finished by floating, brooming and trowelling. For conventional concrete, the end of this phase occurs between 4 to 8 hours after mixing.

In the early hardening/solid phase, significant stiffness develops. This phase is characterised by a significant strength increase and strain capacity decrease. From this time onwards the rate of strength gain is rapid for the next few days, and curing can commence (Illstron & Domone, 2010). Cracking that form as a result of drying shrinkage, thermal volume change and that which is induced structurally in this stage and later on, falls beyond the scope of this study.

Methods that determine setting times are standardised and include the Vicat needle and proctometer. These methods either measure the penetration resistance or the penetration force applied to a sample of concrete paste. Combrinck (2016) compared the reliability and practicality of the Vicat needle and the proctometer in accordance with EN 196-3 (2005) and ASTM C403 (2008). Combrinck (2016) found that the ASTM proctometer is impractical due to preparation time in filling a sample with cement paste. He also found that the setting times obtained from the two methods were comparable and reproducible. With this in mind, the Vicat needle is deemed suitable and is further used in this study.

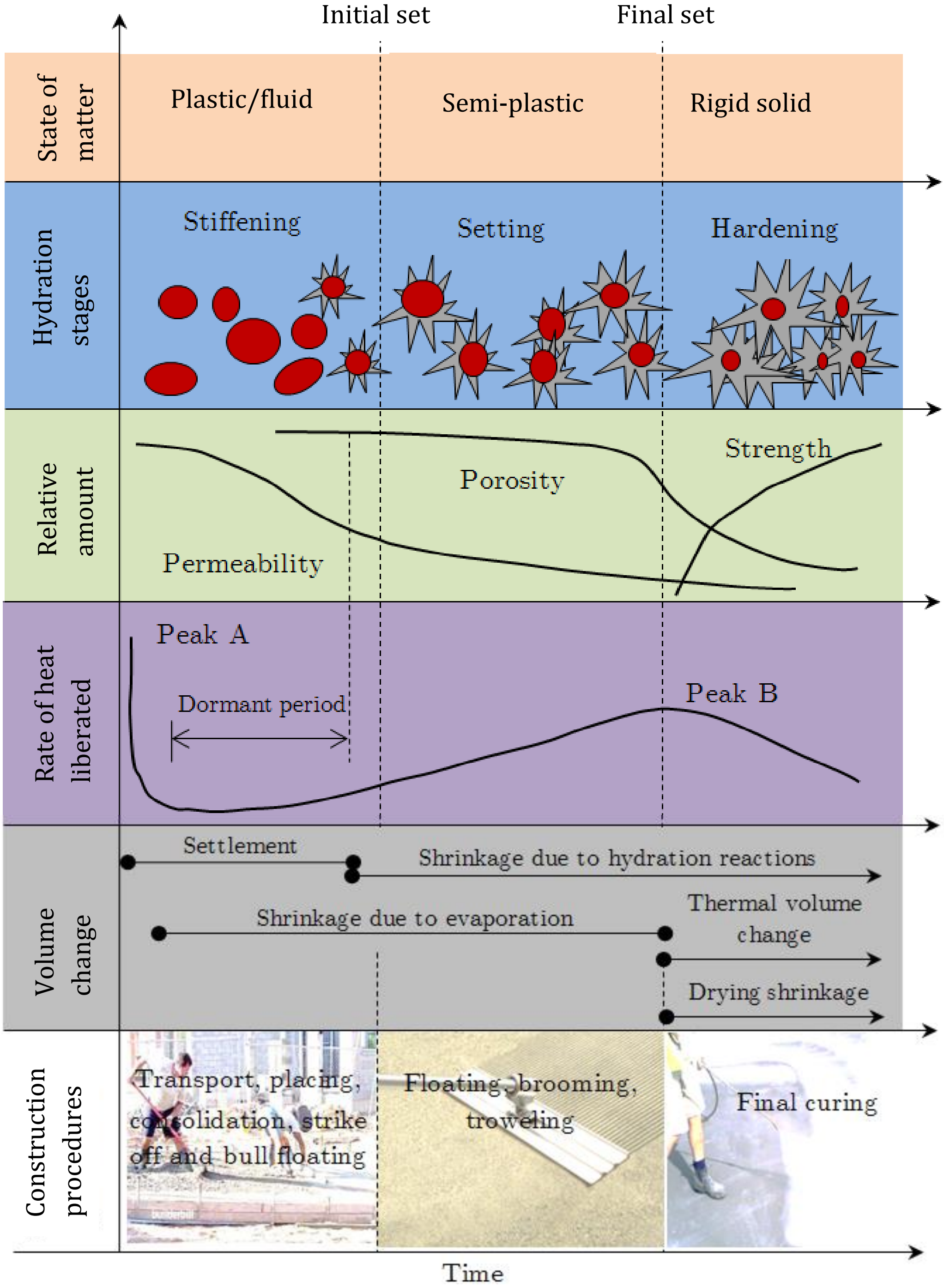

Figure 2.1: Illustration of the different initial stages in the hydration process created by Combrinck, 2016 (Adapted from Powers, 1968; ACI 308R, 2001; Mehta & Monteiro, 2006; Sant et al., 2009 and Domone & Illston, 2010).

Current research investigates the use of ultrasound spectroscopy and oscillating rheometry for predicting setting times. These methods correlate shear and bulk elastic moduli evolution in cement to setting times. This does not form part of the study and more information can be obtained from these sources (Nachbaur et al., 2001 and Hassan et al., 2010).

2.3. Driving forces behind plastic cracking

The driving forces behind the cracking of concrete in the plastic phase are volume change and/or any externally imposed deformation. Externally imposed deformation can be prevented with the use of proper construction techniques and applying the correct finishing operations at the appropriate time. For large concrete decks with a slight slope, the concrete can gradually flow due to gravitational forces. This can ultimately lead to cracking. These cracks can be prevented with a concrete mixture characterised by a low viscosity and high shear yield stress (Hammer, 2007). Cracks due to externally imposed deformation, fall beyond the scope of this study.

Cracks can only initiate if the volume change is restrained. If a concrete element is free to uniformly move (settle or shrink) in all directions, no cracks will form. If concrete is restrained, tensile stresses develop which can exceed its tensile stress capacity (the strain capacity of the concrete). At this critical point in time cracking occurs (Chengqing, 2003; ACI Committee 224, 2008 and Combrinck, 2016).

Cracking caused by volume change is the main focus of the study. In the plastic phase of concrete, volume change can occur due to one or a combination of the following:

- air expulsion
- thermal effects
- autogenous deformation resulting from chemical shrinkage
- bleeding as a result of settlement
- shrinkage due to evaporation

Of the mentioned type of volume change, air expulsion is assumed to be negligible. After mixing, placing and properly consolidating the concrete, most entrapped air should be released and have insignificant influence on volume changes in the plastic period. Volume change due to thermal effects only has a noticeable effect on concrete from the hardening phase and then further on (Neville, 2011). Thermal effects therefore fall beyond the scope of this study. Temperature change before the hardening phase does however have implications on evaporation, as discussed later in Section 2.8.1.

Autogenous deformation is caused by chemical shrinkage or due to the hydration of cement. In the stiffening phase, autogenous shrinkage equals chemical shrinkage as gravity collapses the pores caused by the hydration reaction. In the setting phase, the concrete starts to form an internal structure which can resist the collapsing of internal pores. From this point onwards chemical shrinkage exceeds autogenous deformation (Hammer, 2007).

As pores start to form in the setting phase, water is removed from these internal pores and capillary stress starts to develop. This causes a global volume change called autogenous shrinkage/deformation (Sant et al., 2009). Only 40 % of autogenous shrinkage occurs within the first 24 hours and its magnitude is usually an order less than drying shrinkage (Owens, 2009). Autogenous shrinkage is predominant in high strength or ultra-high strength concrete with water cement (w/c) ratios smaller than 0.4. As a result of these factors, volume change due to autogenous deformation, is assumed to be negligible when compared to settlement and shrinkage deformation, especially for a conventional concrete mix with w/c ratios of more than 0.4 as it is used in this study.

Volume change due to settlement and shrinkage in conventional concrete dominates the plastic phase. To quantify and further simplify these volume changes, deformations are classified as linear, with the vertical and horizontal component called plastic settlement and shrinkage respectively.

2.4. Plastic settlement

Over the past couple of decades, numerous researchers have studied settlement and its effect on plastic settlement cracking (Powers, 1968; Dakhil et al., 1975; Weyers et al., 1982; Sanjuan & Moragues, 1997; Holt, 2000; Kwak et al., 2010 and Combrinck, 2016). Just after placing concrete, solid particles start to settle and in turn displace water upwards. The thin layer of water on the concrete surface is called bleed water. Settlement is the driving force behind the vertical volume reduction of plastic concrete.

Powers (1968) first measured settlement by placing a steel pin on the concrete surface and then measuring the vertical displacement manually. Later on, instead of using a steel pin, researchers used a polystyrene ball and then tracked its movement. Until the late 90s dial gauges were used for measuring settlement. Most recently Kwak et al. (2010) used a non-contact laser to measure the displacement and they found it to be accurate and repeatable.

Plastic settlement occurs primarily before the concrete starts to set i.e. before the setting phase. Settlement in the setting phase is hindered by hydration products forming an internal matrix capable of resisting the gravitational forces acting on the solid particles. Settlement can also seize locally in the stiffening phase when aggregates come in contact with one another or with rigid inclusions. In addition to settlement occurring in the stiffening phase, it was proven that additional settlement can also occur in the setting phase. This is due to high evaporation rates which cause a capillary pressure build-up, that induces horizontal forces on the surface of the concrete matrix.

2.4.1. The behaviour of plastic settlement cracks

Settlement is the primary driving force behind plastic settlement cracking. Uniform settlement in itself does not induce cracks. Rigid inclusions such as embedded reinforcing steel or sudden differences in section depth, provide restraint against the vertical deformation. Numerous researchers have conducted tests where settlement cracking has been isolated from horizontal shrinkage (Powers, 1968; Dakhil et al., 1975; Weyers et al., 1982; Sanjuan & Moragues, 1997; Holt, 2000; Kwak et al., 2010 and Combrinck, 2016). These studies focused on rigid inclusions that cause differential settlement, such as embedded steel and investigated aspects such as varied cover depth, steel bar size and steel bar spacing.

Most recently, Combrinck (2016) studied differential settlement and identified three different defects namely shear cracks, tensile cracks and the formation of a water pocket beneath the steel bar as shown in Figure 2.2.

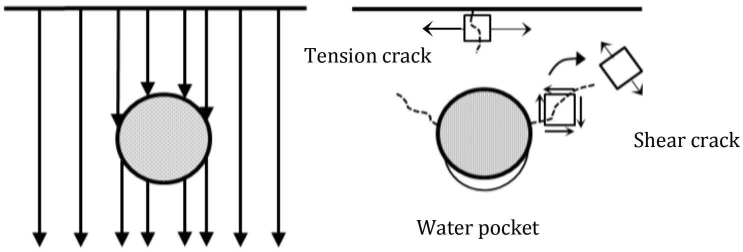

Figure 2.2: Tensile cracks, shear cracks and water pocket formation due to a rigid inclusion (Combrinck, 2016).

Tensile cracks

Tensile cracks usually map the underlying reinforcing steel and form from the top downwards. These cracks are very small which make them difficult to observe. These cracks form when the tensile stress capacity of the plastic concrete is exceeded. Tensile cracks are characterised by initial multiple cracks that form directly above the rigid inclusions or sudden changes in the cross section depth. These cracks are very small and measuring their initial formation accurately, proves difficult. These cracks are further widened by shrinkage which can ultimately form pathways for degrading agents to penetrate the concrete surface (Illstron & Domone, 2010).

Shear cracks

These cracks have not been well documented as they are not visible on the surface and can only be seen from the side. Combrinck (2016) described the formation of these cracks as being initiated by shear stress and they are opened further by principal tensile stress, therefore referred to as shear cracks. These cracks are also indicated in Figure 2.2. They form from the bottom up and generally appear before the tensile cracks (Combrinck, 2016).

Water pocket

As the heavier particles start to settle, water starts migrating upwards. As the water moves upwards, some water particles get trapped under large aggregate particles and/or rigid inclusions like steel bars (Illstron & Domone, 2010). These pockets can reduce the already weak interface zone between aggregate and/or steel bar, as well as increase the porosity of hardened concrete.

2.5. Plastic shrinkage cracking

Plastic shrinkage cracks commonly arise in structural elements with large surfaces such as bridge decks, highway pavements and they are most notable in large concrete slabs exposed to high evaporation rates (Kwak & Ha, 2006). It is well documented that plastic shrinkage cracks are characterised by its unpredictable and sudden formations (Wittmann, 1975; Shah & Weiss, 2006; Slowik, et al., 2008; Boshoff, 2012 and Combrinck, 2016).

If the surface of the concrete is unprotected in a high evaporation environment, the amount of bleed water on the top surface can be removed by the evaporation amount. During this time, tensile stresses develop in the concrete matrix. If the concrete is restrained by rigid inclusions, non-uniform section depths, non-uniform surface geometry, embedded reinforcing steel or the underlying surface, the possibility for plastic shrinkage cracking exists.

These cracks sometimes appear to form random craze-like patterns on the surface, or similar to plastic settlement cracks, map the underlying reinforcing steel. Studies have shown that these cracks can penetrate the full depth of the concrete section (Wittmann, 1975 and Slowik et al., 2008).

2.5.1. The behaviour of plastic shrinkage cracks

Plastic shrinkage, also known as capillary shrinkage, refers to the horizontal shrinkage of concrete and usually starts occurring after the stiffening phase. As for plastic settlement, plastic shrinkage in itself does not induce cracks. Only if the concrete is restrained against volume change in the horizontal direction, do stresses develop which could ultimately lead to plastic shrinkage cracking.

The volume change in the horizontal direction is driven by the build-up of negative capillary pressure in the concrete interconnected pore system, which is the primary driving force behind plastic shrinkage cracking. As the amount of bleed water is removed from the surface by the evaporation amount, negative capillary pressure build-up causes menisci to form between the solid particles. These menisci exert forces, mostly horizontally, on the particles.

Figure 2.3 shows the known events leading up to the formation of plastic shrinkage cracking. The information in Figure 2.3 was gathered through multiple tests conducted over three years at the University of Stellenbosch (Combrinck, 2011; Maritz, 2012 and Boshoff & Combrinck, 2013). Figure 2.3 shows that when the amount of bleed water at the surface is exceeded by the evaporation amount, negative capillary pressure starts to build-up. As the negative capillary pressure reaches its peak in the settlement period just before the initial set, it suddenly drops, which means a weak spot has formed locally and air has entered the concrete interconnected pore system. After the stiffening phase, as the concrete enters the setting phase, the potential for a plastic shrinkage crack is the highest.

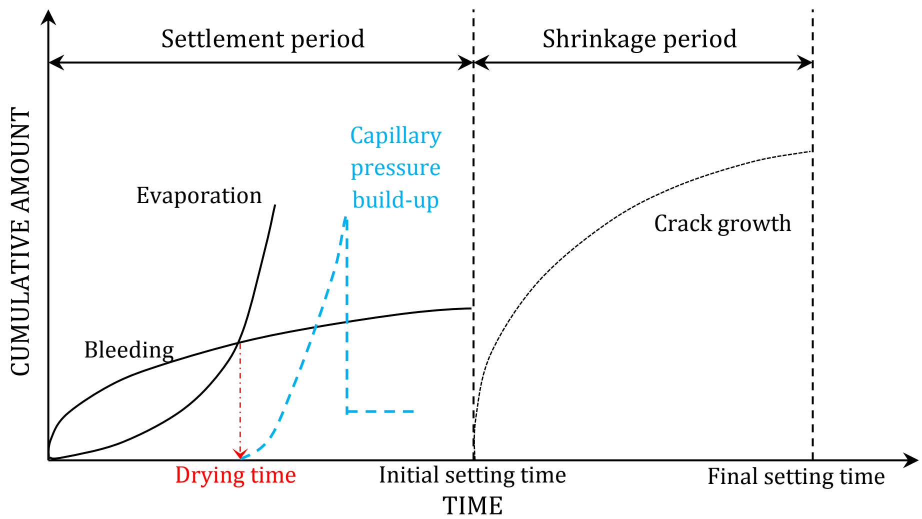

Figure 2.3: Typical phenomenological behaviour of plastic shrinkage cracking (Combrinck, 2011; Maritz, 2012 and Boshoff & Combrinck, 2013).

The plastic shrinkage cracking behaviour illustrated by Figure 2.3 used a mould that is believed to induce an initial weak spot through plastic settlement cracking (Combrinck, 2016). The influence of settlement cracking on shrinkage cracking is unknown. Determining the effect initial settlement cracks have on plastic shrinkage cracking is one of the objectives of this study.

Plastic settlement and shrinkage cracking are influenced by numerous factors. These factors are influenced by a vast number of variables including depth, finishing operations, evaporation, external restraint, capillary pressure, bleeding, setting times, water-cement ratio, concrete cover and fines content. As these factors can have an effect on both plastic settlement and shrinkage cracking, they are considered to influence both cracking types and discussed accordingly in the following sections.

2.6. Influence of depth on plastic cracking

The rate and amount of settlement are directly proportional to the depth of a concrete section (Van Dijk & Boardman, 1971). Bleeding is dependent on settlement, which leads to the conclusion that deeper sections are more prone to plastic settlement cracking (Kwak & Ha, 2006). However, plastic shrinkage cracking starts once the evaporation amount exceeds the total amount of bleeding. This means that the potential for plastic shrinkage cracking could be less in deeper sections (Uno, 1998). No research could be found regarding the effect of concrete depth on plastic cracking. It forms an integral part of this study.

2.7. Influence of finishing operations on plastic cracking

Before finishing operations can commence, the concrete first needs to be placed, consolidated and levelled. Finishing operations is used to either make the concrete aesthetically more acceptable and/or improve its mechanical properties (Owens, 2009).

After placing and consolidating, the concrete is levelled using a darby, bull float or highway straight-edge. This forces larger aggregate into the paste and it also smooths the surface. This should be done before the majority of the bleed water rises to the surface. If the bleed water is reworked back into the surface, it could cause dusting and scaling when the concrete hardens. It should also be taken into account that the surface must not be sealed off before the bleed water rises to the top, which could cause delaminations, blisters and surface scaling (Basham, 2000).

Floating and trowelling begins after the stiffening phase, and can be implemented using either machines or hand tools. These operations should be done before the concrete enters the hardening phase, after the final setting time. The use of hand tools is not obsolete, even with the introduction of machine operations. Hand tools are still vital for edges, steps and locations where machines cannot manoeuvre (Basham, 2000).

Floating removes imperfections from the concrete surface and brings cement paste to the surface for trowelling. Floats are made of various materials but they are most commonly made of magnesium or wood. Of these two, wood floats are less likely to seal the concrete surface and trap the bleed water (Suprenant & Malisch, 1999).

The effect of finishing operations on plastic cracking forms an integral part of this study. No research could be found regarding this.

2.8. Other factors influencing plastic cracking

Various factors can have a direct or indirect influence on the behaviour of both plastic settlement and/or shrinkage cracking. These factors can be divided into either factors influencing plastic shrinkage or plastic settlement, if studied separately. In this study, the effect of these factors is considered influencing both the behaviour of plastic settlement and shrinkage cracking. A discussion on each of these factors and how they influence plastic cracking follows.

2.8.1. Evaporation

Evaporation is the process where water changes from a liquid to a gas or vapour. There exist two means by which water can evaporate. Firstly, water can evaporate if the pressure above the liquid surface is less than in the liquid itself, and secondly if the liquid absorbs heat energy (Uno, 1998). Both these processes cause water molecules to escape, resulting in a transition from a liquid to a vapour. Evaporation is affected mainly by the wind, air temperature, relative humidity, concrete temperature and solar radiation.

High evaporation rates are characterised by high wind speeds, low relative humidity and high air temperatures. The high concrete temperature in combination with lower air temperatures also promotes high evaporation rates. Solar radiation raises the temperature of the concrete surface which increases evaporation. However, previous research done showed that while solar radiation increases the evaporation rate, it also accelerates the hydration process which increases the strength of the concrete near the surface (Van Dijk & Boardman, 1971). Ultimately, if the concrete has higher early age strength, it can resist induced strains due to shrinkage earlier and therefore it can inhibit or reduce the formation of plastic shrinkage cracks. This is not absolute and needs further investigation.

Equation 2-1 developed by Uno (1998), is used for calculating the evaporation rate in terms of kilogrammes per square meter per hour.

$$ER = 5 \times 10^{-6} \times [(T_c + 18)^{2.5} - r \times (T_a + 18)^{2.5}] \times (V + 4) \qquad \text{Eq. 2-1}$$

where:

ER = Evaporation rate [kg/m²/h]
T_c = Concrete temperature [°C]
T_a = Air temperature [°C]
V = wind velocity [km/h]
r = Relative humidity [%]

Eq. 2-1 is highly regarded as a good approximation to calculate evaporation rates and it is used to estimate evaporation rates in this study. Historically it has been shown that if the evaporation rate exceeds 1 kg/m²/h the potential for plastic shrinkage cracking is high (Bentz & Weiss, 2008).

2.8.2. External restraint

External restraint is a fundamental aspect needed for horizontal shrinkage to result in stresses within the concrete. External restraints include the underlying surface, the geometry of the concrete element or any other rigid obstructions, for example columns and walls. External restraint does not include internal rigid objects such as embedded reinforcing steel or differential section depths.

If concrete is left to shrink freely on a frictionless surface without any restraint, no stress would develop, hence no cracking (Slowik et al., 2008 and Hammer, 2007). As the concrete begins to shrink in the setting phase, stress develops first in the region near the top surface. The stress on the surface causes the concrete to contract. Rigid inclusions such as internal columns or change in the geometry of the concrete surface cause non-uniform horizontal shrinkage as illustrated in Figure 2.4. Region A shrinks less when compared to Region B as seen in Figure 2.4. This causes induced stress at the corner where a change in the geometry occurs and the possibility of cracking occurs.

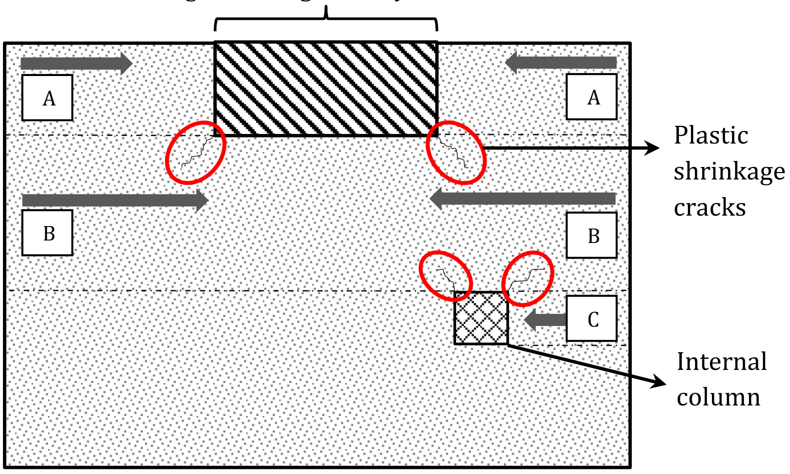

Figure 2.4: Plastic shrinkage cracking on a slab section with external restraint as illustrated in plan.

2.8.3. Capillary pressure

Capillary pressure is the process where a negative build-up of pressure arises in a cementitious material, which is believed to ultimately lead to plastic shrinkage (Slowik et al., 2008). Figure 2.5 illustrates the development of capillary pressure through five stages (A-E).

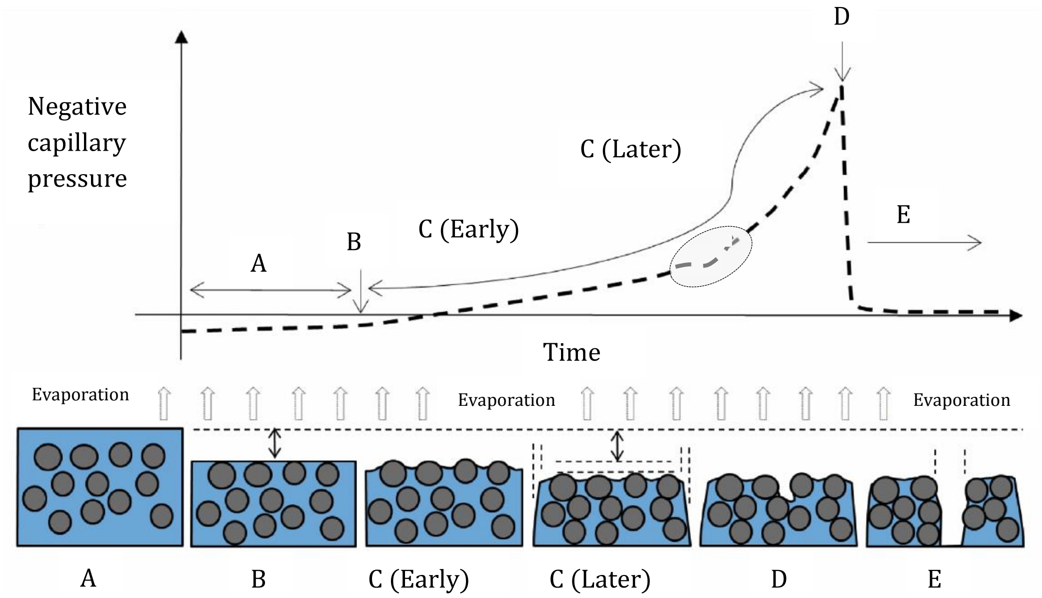

Figure 2.5: Capillary pressure build-up in a drying suspension (adapted from Combrinck 2016).

Combrinck (2016) thoroughly described these phases based on both literature and experience. A Figure similar to that of Figure 2.5 was first described and presented by Slowik et al., (2008) and then further modified by Combrinck (2016).

Stage A is characterised by the bleeding of the concrete mixture. Bleeding is the process where the heavier solid particles settle in concrete and forces water to the surface. The accumulation of this water on the surface is called bleed water. This is discussed further in the next section.

As the evaporation amount exceeds the amount of bleed water, top particles become exposed. The latter is illustrated by Point B on Figure 2.5 and initiates the rise in capillary pressure. Throughout the rise of capillary pressure, the pressure can be calculated using the well-known Gauss-Laplace equation:

$$P = \sigma_t \times \left(\frac{1}{R_1} + \frac{1}{R_2}\right) \qquad \text{Eq. 2-2}$$

where:

P = Capillary pressure [Pa]
σ_t = Surface tension [N/m^2]
R_1 and R_2 = maximum and minimum radius of water meniscus respectively [mm]

Figure 2.6 further illustrates the parameters used in Equation 2-2. The pressure induced by the formation of menisci, creates forces acting on the solid particles near the top surface of the still plastic concrete. Equation 2-2 clearly indicates that as the radius between the particles decreases, the force acting on these particles increases. The radius is thus indirectly proportional to the capillary pressure build-up.

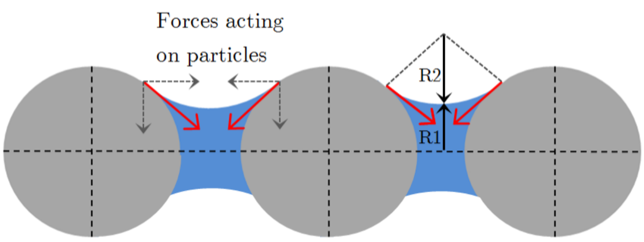

Figure 2.6: Forces caused by menisci forming in capillary pores (Combrinck, 2016).

Early in Stage C and onwards the continual evaporation increases the pressure due to particles moving closer to each other and the surface that starts drying out. Capillary pressure acts in all directions. To simplify volume change caused by capillary pressure, volume change is divided up into a vertical and horizontal component. Settlement refers to the vertical component where shrinkage refers to the horizontal component.

Settlement, to a lesser degree than initial settlement which occurs in the stiffening phase, is prominent for some time from Stage C onwards (Wittmann, 1975; Slowik et al., 2008 and Combrinck, 2016). Combrinck (2016) indicated the point in time when the capillary pressure build-up is relieved through settlement. The grey circle in Figure 2.5 in Stage C indicates this point. As the concrete pore water continually evaporates, forces acting on these particles pull them in either a downwards or sideward direction. Forces acting in the vertical direction further compacts the concrete surface (Combrinck, 2016). This settlement causes additional bleed water to rise to the surface and relieves capillary pressure for a short time period. If further cracking is avoided after the additional settlement, it can even improve the mechanical behaviour of the hardened concrete (Wittmann, 1975).

Later in Stage C when the concrete can no longer relieve the stress through vertical settlement, it mainly shrinks horizontally. Point D is characterised by the point in time when the concrete can no longer relieve stress through volume change and air entry occurs. Air enters the concrete locally at certain locations where the radii of the menisci between the particles become too small to bridge the gap. The solid particles present on the concrete surface are irregular and are not all the same size or shape. Local air entry is only the beginning, and negative capillary pressure still rises in the interconnected pore system where air has not entered (Slowik et al., 2008).

From Stage E onwards, the capillary pressure continues to rise at all other locations where air has not penetrated the surface. Forces between particles, due to capillary pressure, are considerably higher compared to regions where air has entered the concrete pore system (Slowik et al., 2008). Air entry does not mean the surface has cracked, it only indicates a weak spot created on the surface locally in the concrete matrix. Factors influencing capillary pressure include evaporation rate, particle size distribution, air content, the geometry of particles and water–solid ratio (Slowik et al., 2008).

2.8.4. Bleeding

Bleeding is a direct result of settlement (Illstron & Domone, 2010). Solid, denser particles in concrete gradually settle downwards due to gravitational forces acting on them. As these particles gradually displace downwards, water is simultaneously displaced upwards. This is called bleeding and it occurs in the stiffening phase. Gravitation is the driving force behind bleeding (Josserand, et al., 2006).

As the water continually rises to the surface of the concrete, a thin layer of water is observed which is called bleed water. Before the concrete stiffens, the initial rate of bleeding is constant. As the rate of bleeding gradually decreases, bleed water steadily disappears from the surface. The latter can be due to high evaporation rates or reabsorption. The former causes a build-up of capillary pressure which can lead to additional settlement. Reabsorption of the bleed water is related to the hydration of the cement paste and occurs when the initial maximum settlement is reached (Combrinck, 2016).

Factors influencing bleeding include fines content, water-cement ratio, aggregate characteristics, setting times and section depth. Higher bleeding leads to larger settlement and increases the risk of plastic settlement cracking. However, bleeding relieves the pressure caused by capillary pressure build-up and can reduce the risk of plastic shrinkage cracking.

Other defects caused by bleeding include the formation of water pockets beneath embedded reinforcing steel, sand streaking, and the occurrence of a surface laitance which decreases the quality of the top surface. If bleed water is reworked back into the surface by finishing operations, it can also decrease the strength of the top surface.

2.8.5. Setting times

An in-depth discussion on the development phases of plastic concrete was given in Section 2.2. The initial and largest part of settlement occurs in the stiffening phase of concrete. The duration of this period relates to the hydration process. The faster the hydration products can bridge the inter-particle gaps and form an internal matrix, the faster plastic settlement can cease (Owens, 2009). The latter also accounts for higher early age strength which could assist in resisting plastic shrinkage cracking. Prolonged setting times increases the stiffening phase. Increasing the stiffening phase increases bleeding which could assist in reducing plastic shrinkage cracks. This, however, requires more investigation as some argue that a prolonged stiffening phase could increase plastic shrinkage cracking. Factors affecting setting times include water-cement ratios, mix proportions, the temperature of constituents and ambient temperatures.

2.8.6. Water-cement ratio

For normal concrete, the water-cement ratio governs the hardened strength of concrete. For high water-cement ratio mixtures, more water is present in the concrete mix. This could result in higher bleeding rates and thus minimise the potential for plastic shrinkage cracking. However, higher bleeding rates could lead to higher settlement values which could increase the risk of plastic settlement cracking.

2.8.7. Concrete cover

The concrete cover is a term used in reinforced concrete structures and supplied by the design engineer. The concrete cover is the minimum distance between the top most embedded reinforcing steel and the surface of the concrete. Smaller cover leads to higher risk of settlement cracking due to an increased differential settlement. This has been verified numerous times with the latest research done by Combrinck (2016).

Not only does insufficient cover increase the risk of plastic settlement cracking, it creates a weak spot that is further widened by horizontal plastic shrinkage.

2.8.8. Fines content

Fines increase the cohesiveness of concrete. This leads to less settlement and therefore less bleeding. It is obvious that the latter reduces the risk of plastic settlement cracking. Fines are usually classified as smaller than 300 μm (Owens, 2009). Due to the size of fine particles, they increase the capillary pressure build-up. This is a direct result of smaller menisci forming between particles, as discussed in Section 2.8.3. This increase in capillary pressure increases the risk of plastic shrinkage cracking.

2.9. Interaction between plastic settlement and shrinkage cracking

Plastic settlement and plastic shrinkage potential have predominantly been seen as a ratio that changes between zero and one up until the beginning of the hardening phase. Settlement potential is the highest just after placing where the potential for plastic shrinkage is zero. As the potential for plastic settlement decreases to zero at initial set, the plastic shrinkage potential rises (Hammer, 2007).

Exactly how these cracks interact, as well as which factors influence their interaction, is largely unknown (Combrinck, 2016). This is a cause for concern, as plastic cracking still appears to be unpredictable even when proper construction techniques are followed. A reason for this is that no universally used standard test methods exist which isolate plastic shrinkage cracking from initial settlement cracks. Most researchers studied either plastic settlement cracks or settlement induced shrinkage cracks, as discussed in the following section.

The only research found that mentioned experimental tests regarding the interaction between plastic settlement and shrinkage cracking were a PhD study conducted by Combrinck (2016). However, Combrinck (2016) realised only later in his study that settlement plays an integral part in the mould he used to observe plastic cracking. After his study, Combrinck (2016) stressed the need for a mould that would be able to isolate and in turn evaluate plastic shrinkage cracking without the influence of plastic settlement.

Creating a mould that induces a plastic shrinkage crack without the influence of settlement, forms a large part of this study.

2.10. Current methods evaluating plastic shrinkage cracking

Plastic shrinkage cracking has been studied for numerous years using mainly three different types of mould geometries. These geometry types include rings (NT Build 433, 1995), slabs (Kraai, 1985 and Schaeles & Hover, 1988) and beams (Mora, et al., 2000 and Combrinck, 2016). The difference between a beam and a slab is the length to width ratio of the specimen. A beam is classified having a high length to width ratio, while a slab has a much lower length to width ratio. The ASTM C1579 mould along with variations on this mould, is the most widely used standard test method for evaluating plastic shrinkage cracking.

The ASTM C1579 specifies that the mould should be 560 x 355 x 100 mm as shown in Figure 2.7. This mould uses two smaller side triangles to provide restraint against horizontal shrinkage, and a central bigger triangle to reduce the cross-sectional area of the concrete, which in turn creates a weak spot for crack localisation. The cracking performance of concrete with different mix proportions, fibre volumes, fibres type and different kind of admixtures can be compared by using this method.

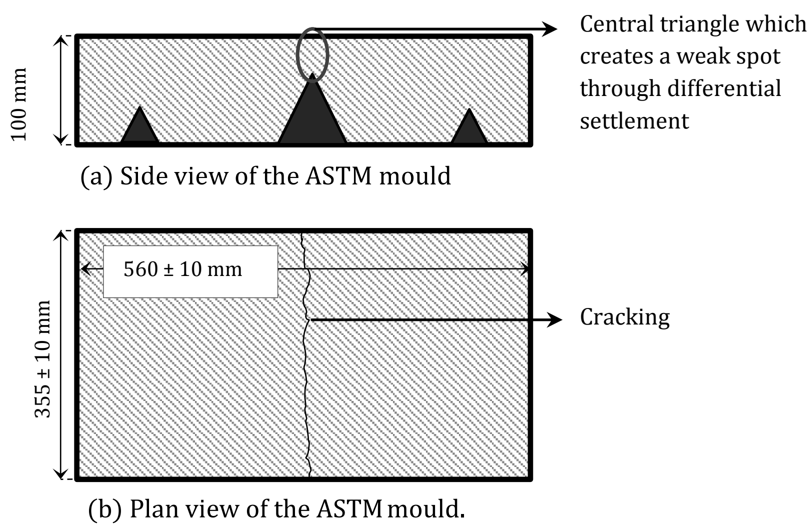

Figure 2.7: ASTM C1579 test mould.

Most research done on plastic shrinkage cracking has been conducted using a mould having more of a slab-like geometry. The most recent research on plastic shrinkage cracking was done at the University of Stellenbosch (Combrinck, 2016). Combrinck, (2016) adjusted the width and length of the standard ASTM C1579 mould to create a beam-like geometry as shown in Figure 2.8. He further added a steel bar to the sides to further increase the horizontal restraint and to increase the severity of the central crack.

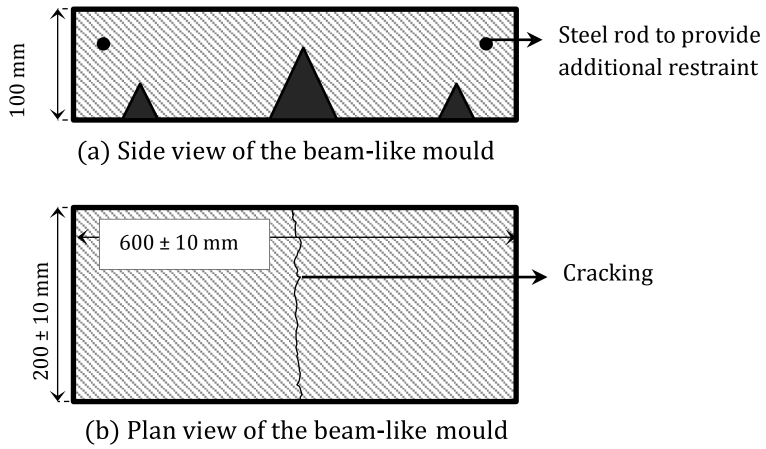

Figure 2.8: Plastic shrinkage cracking mould used by Combrinck (2016).

Lastly, the Nordtest method, otherwise known as the ring test, is also used to investigate plastic shrinkage cracking. The test setup consists of two ring-shaped test moulds made of steel and that are mounted to a steel platform as shown in Figure 2.9. The procedure for calculating the average crack width per specimen entails drawing two radial lines on the surface. The two lines are drawn on the top surface, one 50 mm from the outer edge and the other one 50 mm from the inner edge. The average crack width (crack tendency) is taken as the width where the lines intersect a crack, divided by the amount of points where the crack and radial lines intersect.

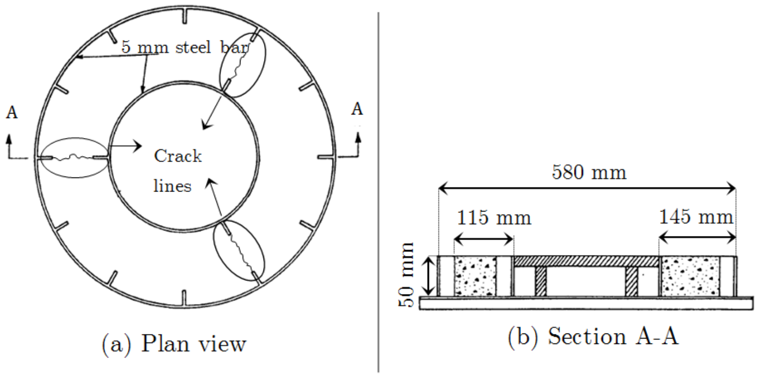

Figure 2.9: Nordtest method ring test.

2.11. Concluding summary

This chapter gives background on the plastic cracking of concrete. The chapter firstly describes the early development phases of plastic concrete and the characteristics of each phase. Secondly, the driving forces behind plastic cracking, which include settlement and capillary pressure build-up (shrinkage) are considered. The basic mechanisms causing plastic settlement and shrinkage cracking are then discussed followed by factors influencing them. These mechanisms include differential settlement and restrained shrinkage. Current research on the interaction between plastic settlement and shrinkage is given. Lastly, current methods evaluating these plastic cracks are outlined.

Chapter 3 : Mould design

Normal strength concrete plastic cracking mainly consists of two types, namely plastic shrinkage and settlement cracking. Isolating plastic settlement cracking can be done with relative ease, while few experimental test methods exist that isolate and study plastic shrinkage cracking without the influence of an initial differential settlement weak spot. This chapter aims to design and finally propose a standard test method and mould that can be used to investigate plastic shrinkage cracking without any influence of settlement cracking.

Not only does this enable a better understanding and prediction of plastic shrinkage cracking, but it also allows future investigations on the interaction between plastic shrinkage and settlement cracking. The first objective of this chapter is to evaluate existing methods and moulds that are believed to induce plastic shrinkage cracks. The final aim is to design a mould that induces one plastic shrinkage crack without the influence of differential settlement. This process essentially consists of preliminary experimental tests that are followed by optimising the mould geometry using the finite element method.

To conclude this chapter, final adjustments are made to the mould which is also experimentally verified.

3.1. Shortcomings of previous methods

The so-called ring test uses the geometry of the mould itself to ensure that cracks occur. As the concrete starts to shrink, stress is firstly induced at the inner surface of the ring. To relieve this induced stress, a crack or multiple cracks start forming along the inner ring. These multiple cracks are a cause for concern, as previous research clearly shows this non-uniform stress over the concrete surface and thus the length of the crack (Shah & Weiss, 2006). This non-uniform stress can have an unpredictable effect on the formation and characteristics of the crack. Therefore, the ring test is not considered as a viable option for this study due to the above mentioned and its relative small surface area compared to the other moulds. However, an important aspect of the ring test is the ability of the mould to induce a crack without creating a weak spot through differential settlement.

To design a mould that induces one pure uniform plastic shrinkage crack, it is clear that a symmetrical mould (uniform stress over crack) without internal restraint such as steel bars or triangles is sought after. The ASTM C1579 (2004) mould, or slight variations of the mould, has been used numerous times to evaluate plastic shrinkage cracking. Variations of the ASTM C1579 include the geometry and degree of restraint. Nevertheless, all these variations of the mould still induce a crack with by means of a central stress riser located in the middle of the mould. The ASTM C1579 mould is symmetrical but the formation of internal cracks at the internal restraint is evident. Figure 3.1 shows these cracks that cannot be seen from the surface. This image was taken while doing preliminary experimental cracking tests. The effect these cracks have on the single crack that forms in the middle of the mould, is unclear and could be a source of inconsistency.

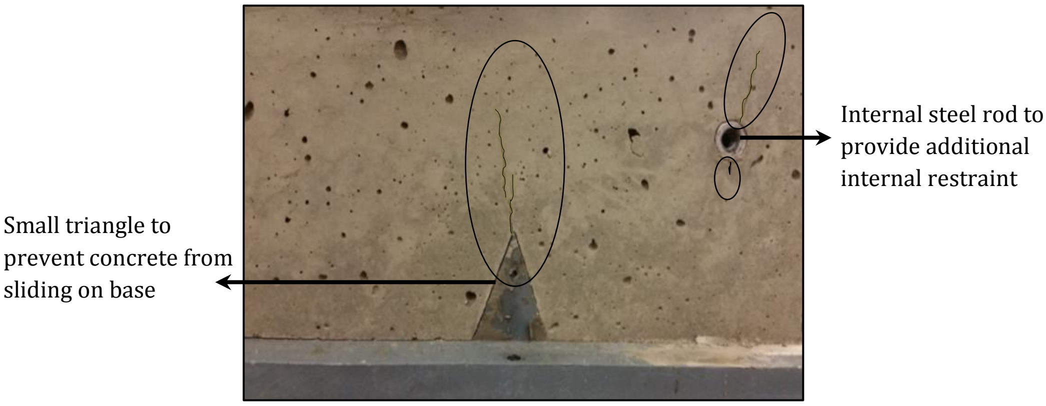

Figure 3.1: Internal cracks due to restraint located on both sides of the ASTM C1579 mould as seen from the side.

No explicit research could be found regarding the effect of the central stress raiser on the formation of the plastic shrinkage crack. Combrinck (2016) mentioned the effect of the differential settlement, but he only realised it later in his tests and he recommended that it should be investigated further. Combrinck (2016) did however find that the crack that forms over the central stress raiser, is settlement induced and it is not a pure plastic shrinkage crack. This is supported by initial fine cracks that are appearing on the surface before capillary pressure begins to rise (Combrinck, 2016). Differential settlement initially causes multiple small cracks - some close while others widen further, especially once plastic shrinkage starts. This is illustrated in Figure 3.2. The images displayed in Figure 3.2 was taken while doing preliminary experimental cracking tests.

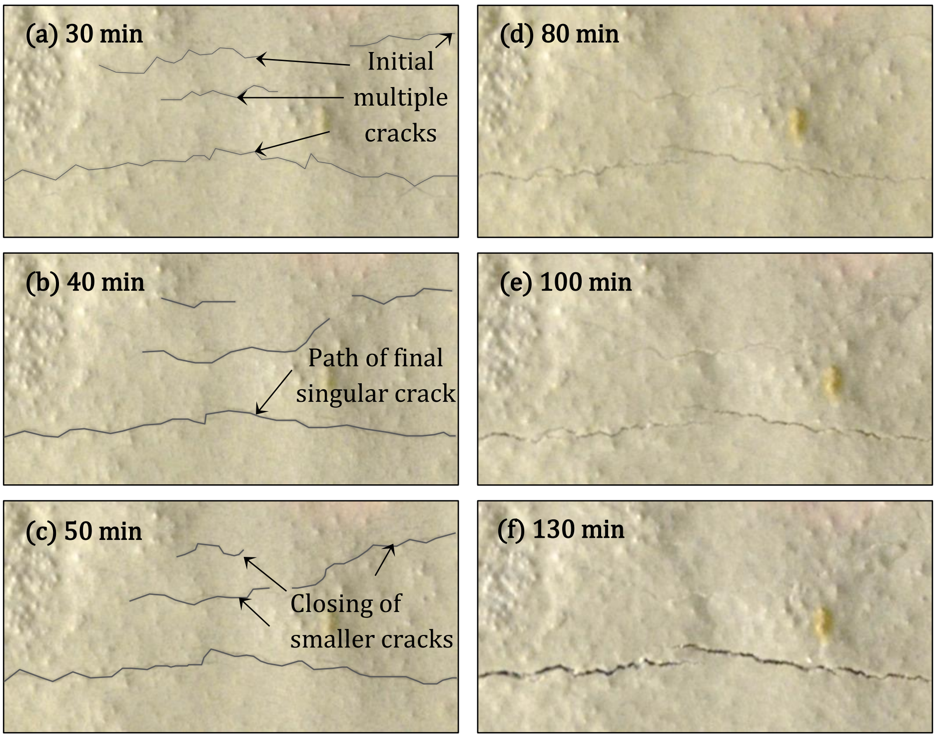

Figure 3.2: Initial settlement cracks observed above the central triangle of the ASTM C1579 mould obtained from preliminary experimental tests.

Figure 3.3 illustrates the effect of these initial settlement cracks schematically. The plastic shrinkage does not form the crack, but it only widens the crack (Figure 3.3 a). If the central triangle is removed (Figure 3.3 b), the concrete finds other ways to relieve the stress as a result of shrinkage. The induced stress can be relieved by forming a central crack, pulling away from the sides or forming internal cracks at restraints (Combrinck, 2016).

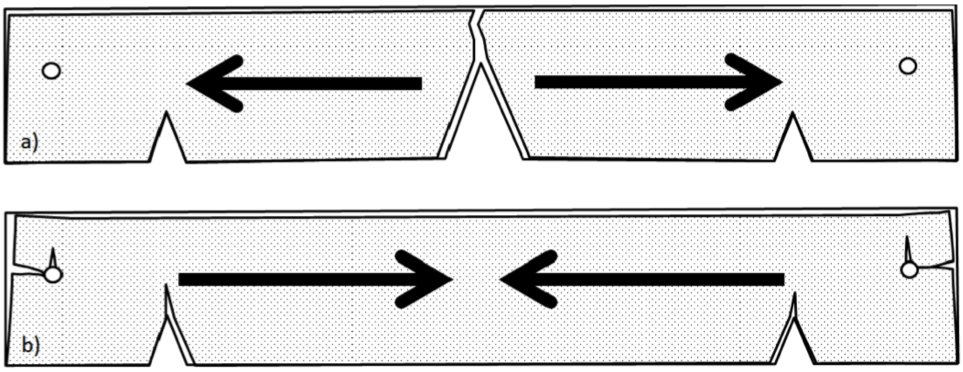

Figure 3.3: Illustration of cracking and shrinkage observed for a) Normal shrinkage cracking mould with 64 mm bottom triangular insert at centre. b) Modified shrinkage cracking mould with no triangular insert at centre (Combrinck, 2016).

Undoubtedly more research is required in order to fully understand the behaviour of plastic shrinkage cracking without the effect of an initial plastic settlement crack. Designing a practical mould that induces a plastic shrinkage crack without a central stress raiser (differential settlement), is essential in understanding the formation and interaction of plastic shrinkage and settlement cracking.

3.2. Initial mould design considerations

Taking the shortcomings of previous moulds into account, it is evident that the stress over the crack area needs to be uniform and that vertical internal restraint should not be used as this causes formation of settlement cracks as well as internal cracks at unwanted locations. However, some characteristics of the previous moulds should not be ignored and should be further investigated when designing a new mould. The sample size is an important aspect to be considered when designing a new mould and method. This ensures that comparisons can be made between different methods. This is further discussed under crack length and sample size.

3.2.1. Crack length

Considering the ASTM C1579 mould, it is clear that the length of the crack that forms over the central stress raiser is 355 mm. The test method recommends that two specimens are tested at the same time. This provides a total combined crack length of ± 700 mm that can then be measured and further examined. The crack that forms during these tests is generally only monitored from the top and not from the side. With the height of the central larger triangular stress raiser at 65 mm, the crack propagates through an area of 12250 mm^2 per mould.

The latest beam-like plastic shrinkage cracking tests were carried out by Combrinck (2016). He used four moulds with a total combined crack length of 800 mm. These moulds also induced an initial crack by using a central stress raiser with a height of 63.5 mm. Each crack propagated through an area of 7000 mm^2 per mould. This is further summarised in Table 3.1.

Table 3.1: Crack area for most commonly used moulds.

Mould type	Crack length per mould (mm)	Crack formation depth per mould (mm)	Concrete crack area per mould (mm^2)	Total concrete sample crack area (mm^2)
Common Beam-like mould	200	35	7000	28000
ASTM C1579	350	35	12250	24500

The different methods use different crack lengths, the number of specimens and depth of moulds as shown in Table 3.1. However, all the methods present similar crack propagation areas, as shown in the final column of Table 3.1. Care must be taken when designing a mould with a similar or even larger crack propagation area. The length of the crack on the surface must preferably be as long as possible. The latter has limitations due to the geometry and practical size of the mould. A crack length of 200 mm is chosen to correlate with the other standards as summarised in Table 3.1.

3.2.2. Sample size

The maximum size of the mould is limited as a result of various factors. These factors include the maximum size of the test environment (e.g. climate chamber) and the maximum size of common laboratory concrete mixers. This is hugely important with regard to practical implications. The weight of the mould is also an important practical consideration. The weight of the moulds filled with concrete should be limited to 60 kg. A test specimen which exceeds 60 kg becomes difficult and dangerous to transport and place.

The maximum width and length of the mould are limited to 400 mm and 1500 mm respectively, due to the size of the current climate chamber at the University of Stellenbosch where tests are done. Not only is the size of the mould limited, but also the maximum concrete volume per mould, which also directly correlates to the weight of the mould. Most concrete pan mixers in experimental laboratories either have a maximum capacity of 25 or 50 litres.

For the future mould, it is assumed that two moulds are cast simultaneously. This leads to the conclusion that a 50-litre mixer is required. Limiting the mixture volume to 22 litres, satisfies both practical considerations. A standard 50-litre pan mixer can be used to cast two moulds without spillage and the weight of a single sample does not exceed 60 kg.

3.3. Mould design requirements

Considering the shortcomings of previous moulds and methods it is clear that certain requirements should be met throughout the design process. Not only are the shortcomings taken into account but also practical considerations as discussed in the previous section. These five principal design requirements are:

1. The mould should induce a single pure plastic shrinkage crack.

2. The use of differential settlement to induce an initial weak spot should be avoided.
3. For normal concrete, the final average crack width should be greater than 1 mm for evaporation rates exceeding 1 $kg/m^2/h$ as discussed in Section 2.8.1.
4. No internal restraint which could lead to multiple internal cracks which cannot be measured, should be present in the mould.
5. The size and weight of the mould should be suitable for experimental laboratory tests.

These requirements form an integral part of the mould design. The requirements are taken into account when modelling the mould using finite element analysis (FEA) and when conducting experiments.

3.4. Mould design

The mould design requirements form an integral part of this chapter. The methodology followed to design and propose a mould that is suitable for evaluating pure plastic shrinkage cracking is as follows:

- Preliminary experiments.
- Optimising the mould geometry using FEA.
- Verifying FEA results and effectiveness of the final mould through experiments.

Each of these steps, including the results, is discussed in the following sections.

3.4.1. Preliminary experimental tests

Figure 3.4 shows selected preliminary experimental moulds that were used for testing.

Throughout these tests, it became clear that any type of internal vertical restraint caused unpredictable internal cracking as shown in Figure 3.4 (a and c). To prevent this, a dog-boned shaped mould without any inclusions that should be suitable for the testing of pure plastic shrinkage cracking was chosen as the appropriate shape for the new mould.

A preliminary test with such a mould was conducted as shown in Figure 3.4 (d). This mould resulted in a single crack in the centre of the mould and did not show any settlement and/or internal cracking.

3.4.2. Finite Element Modelling

The finite element analysis (FEA) software Diana version 9.6 (2010) was used to optimise the geometry of the dog-boned shaped mould. Before the mould could be modelled, various practical aspects and limitations needed to be taken into account. These limitations form part of requirement five of the mould design requirements. These aspects include:

- The maximum size of mould in terms of length, width and height is 1000 x 400 x 200 mm.
- The maximum volume of the concrete mixture per mould is 22 litres.
- The minimum length of the crack that forms in the middle of the mould is 200 mm.

It should be noted that results acquired from FEA is not exact and it is merely a tool to help design and optimise the plastic shrinkage crack mould shape. Effects such as adhesion is not taken into account and assumed to be negligible.

(a) Enlarged photo of internal cracks present in the concrete after the side panel was removed as seen from the side

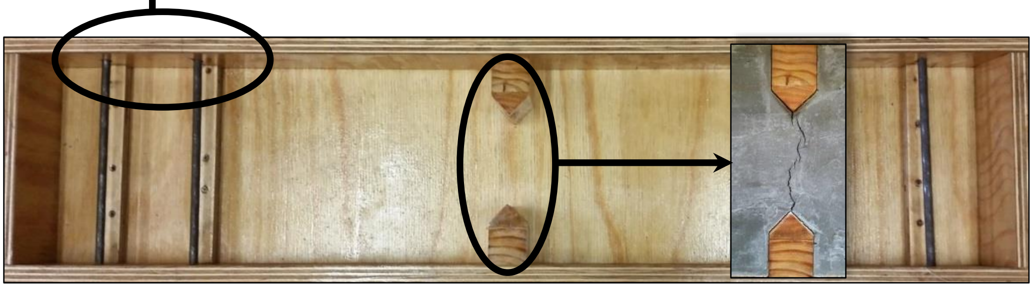

(b) Beam-like mould with internal restraint and reduced middle cross section

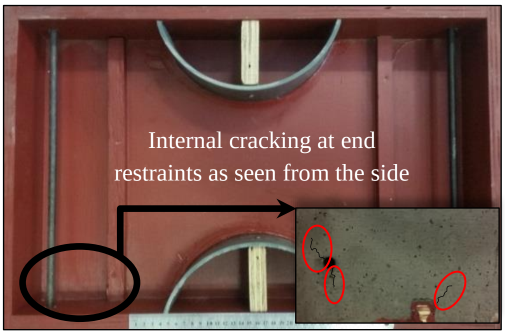

(c) Slab-like mould with internal restraint and reduced middle cross section

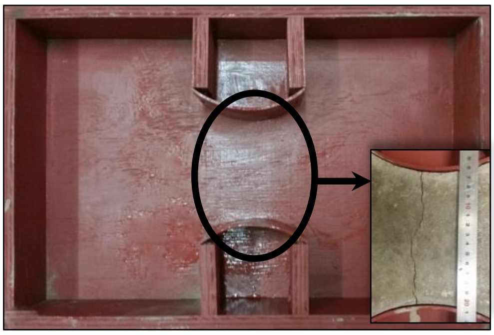

(d) Slab-like mould with no internal restraint and single crack

Figure 3.4: Preliminary experimental moulds and their respective results.

3.4.3. FEA input parameters

The mould as shown in Figure 3.5 is modelled with the following input parameters:

- The inside boundary of the mould is modelled with one node spring elements. The stiffness of these elements is infinite in the direction towards the mould sides and near zero in the direction away from the mould sides. This simulates the real behaviour of the concrete, allowing the concrete to displace freely away from the mould sides and not into the mould sides.
- Translation in the x- and y-directions at the centre of the web is fixed. Due to the symmetry of the mould, fixing a node in the centre of the mould does not have an effect on the stress distribution of the concrete in the mould.
- Quadrilateral, four node, elements are used to model the mesh.
- A mesh size of 5 x 5 mm is used.
- Lastly, an initial volume shrinkage of 0.01 mm/mm is placed on the specimen.

- The initial size of mould in terms of length, width and height are first chosen as 600 x 400 x 100 mm.

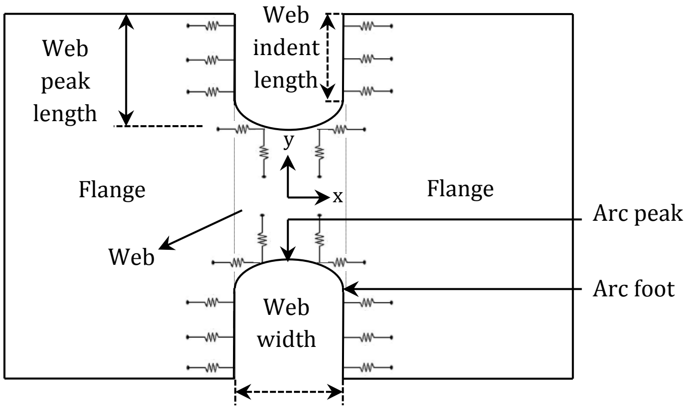

Figure 3.5: Plastic shrinkage cracking mould shape

Four different aspects are considered to be of importance when using the FEA results for choosing the appropriate geometry of the new mould (see Figure 3.5 for the appropriate labels):

1. The maximum stress at the arc peak.
2. The relationship between the arc peak and arc foot stress (The ratio between the arc peak and arc foot stress is further referred to as the stress ratio).
3. The web width of the mould.
4. The web indent length.

The mould with the highest arc peak stress will have the most severe crack, but if the stress at the arc foot is near the stress at the arc peak, meaning a high stress ratio, a small crack could form at the arc foot. This is unwanted since the first design requirement of the mould is to induce a single plastic shrinkage crack.

3.4.4. FEA results

The first variations to the mould are shown in Figure 3.6 and entail the changing of the web arc shape by altering the web indent length while keeping the crack length constant at 200 mm. Figure 3.7 shows the arc peak stress and stress ratio as a function of the arc ratio. Figure 3.6 shows the stress contours throughout the surface of the mould. Moulds 1, 2 and 3 in Figure 3.6 have similar colour codings with regard to the size of the stress contours. The results show that the larger the web indent length, the larger the stress at the arc peak.

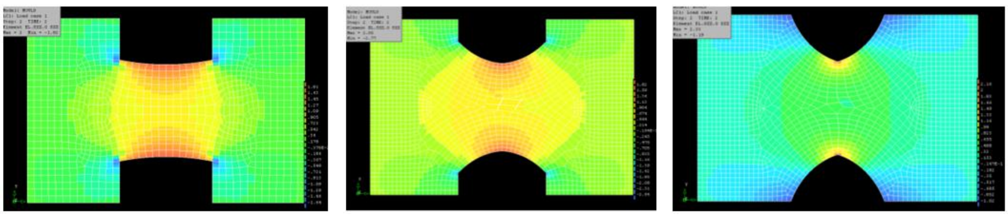

(a) Mould 1 (b) Mould 2 (c) Mould 3

Figure 3.6: Variation in the arc shape of the web arc of the mould with stress contours.

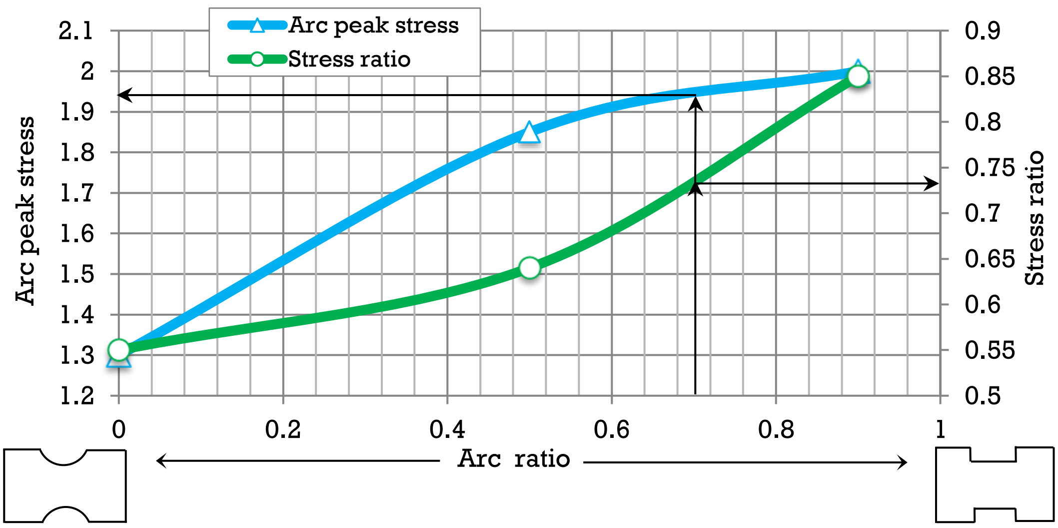

Figure 3.7: FEA mould Variation 1 results.

A large web indent ensures that the concrete 'kicks' against the side of the mould once shrinkage starts, which increases the stress in the mould. This fundamental characteristic forms an integral part of the design as it is the only form of restraint present in the mould.

After careful consideration, it is observed that a well-defined web indent is needed to provide restraint against shrinkage. The arc ratio in Figure 3.7 refers to the web indent length divided by the web peak length. The results show that the arc ratio of the mould must result in a high arc peak stress and a relatively low stress ratio as indicated in Figure 3.7. An arc ratio of 0.70 is chosen since this corresponds to a combination of a high arc peak stress and low stress ratio, which results in a single crack in the centre of the web without additional cracks at the arc foot. This choice is verified through experiments reported in Section 3.5.

The next step in the design of the mould is to further increase the arc peak stress since this will increase the severity of the crack. The moulds shown in Figure 3.8 have similar colour codings with regard to the size of the stress contours. Once again three different mould shapes are modelled in order to obtain insight on how the variation of web width, changes the stress distribution in the mould.

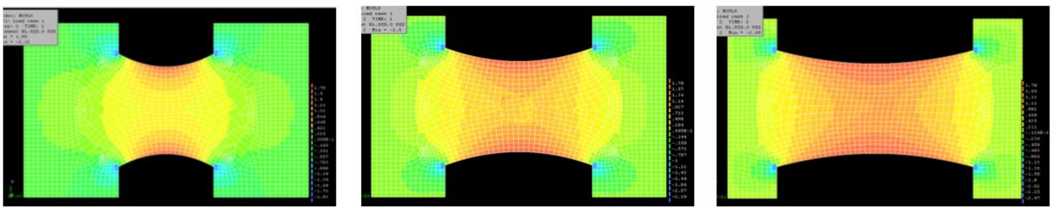

(a) Mould 4 (b) Mould 5 (c) Mould 6

Figure 3.8: Variation of the web width of the mould with stress contours.

The web width ratio in Figure 3.9 refers to the web length divided by the total length of the mould. From the results in Figure 3.9 it can be concluded that the increase in the web width ratio leads to an almost linear increase in the arc peak stress.

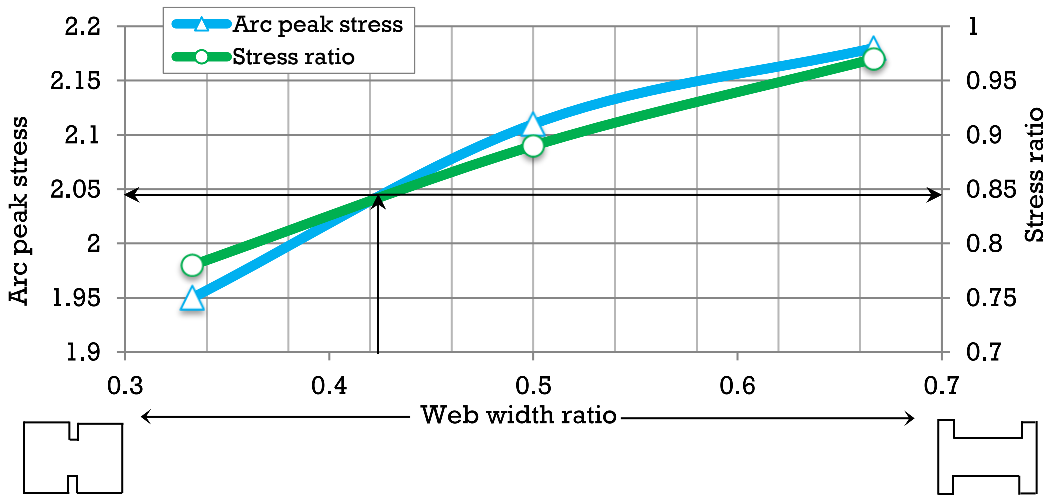

Figure 3.9: FEA mould Variation 2 results.

The same can be said for the relationship between the web width ratio and stress ratio. To avoid a crack forming at the arc foot and ensuring that a crack will start forming at the arc peak, care must be taken in selecting a web width ratio. A final web width ratio of 0.42 is chosen since this results in a relatively high arc peak stress, without significantly increasing the stress ratio. This choice is verified through experiments reported in Section 3.5. Based on the FEA results in terms of the chosen 0.7 arc ratio and 0.42 web width ratio, the geometry of the mould was determined using the 22-litre concrete capacity as governing requirement. This means the overall volume of the mould must stay within the limit of a 22-litre concrete mix. This resulted in mould dimensions of 650 x 400 x 100 mm, with a web width of 270 mm and web indent length of 70 mm. The final FEA mould along with its respective stress distribution is shown in Figure 3.10.

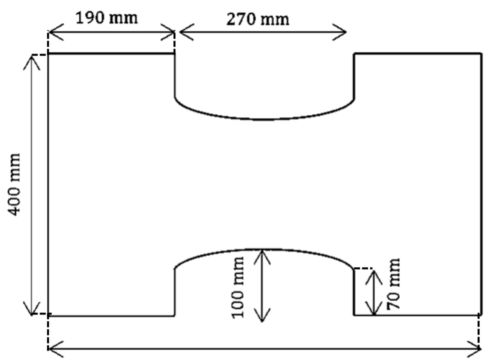

(a) Final FEA mould geometry

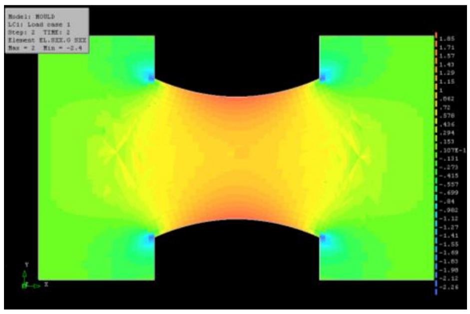

(b) Stress distribution in final mould

Figure 3.10: Final FEA mould geometry with respective stress distribution

3.5. Experimental results

For the experimental tests, a typical concrete mixture exposed to an extreme condition with an evaporation rate of 1 kg/m^2/h was used. The purpose of these experimental tests was to verify the assumptions made in the FEA. These assumptions are as follows:

- A large web indent length is required to ensure restraint against horizontal shrinkage. This is referred to as FEA Assumption 1.
- If the stress at the arc foot nears or exceeds the stress at the arc peak, a second small crack could form at the arc foot. This is referred to as FEA Assumption 2.

Figure 3.11 (a) shows the results of the tests conducted to substantiate FEA Assumption 1. A large indent length ensures that the concrete 'kicks' against the mould side which increases the stress in the mould.

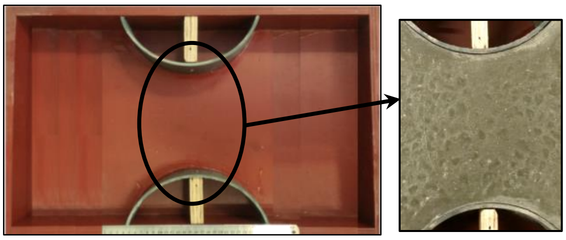

(a) FEA Assumption 1

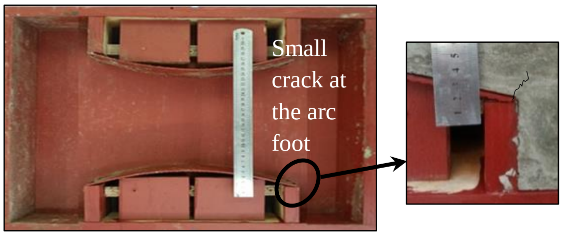

(b) FEA Assumption 2

Figure 3.11: FEA assumptions experimentally tested

If no apparent web indent is present, the horizontal volume change cannot be restricted and no crack forms. This is confirmed by Figure 3.11 (a) which shows a mould with zero web indent length that resulted in no cracking. Figure 3.11 (b) shows the results of the test conducted to substantiate the FEA Assumption 2. An increase in the web width leads to an almost linear increase in the arc peak stress. However, increasing the web width directly, increased the arc foot stress, which resulted in cracking at the arc foot as shown in Figure 3.11 (b).The optimum mould obtained from the FEA for testing was first made out of wood as shown in Figure 3.12. No cracks formed at the arc foot which further substantiate the correctness of the FEA Assumptions 1 and 2. The test results showed a single pure plastic shrinkage crack in the middle of the mould, as required. However, the crack was only 0.7 mm in width, which is smaller than the required 1 mm. This is cause for concern because according to Design Requirement 3 this mould needs to accommodate various concrete mixtures and still manage to induce large and visible plastic shrinkage cracks. The small crack width could be as a result of the mixture not shrinking enough, or the geometry of the experimental wood mould not preventing the shrinkage efficiently.

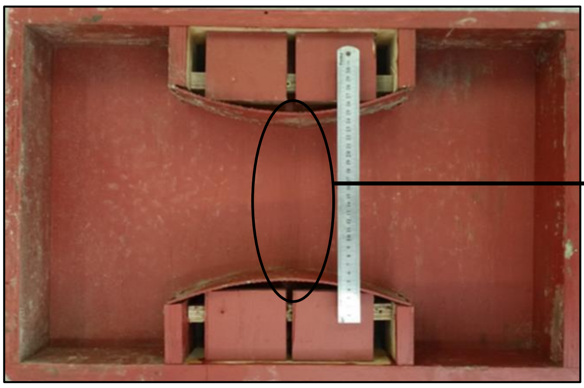

(a) Experimental wood mould

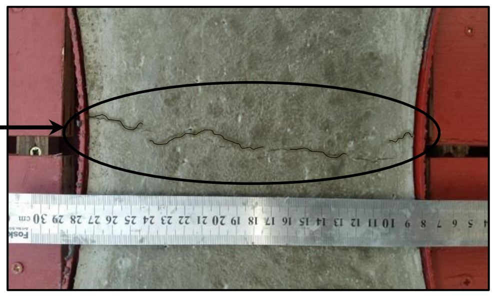

(b) Experimental wood mould final crack

Figure 3.12: Experimental wood mould with 200 mm crack length.

The mixture used for this test was very susceptible to plastic shrinkage which leads to the conclusion that the restraint provided by the geometry of the mould is not sufficient. The only aspect of the mould that can be changed to ensure a more severe crack, is to reduce the length of the crack (width of the web). Making the width of the web smaller will decrease the concrete cross-sectional area and increase the restraint of the mould. Both these aspects will increase the severity of the crack.

3.6. Final mould adjustments

The aspects of the mould that can easily be changed to increase the size of the crack, are the length of the crack as well as the level of horizontal restraint. However, these aspects should not be changed to such an extent that the mould does not comply with the five design requirements. Each of these aspects is discussed in the following sections.

3.6.1. Crack length

An aspect of the mould that can be changed to ensure a more severe crack, is to reduce the length of the crack. This increases the stress induced on the concrete by the mould, thus increasing the severity of the crack. However, the crack length should not be reduced to such an extent that the crack cross section area becomes too small, since this could influence the plastic shrinkage cracking behaviour.

Table 3.2 summarises the crack length and crack cross-sectional area of the three most commonly used mould geometries. Reducing the crack length of the mould from 200 mm to 150 mm still gives a crack cross-sectional area of 15 000 mm^2 which is larger than that of the other moulds as shown in Table 3.2. It is therefore reasoned that this change in crack length is acceptable and does not significantly influence the plastic shrinkage cracking behaviour.

Table 3.2: Crack cross-sectional area of three common mould geometries.

Mould type	Crack length per mould (mm)	Crack formation depth per mould (mm)	Concrete crack cross-sectional area per mould (mm^2)
Beam-like mould	200	35	7000
ASTM slab-like mould	350	35	12250
Ring test	170*	50	8500

*It is assumed that at least a minimum of two crack will for on the surface of the ring

An experiment with the mould made from wood where the crack length was reduced to 150 mm was conducted, using the same concrete mixture exposed to the extreme condition. The mould with its reduced crack length and final crack is shown in Figure 3.13. The results fulfilled the design requirement and showed an average crack width of 1.9 mm compared to the 0.7 mm for the mould with a crack length of 200 mm.

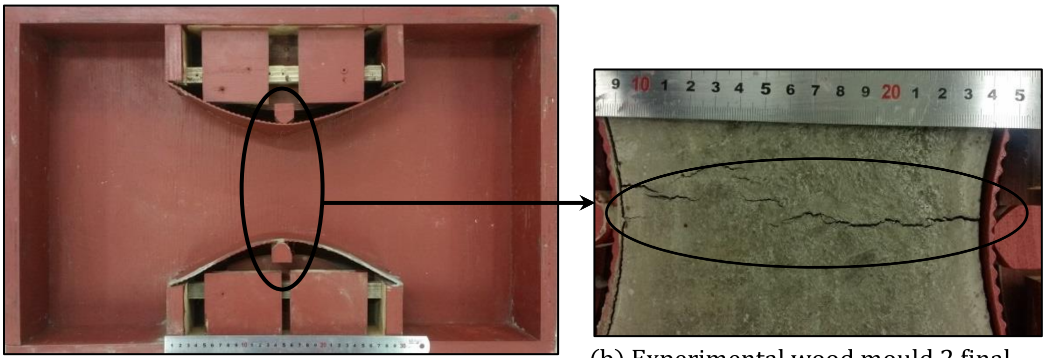

(a) Experimental wood mould 2

(b) Experimental wood mould 2 final crack

Figure 3.13: Experimental mould with 150 mm crack length.

3.6.2. Influence of restraint

To further increase the durability and practicality of this final proposed mould, it was made out of PVC as shown in Figure 3.15. PVC has a much smaller friction coefficient, especially after being painted with mould oil, compared to a wooden mould used for the previous experiments.

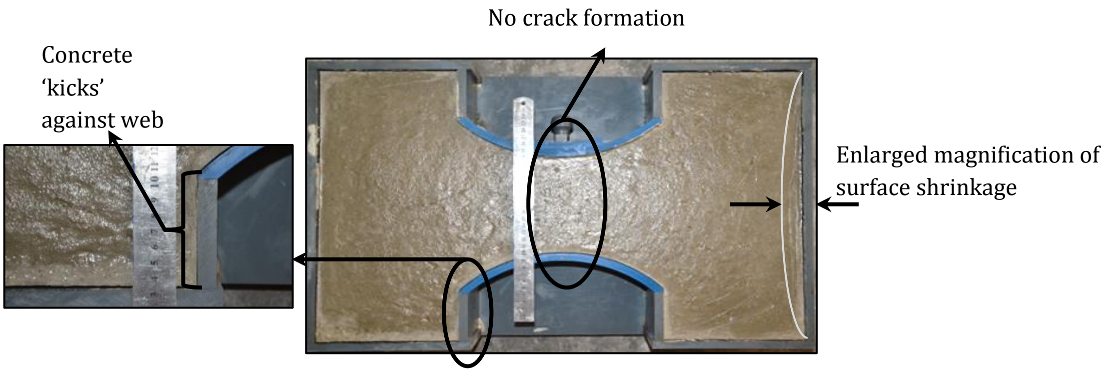

Figure 3.14: Frictionless PVC mould final test results.

Experimental results showed that the PVC mould resulted in no cracks forming due to this near zero friction between the mould and the concrete. This means that as stress rises in the concrete, it is relieved by simply sliding on the bottom surface of the mould as shown in Figure 3.14. Figure 3.14 not only demonstrates the way in which the concrete shrinks away from the side surface, but it also shows how the concrete 'kicks' against the web indent.

To prevent the concrete from sliding on the surface, before stiffening, small 1 x 1 mm right-angled triangular grooves were cut on the bottom surface of the mould - every 5 mm for 140 mm - measured from each side of the mould as shown in Figure 3.15.

The additional friction resulted in an average crack width of 1.5 mm during experiments with the same mix and extreme conditions. In addition, a concrete mixture with a higher bleeding than used previously, was tested in the mould at the same extreme conditions. The results showed an average crack width of 1.2 mm. This is clearly larger than the required crack width of 1 mm and much larger than the average minimum required crack width of 0.5 mm as required by the ASTM C1579.

This verifies the effectiveness of the proposed mould in providing a single pure plastic shrinkage cracking, even for concrete mixes with a high bleeding and therefore reduced potential for plastic shrinkage cracking. However, the grooves used as a restraint in the proposed mould, proved to be difficult to cut onto the surface of the mould and to be cleaned ultimately after testing. This led to the need for more effective and practical implementation of restraint.

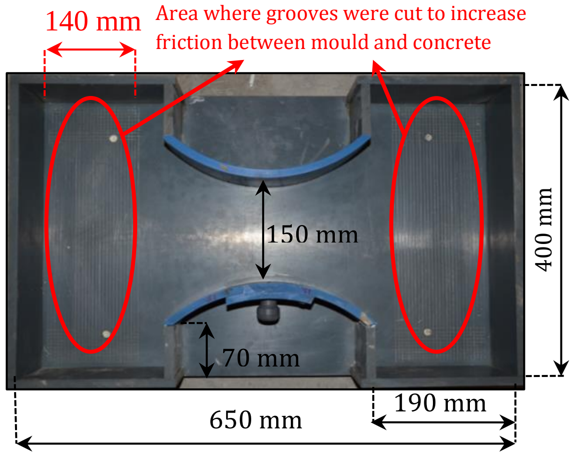

Figure 3.15: Proposed mould with grooves to increase restraint.

After testing different types and degrees of restraint the final mould as shown in Figure 3.16 is proposed. The use of three triangular shaped PVC blocks on each side, proved to be a practical solution to provide restraint while complying with all the mould design requirements. For the same concrete mixture, susceptible to plastic shrinkage cracking, the final mould resulted in a final crack width of 1.6 mm.

Finally, to further improve the mould, a removable side door was added to monitor the formation of the crack from the side. The side door can be removed before the crack starts to form. This point in time corresponds to initial setting. This allows the simultaneous monitoring of the crack formation from the top and from the side, which can ultimately provide valuable insight into the cracking behaviour.

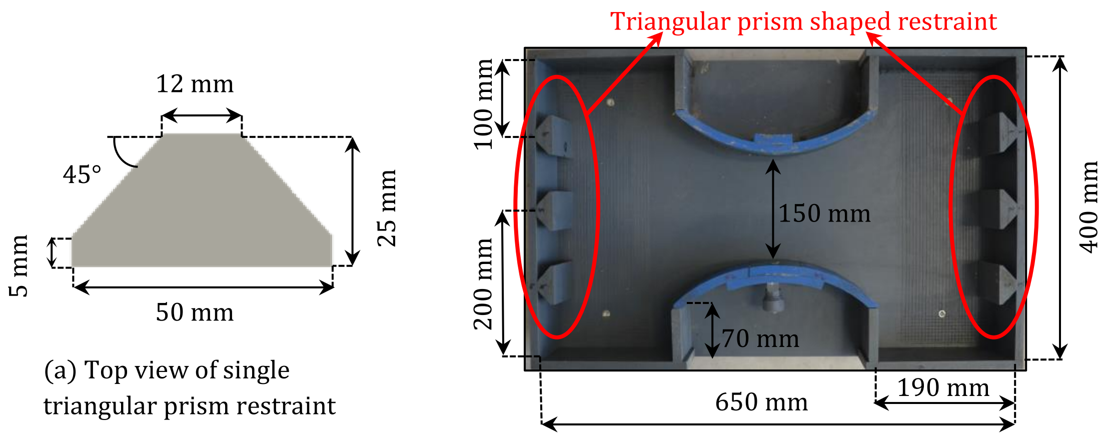

(a) Top view of single triangular prism restraint

Figure 3.16: Final proposed mould with triangular prism restraint.

An example of such a step-by-step crack formation is shown in Figure 3.17. The figure shows that the formation of the crack was sudden, where most of the crack growth occurred between 120 minutes and 145 minutes after casting. The figure also suggests that the formation of the crack was almost immediately through the depth of the concrete and not gradually from the top to the bottom as would be expected. Such conclusions and investigations on the behaviour of pure plastic shrinkage cracking are now possible with this new mould.

(a) Propagation of cracking as seen from the top

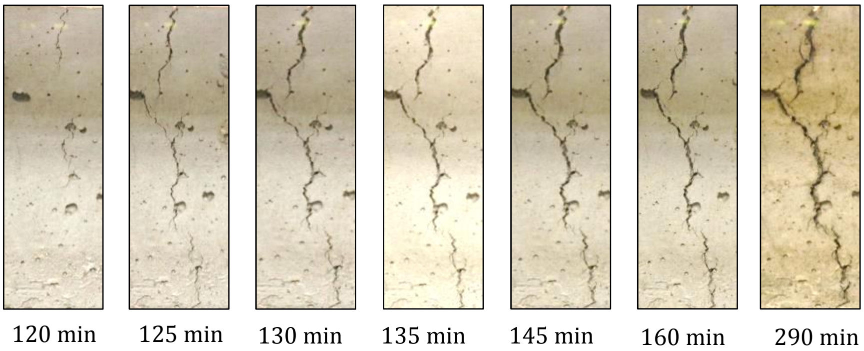

(b) Propagation of cracking as seen from the side

Figure 3.17: Plastic shrinkage cracking monitored in the final proposed mould.

3.7. Concluding summary

This chapter consists of preliminary experimental tests followed by the optimising of the mould geometry using FEA. The assumptions made in the FEA are also verified by experiments, where after a new mould is proposed that can induce a single pure plastic shrinkage crack. This chapter showed that there exist numerous variables that have an influence on the design of a mould and the cracks it induces. Regardless of this, the final mould as shown in Figure 3.16 was designed using FEA along with experimental tests. This mould met all the design requirements and is suitable for the testing of pure plastic shrinkage cracking.

Chapter 4 : Experimental framework

This chapter contains all the information on the plastic cracking tests conducted in this study. Firstly, all the test apparatus and moulds used are discussed in detail. This is followed by a description of the test setup, measurements and methods used. Then information regarding all the materials, climate conditions, mixture proportions and other principal mixture properties is given. Lastly, a summary of the test program that was followed throughout this study is given.

4.1. Climate chamber

To ensure all tests were done under controlled climate conditions, all test specimens were placed and monitored in the climate chamber as shown in Figure 4.1. The climate chamber can simulate extreme environmental conditions that equal evaporation rates as high as 2.5 kg/m^2/h. The latter is a combination of wind speeds of 70 km/h, an ambient air temperature of 50 °C and a relative humidity of 10 %. For the purpose of this study, these climate condition ranges are more than sufficient. More information on the climate chamber can be obtained from this source (Combrinck, 2011).

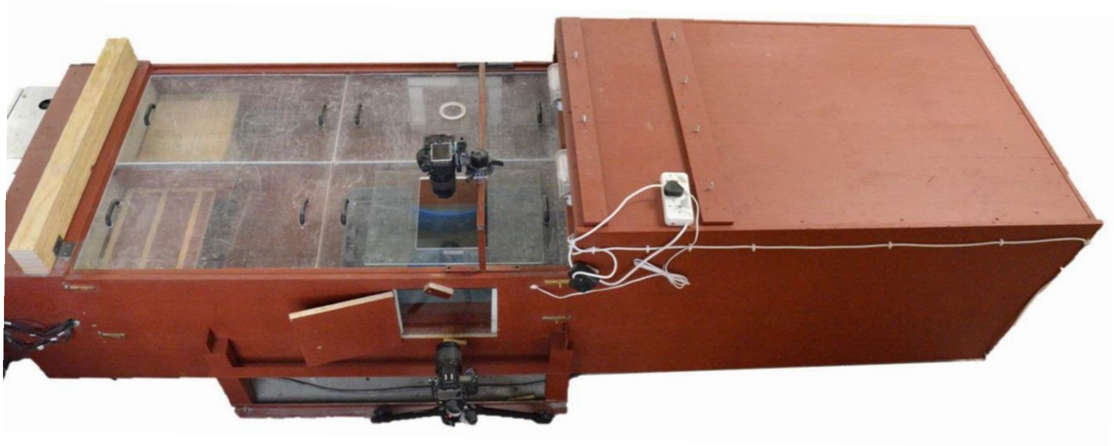

Figure 4.1: Climate chamber used with camera setup.

4.2. Experimental moulds

To increase the durability and practicality, all moulds were made out of PVC, unless stated otherwise. Mainly two types of moulds were used in this study. These two mould types can be divided into either cracking related moulds or moulds determining selected properties of the concrete mixtures. A description of these moulds and their respective purpose and geometry is given in the following sections.

4.2.1. Plastic cracking

The majority of tests that were done in this study used the plastic cracking mould as shown in Figure 4.2. The mould makes use of a dog-boned shape along with side triangular restraints (Figure 4.2 a) to restrict the horizontal shrinkage of the concrete mixture. The formation of the crack in the centre of the mould can be monitored from the top and from the side. The mould has a built-in side door which can be removed after the concrete is stiff enough. Not only can this mould be used to study plastic shrinkage cracking, but also plastic settlement cracking as well as a combination of the two. Figure 4.2 (c) shows the mould with an embedded steel rod at a depth of 25 mm. The steel rod is fully fixed at the wall of the web as shown in Figure 4.2 b. This is to prevent any vertical displacement of the steel rod before and after the removal of the side door, to ensure no disturbances to the crack formation.

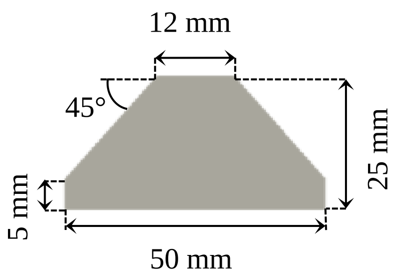

(a) Top view of single triangular prism restraint

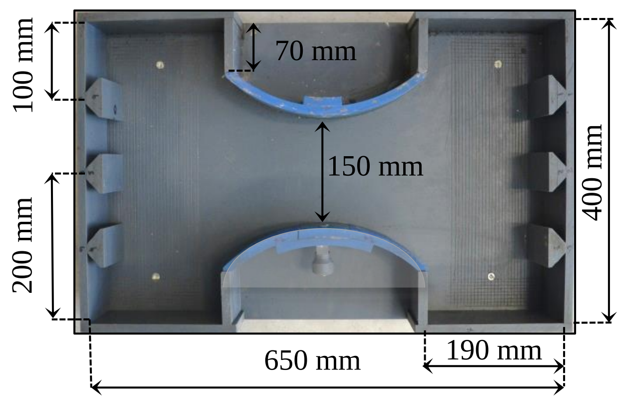

(b) Plastic cracking mould

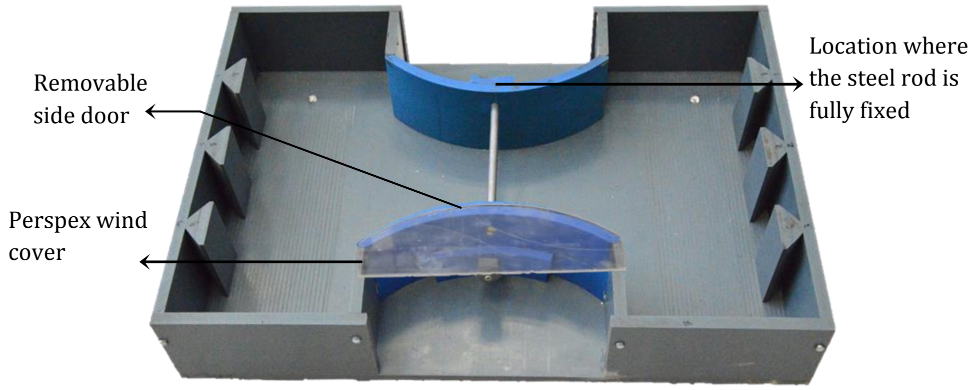

(c) Plastic cracking mould with embedded steel rod

Figure 4.2: Plastic cracking mould.

The effect of depth on plastic cracking is an important aspect that is investigated in this study. Variations in the height of the mould as shown in Figure 4.2 include 100, 150 and 200 mm. All the other dimensions stay constant when varying the overall depth of the mould. Further information regarding the design of the mould can be found in Chapter 3.

4.2.2. Shrinkage and settlement

The shrinkage and settlement of the plastic concrete are measured in a mould with dimensions of 300 x 300 x 100 mm. As for the cracking mould, the height of the shrinkage and settlement moulds include 100, 150 and 200 mm. The mould also consists of an LVDT holder for the shrinkage and settlement measurements. The shrinkage is measured with the use of embedded anchors, while the settlement is measured using a wire lattice, placed on the surface of the concrete.

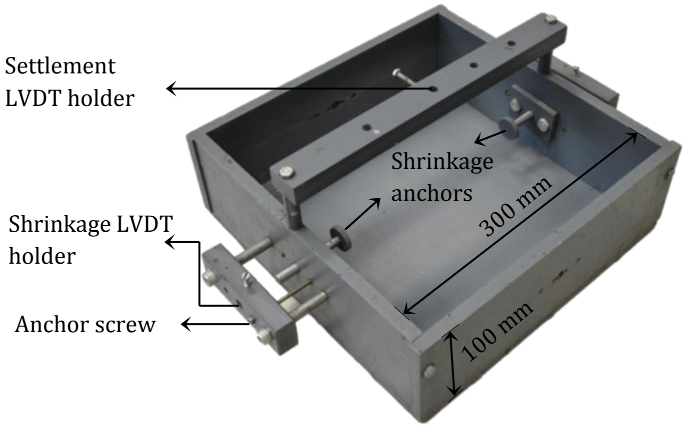

Figure 4.3: Shrinkage and settlement mould.

4.2.3. Capillary pressure

The capillary pressure in the plastic concrete is measured in a mould with dimensions of 300 x 300 x 100 mm. As for the cracking mould, the height of the capillary pressure moulds included 100, 150 and 200 mm. The mould also consists of a hollow steel tube and a capillary pressure sensor which is connected to a data acquisition programme.

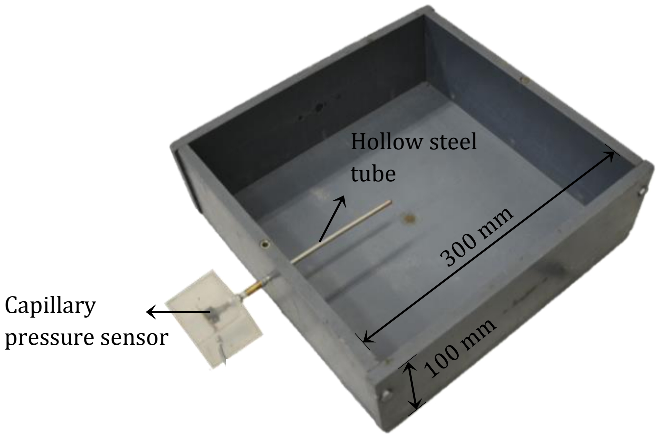

Figure 4.4: capillary pressure moulds.

4.2.4. Setting times

The setting times in this study were measured according to the EN 196-3 (2005) standard. The Vicat apparatus, concrete mould and setting needles are shown in Figure 4.5. The Vicat apparatus makes use of two needle types namely, initial set needle and final set needle, as shown in Figure 4.5.

4.3. Measuring methods

This section entails a description of the different measuring methods used in this study. Each of the moulds, presented in the previous section has a systematic measuring method to obtain the required results. The methodology used for each measuring method is given in the following section.

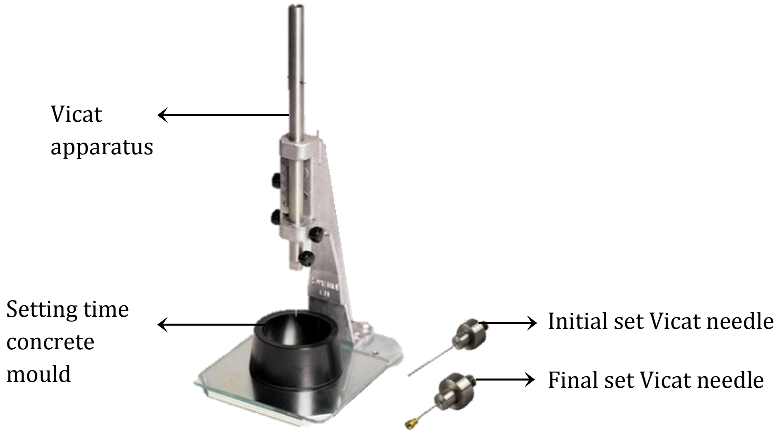

Figure 4.5: Setting time apparatus.

4.3.1. Average crack width

After the two specimens were placed in the climate chamber, two digital cameras were strategically placed above and on the side of the specimen as shown in Figure 4.6. The images were taken automatically through glass windows, using Interval Timer Shooting (ITS) with a general time interval of 30 seconds. This proved to be sufficient for all the standard tests in monitoring the crack throughout its development. For selected tests, the time interval was reduced to 15 seconds. These photo sequences were used to create videos to visually track the formation of the crack.

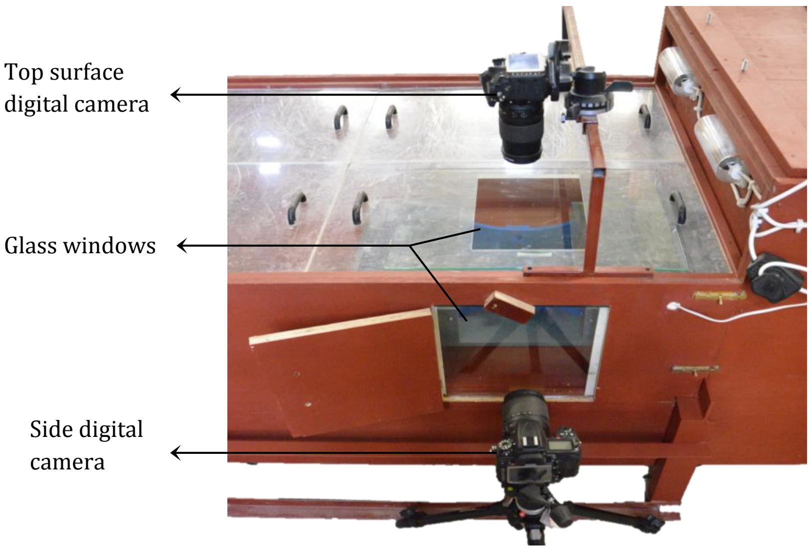

Figure 4.6: Plastic cracking mould test setup.

Glass windows were used to cover the holes to ensure the environmental conditions in the climate chamber remained constant. The ITS for the top camera was activated as the specimens were placed in the climate chamber while the side camera was only activated once the side door was removed.

The side door was only removed once the concrete was stiff enough. This varied for different concrete mixtures and climate conditions. A good estimation of when the side door can be removed, is the time the concrete starts to pull away (shrink) from the side of the mould. Once the side door was removed, a Perspex cover was placed on the web as shown in Figure 4.2. The purpose of the Perspex cover was to minimise water evaporation from the side surface, especially as a result of the wind, once the door was removed.

The average crack width was calculated from high-resolution digital images using a Digital Image Processing Program (DIPP). The DIPP used was ImageJ IJ 1.46r (2012). An example of how the DIPP converts a raw image into a greyscale version is shown in Figure 4.7. Firstly, the digital image is scaled according to its true size. Then 10 mm was removed from each side of the crack to account for the influence of the side wall effect. The ASTM C1579 prescribes the removal of 25 mm from each side but it was found that 10 mm is sufficient. Using a tracing tool to select the crack (white area) the DIPP returns the area of the selected crack section. This area is then divided by the total crack length to obtain the average crack width for the required crack section. The average crack width of two specimens were taken per test, unless stated otherwise.

(a) Raw final surface crack

(b) Processed final surface crack

Figure 4.7: Average surface crack width measuring example

4.3.2. Capillary pressure

The capillary pressure was measured using a metal tube connected to an electronic capillary pressure sensor. The capillary pressure sensor was then connected to a data acquisition programme which took a measurement every second. The capillary pressure was measured using the same test method as followed by Combrinck (2016), which he adopted from Slowik et al. (2008).

Firstly, the metal tube was connected to a pressure sensor and then filled with distilled water. The metal tube was carefully filled using a syringe and a needle. A small piece of sponge was inserted at the tip of the metal tube to prevent concrete from entering the metal tube while the mould was filled and consolidated. After the mould was filled with concrete to just below the electronic capillary pressure tube hole, the tube was inserted into the mould. The mould was then further filled to the top and consolidated on a standard vibrating table. After the mould was placed in the climate chamber, it was connected to the data acquisition programme. For the 100 mm deep mould, the sensor was placed at a depth of 50 mm. For the 200 mm deep mould capillary pressure tubes were placed at depths of 50, 100 and 150 mm. An average of three capillary pressure moulds were used per test, unless stated otherwise.

4.3.3. Shrinkage and settlement

As for the capillary pressure, the shrinkage and settlement were measured using the same test method as followed by Combrinck (2016), which he adopted from Slowik et al. (2008).

The shrinkage was measured using spring loaded LVDTs (Linear variable differential transformer) that were connected to a data acquisition programme which took measurements every second. For the 100 mm shrinkage mould, two LVDTs were used per mould — one each on opposite sides of the mould placed at a height of 50 mm. For the 200 mm deep mould, six LVDTs were used per mould, one each on opposite sides of the mould placed at a height of 50, 100, or 150 mm.

The LVTDs were connected to shrinkage anchors as shown in Figure 4.3. A screw was used to hold the shrinkage anchor in place while filling, consolidating and placing the mould in the climate chamber. Once the mould was placed in the climate chamber and after the LVDTs were connected and screwed in place, the screws keeping the anchors in place were loosened. From this point in time the shrinkage anchors were free to move as the concrete shrunk. The shrinkage was also measured on the surface of the concrete. Digital images were taken every 20 minutes on opposite sides (above the shrinkage anchors) of the mould.

The settlement was measured using non-spring loaded LVDTs. One settlement LVDT was used per mould as shown in Figure 4.3. After filling, consolidating and placing the mould in the climate chamber the LVDT was screwed to a wire lattice which was then placed on the top of the concrete's surface. A wire lattice was used to allow bleed water to pass through it without influencing the settlement results. The same process was followed for the 100 and 200 mm deep moulds. The average of three settlement and shrinkage moulds were used per test, unless stated otherwise.

4.3.4. Setting times

The standard ASTM C403 (2008) method can be used to calculate the setting times of normal concrete mixtures. However, the method used in this study to calculate the setting times was done according to the standard EN 196-3 (2005). This is due to the size and difficulty in preparing samples for the ASTM C403 (2008) method compared to the EN 196-3 (2005) method. Not only is the EN 196-3 (2005) method more practical, but its results do not differ significantly from the ASTM C403 (2008) method (Combrinck, 2016).

Preparing a sample for the EN 196-3 (2005) includes sieving the fresh concrete mixture through a 4.75 mm sieve. This is to ensure no large aggregate (> 4.75 mm) obstructs the penetration needle from entering the sample. A Vicat apparatus is then used to test the penetration resistance of the sieved concrete sample. The initial set is reached when the initial set needle penetrates the concrete to a depth of 6 ± 3 mm from the bottom. The final set is reached when the outer ring of the final set needle no longer leaves a mark on the concrete surface.

4.4. Test procedure

The same mix procedures were followed throughout the entire test program spanning over a ten month period. One day before a test, the material would be measured and stored in a climate controlled room at a constant temperature of 23 °C and a relative humidity of 65 %. For all the tests either a standard 25-litre and/or 50-litre pan mixer was used.

Before the dry constituents were added to the concrete mixer, the pan was rinsed with water to prevent absorption of mixing water and contamination of previous experiments. The inside of the pan was wiped with a paper towel to remove any excess water. The dry material was then added to the pan mixer in the order of sand, cement and stone. After the dry material was added to the mixer and mixed for one minute to thoroughly disperse all the dry material, water was steadily added at a constant rate. The concrete was then mixed for a further three minutes. A total mixing time of four minutes proved to be sufficient and is in accordance with SANS 2001-CC1:2007.

After the concrete was mixed a hand shovel was used to fill the moulds. The moulds were then placed on a vibrating table and vibrated until no more air bubbles appeared on the surface. This process usually took between three to four minutes. For the 200 mm deep plastic cracking mould, a poker vibrator was used for consolidation because of the weight of the mould exceeding the weight capacity of the vibrating table.

After the concrete was placed in the mould and vibrated, the surface was gently levelled using a steel trowel. The moulds were then transported to the climate chamber which was switched on two hours prior to mixing. This was done to ensure the chosen climate conditions were stable. From adding the water to the dry material to placing the moulds in the climate chamber took between 15 to 20 minutes. However, all the tests measurements started only the instant the moulds were placed in the climate chamber at time.

4.5. Materials

The same materials were used throughout all the experimental tests spanning over a ten-month period and their respective properties are illustrated in Table 4.1. Two types of fine aggregates (< 4.75 mm in size) were used namely, a natural pit sand, known locally as Malmesbury sand and crusher dust.

Table 4.1: Material properties.

	Material properties			
	Relative density	Fines modulus	Dust content (%)	Particle shape
CEM III/A-S 42.5 N	3.05	-	-	-
13 mm stone	2.71	-	0.36	Angular
Crusher dust sieved through a 2.36 mm sieve	2.7	3.42	7.8	Angular
Natural pit sand	2.6	2.69	7	Round

The pit sand used was formed by water erosion and is abundantly found in the Western Cape region of South Africa. The particles of the sand are round and the sand has a fine modulus of 2.69 and dust content of 7 %. The crusher dust is a by-product gathered from the crushing of Greywacke stone. The crusher dust particles have an angular shape due to this crushing process. The crusher dust has a fine modulus of 3.42 and dust content of 7.8 %. Both sands are fairly well graded as shown in Figure 4.8. The grading of the fine aggregate was done in accordance with SANS 1083 (2002).

The Greywacke stone used in this study had a nominal particle size of 13 mm. The greywacke stone is made up of a variety of sandstone types and this larger stone is then further crushed to achieve its required size. The angular shape of the stone is a result of this artificial crushing process. The grading of the stone was done in accordance with SANS 1083 (2002) and is shown in Figure 4.9.

The stone has a good grading with a fine and dust content of 0.1 % and 0.36 % respectively. CEM III/A-S 42.5 N cement was used throughout this study. The cement has a blast furnace slag content of between 35 % and 65 % as specified by the supplier.

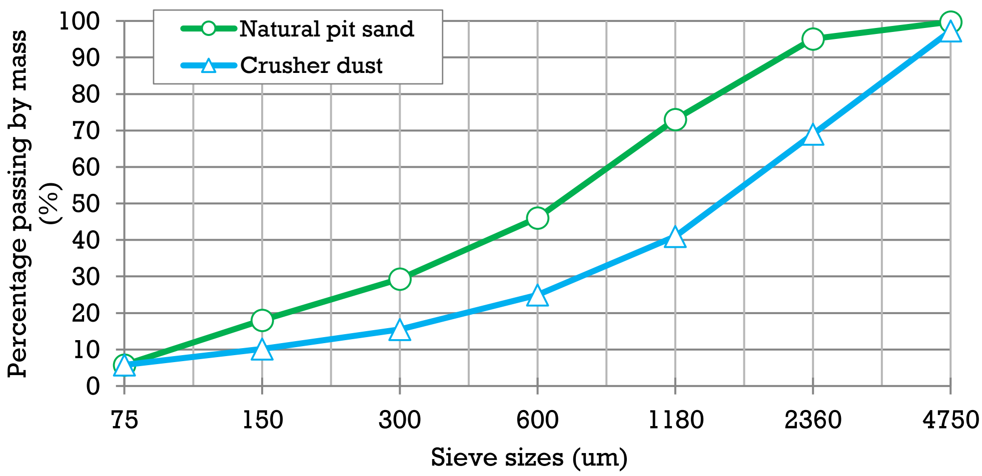

Figure 4.8: Sieve analysis of fine aggregate (sand).

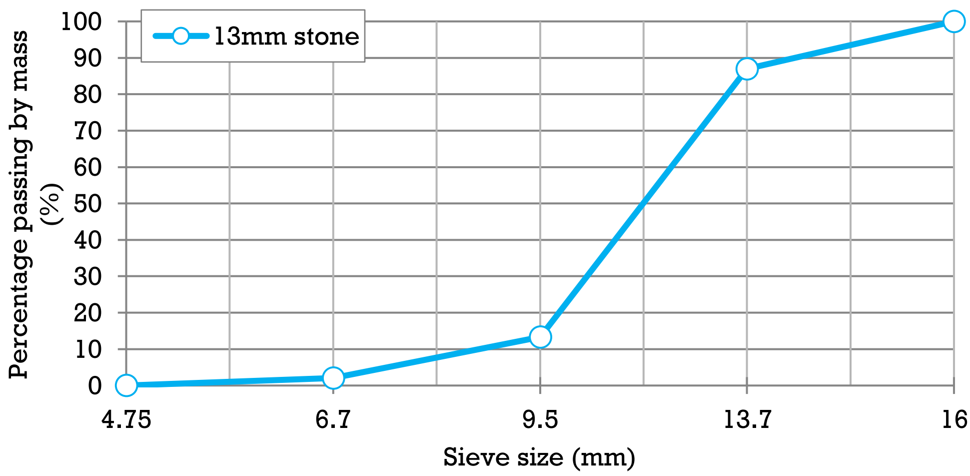

Figure 4.9: Sieve analysis of coarse aggregate (stone).

4.6. Mixes and climate conditions

In this study, two concrete mixtures were used along with three different climate conditions. The two mixes are referred to as the Normal Bleeding Mix (NB-Mix) and High Bleeding Mix (HB-Mix) as shown in Table 4.2. The mixes were chosen to represent similar mixes that were used in the industry for floor and slab construction. The NB-Mix has a smaller slump with lower bleeding compared to that of the HB-Mix. The NB-Mix is designed to be more prone to plastic shrinkage, while the HB-Mix is more prone to plastic settlement.

Three different climate conditions were used in this study and are characterised as either being extreme, medium or normal as indicated in Table 4.3. These climate conditions with their respective evaporation rates, were specifically chosen to cover a broad range of climate conditions as it is encountered in South Africa. The evaporation rate of the climate conditions ranges from 1.11 kg/m^2/h for the extreme climate Climate E, to 0.26 kg/m^2/h for the normal climate, Climate N. The evaporation rates were calculated using Equation 2-1. The respective temperatures, relative humidity and wind speeds were controlled in the climate chamber and they were kept at a constant throughout the experiments.

Table 4.2: Mixture constituents and properties.

Mixture type	NB-Mix	HB-Mix
Mix constituents (kg/m^3)		
CEM III/A-S 42.5 N	342	342
Water	205	205
Natural pit sand	605	847
13 mm greywacke stone	950	950
Crusher dust sieved through a 2.36 mm sieve	342	100
Mixture properties		
Slump (mm)	75	125
28 day strength (MPa)	37.7	35.2
w/c ratio	0.6	0.6

Table 4.3: Climate conditions.

		Evaporation properties			
Climate type	Evaporation rate kg/m^2/h	Concrete temperature (°C)	Ambient temperature (°C)	Relative humidity (%)	Wind speed (km/h)
Climate E	1.11	23	40	10	23
Climate M	0.56	23	40	20	16
Climate N	0.26	23	30	40	8

4.7. Test program

This section entails a brief description of the different tests and their respective objectives that were done in this study. All the different tests that were done in this study were designed to isolate and study a specific objective. The objectives can be divided into six sections.

Objective 1: Plastic shrinkage cracking

The purpose of this objective was to study the formation of a plastic shrinkage crack without the influence of differential settlement. Chapter 3 outlines the process that was followed in designing a mould which was used to study plastic shrinkage cracking. Climate and the concrete mixtures were varied for this objective.

Objective 2: The effect of depth on plastic shrinkage cracking

The purpose of this objective was to study the formation of a plastic shrinkage crack with variation in the cross-sectional depth of the concrete. In this section three different concrete depths were tested namely, 100, 150 and 200 mm.

Objective 3: Interaction between plastic shrinkage and settlement cracking

The purpose of this objective was to study the interaction between plastic shrinkage and settlement cracking. The cover depth was varied along with climate, the concrete mixture and overall concrete depth.

Objective 4: Settlement, shrinkage, capillary pressure and setting time

The purpose of this objective was to study the material properties which included settlement, shrinkage, capillary pressure and setting time. Mainly three aspects were varied namely, climate, mixture type and concrete sectional depth.

Objective 5: Effect of restraint

The purpose of this objective was to study the effect of various degrees of restraint on plastic cracking. The degree of differential settlement was varied along with the restraint located on the sides of the mould.

Objective 6: Effect of finishing operations on plastic cracking

The purpose of this objective was to study the effect of finishing operations on plastic cracking. Its effect on plastic shrinkage cracking and a combination of settlement and shrinkage cracking were studied. The time the finishing operation was applied was also varied and investigated.

Table 4.4 contains a summary of the various objectives used along with their respective mixes, climate conditions and moulds.

Table 4.4: Summary of the experimental plan.

Objective	Climate conditions	Mixture type	Mould type
Plastic shrinkage cracking	Climate E, M and N	NB-Mix and HB-Mix	100 mm deep plastic cracking mould (without an embedded steel rod)
The effect of depth on plastic shrinkage cracking	Climate E	NB-Mix	100, 150 and 200 mm deep plastic cracking mould (without an embedded steel rod)
Interaction between plastic shrinkage and settlement cracking	Climate E and N	NB-Mix and HB-Mix	100 and 200 mm deep plastic cracking mould (selected tests with an embedded steel rod)
Settlement, shrinkage, capillary pressure and setting time	Climate E, M and N	NB-Mix and HB-Mix	Shrinkage and settlement mould, capillary pressure mould and Vicat penetration moulds
Effect of restraint	Climate E	NB-Mix	100 and 200 mm deep plastic cracking mould (without an embedded steel rod)
Effect of finishing operations on plastic cracking	Climate M	NB-Mix	100 mm deep plastic cracking mould (selected tests with an without embedded steel rod)

4.8. Concluding summary

This chapter contains information regarding all the different types of tests that were done in this study. The different types of moulds that were used are presented first, followed by their respective measuring methods and procedures. The mixes, materials and climate conditions that were used for all the experiments are then discussed. Finally, the test program that was used and followed is presented.

Chapter 5 : Experimental results and discussion

The focus of this chapter is on the fundamental behaviour of pure plastic shrinkage cracking in concrete. The term pure plastic shrinkage cracking refers to plastic shrinkage cracking without the influence of any initial settlement cracks. Furthermore, to fully understand plastic cracking the interaction between plastic settlement and shrinkage cracking is also considered while varying the depth. Lastly, the implementation and effectiveness of finishing operation in preventing plastic cracking are considered.

All the results discussed in this chapter were obtained from experiments conducted over a ten-month period at the University of Stellenbosch.

5.1. Plastic shrinkage cracking

The objective of these tests was to observe and ultimately describe the formation of a pure plastic shrinkage crack without the influence of an initial weak spot created through differential settlement. The moulds used in these tests included the plastic cracking mould, shrinkage and settlement mould as well as the capillary pressure mould. Three different climates were used in combination with two concrete mixtures.

5.1.1. Crack formation characteristics

Figure 5.1 shows the average crack width of a pure plastic shrinkage crack for the NB-Mix in Climate E, together with its mixture properties such as shrinkage, settlement and capillary pressure, all a function of time. The average crack width is scaled according to the left-hand axis in millimetres while the right-hand axis scales the average settlement and shrinkage strain in millimetres per meter together with the negative capillary pressure in kPa.

After the samples were consolidated and placed in the climate chamber, the denser solid mix constituents started to settle. The rate of settlement up until just before 50 minutes was gradual at first and then it tended to decrease at around 50 minutes as seen in Figure 5.1. As the negative capillary pressure started to rise, the settlement rate changed and further increased. The capillary pressure build-up causes suction within the concrete water pore system, which pulls the solid particles closer to one another.

The forces acting on the solid particles act both horizontally and vertically. The additional settlement (from 60 minutes onwards) can be explained through these forces. At a certain point in time, the volume change can no longer be relieved through vertical and horizontal shrinkage and then local air entry occurs. This is indicated by the peak capillary pressure value at around 127 minutes. This also coincides with the maximum settlement as observed by Slowik et al., (2008).

The horizontal shrinkage was measured at a depth of 50 mm, which coincides with the middle of the concrete section. The horizontal shrinkage at a depth of 50 mm started after the capillary pressure started to rise and before the pure plastic shrinkage crack formed.

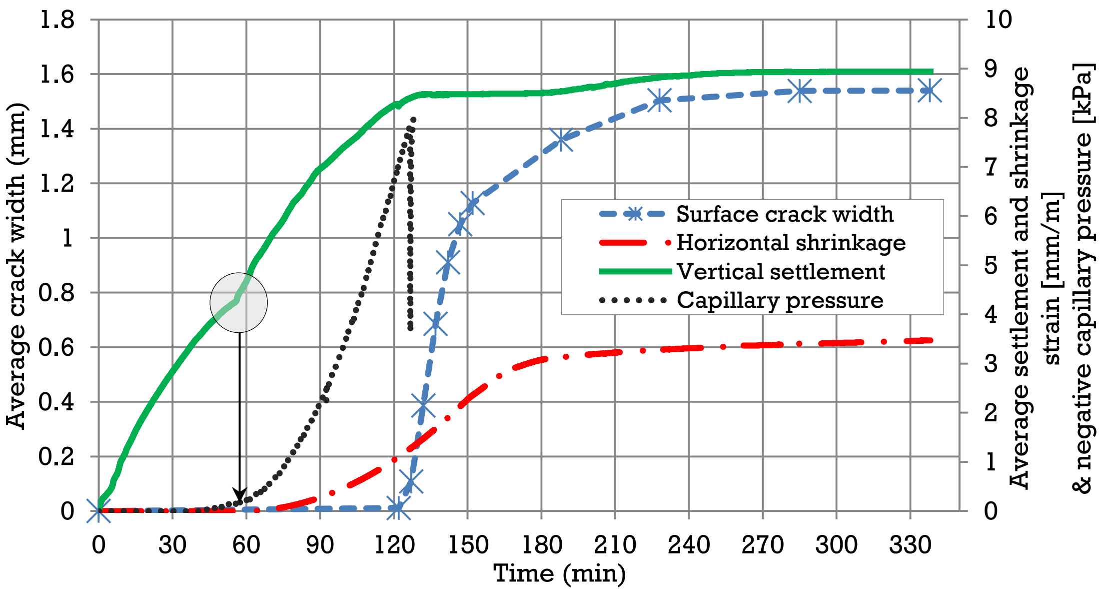

Figure 5.1: Plastic shrinkage cracking results in the 100 mm deep mould with the NB-Mix in Climate E.

Capillary pressure and horizontal shrinkage are much better observed when varying the depth, and are further discussed in Section 5.1.3. For now, it can be said that capillary pressure build-up and horizontal shrinkage coincide, but a drop in capillary pressure does not necessarily coincide with the formation of the pure plastic shrinkage crack. The formation of the pure plastic shrinkage crack was also rapid and the majority of the surface crack formation occurred within a 15 minute time period.

Figure 5.2 shows the formation of the crack not only from the surface but also from the side. Not only does Figure 5.2 present average crack width measurements, but also high-quality digital images taken from the side after the side door was removed. The average crack width measurements from the side are further split up into the top quarter and the bottom three quarters of the crack.

This provides valuable information regarding the principal formation of the pure plastic shrinkage crack through the concrete depth. The results show that a pure plastic shrinkage crack does not form from the top to the bottom as one would expect. In the initial plastic shrinkage phase, as indicated in Figure 5.2, the average crack width of the surface, side bottom three quarters and side top quarter, all had the same average crack widths. This substantiates that the initial formation of the crack is uniform and sudden throughout the entire height of the concrete section.

It is only from Time B, shown in Figure 5.2, and onwards that the average width of the crack changes along the height of the concrete section. The top quarter of the side has an average final width of 1.4 mm compared to 0.8 mm for the bottom three quarters for the final crack, as shown at Time E. The initial hairline cracks that can be seen at Time A and B form randomly over the height of the section on the path of the final crack seen at Time E. It is important to realise that the formation of a pure plastic shrinkage crack is sudden through the concrete section and not from the top to the bottom. This can be an explanation for cases where plastic cracks appear suddenly without any initial warning signs.

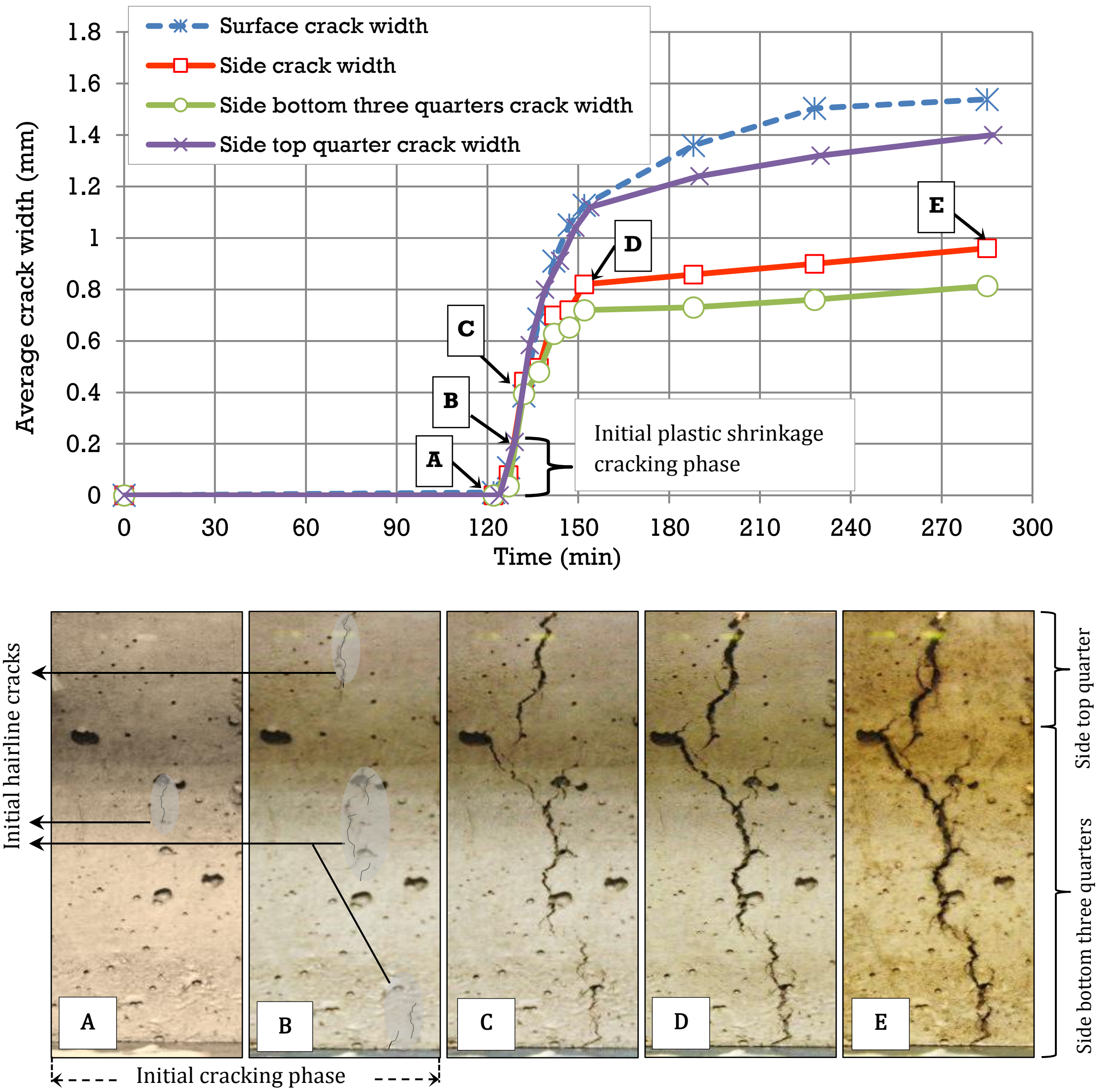

Figure 5.2: Cracking results for the NB-Mix exposed to Climate E along with digital images of the crack as seen from the side at selected times.

The formation of the pure plastic shrinkage crack exhibited similar behaviour for the NB-Mix exposed to Climates M and N. The formation of the pure plastic shrinkage crack in Climate M and N together with the mixture properties such as shrinkage, settlement and capillary pressure are shown in Figure 5.3 and 5.4. Figure 5.3 and 5.4 also contain a digital image of the final crack as observed from the side.

For Climates M and N the pure plastic shrinkage crack started to form at 150 min and 245 minutes respectively, compared to the 125 min for Climate E. As the evaporation rate is reduced by testing at Climates M and N, the build-up of capillary pressure takes longer and shrinkage through the concrete section is delayed. Not only does the formation of the pure plastic shrinkage crack take longer to form at reduced evaporation rates, but the severity of the crack is also reduced.

However, even when the evaporation rate is reduced, the initial crack formation remains sudden through the concrete section. Figures 5.3 and 5.4 also shows an image of the final crack, as seen from the side.

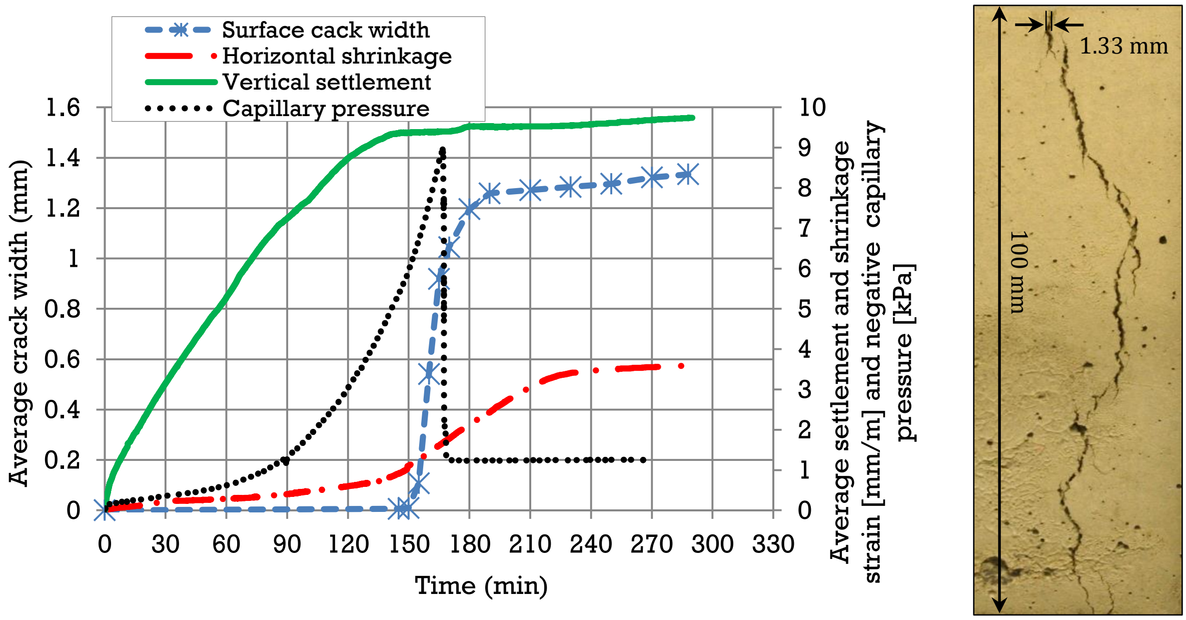

Figure 5.3: Plastic shrinkage cracking results for the NB-Mix in Climate M along with a digital image of the final crack width as seen from the side.

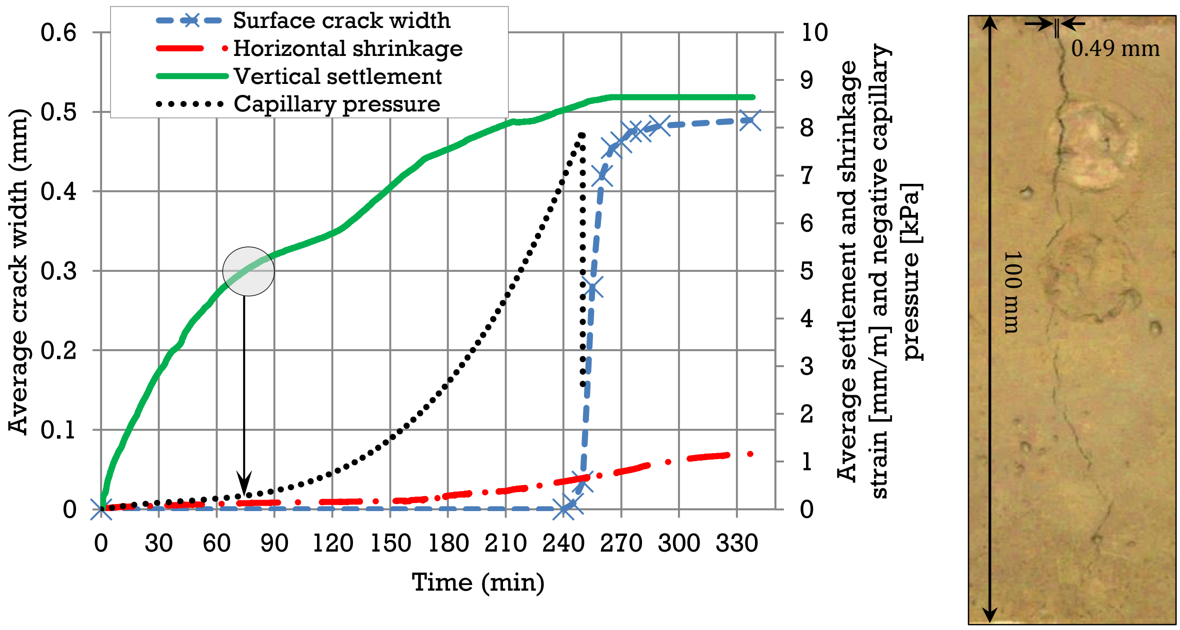

Figure 5.4: Plastic shrinkage cracking results for the NB-Mix in Climate N along with a digital image of the final crack width as seen from the side.

The effect of the capillary pressure build-up on the settlement can again be seen when considering Climate N as indicated by the shaded circle in Figure 5.4. As discussed for Climate E, the capillary pressure build-up causes suction within the concrete matrix which pulls all the solid particles closer to one another, which results in additional vertical settlement. For the NB-Mix at Climates N and M, air entry also coincides with the maximum settlement. Monitoring the crack from the side for Climates M and N showed similar crack formation characteristics as indicated in Figure 5.2 for Climate E. The average crack width decreased while the time of initial crack formation increased with an increase in evaporation rate.

Monitoring the settlement for the NB-Mix in the different climates also provides important information. The initial settlement in Climate E occurred at 50 minutes compared to 77 minutes for Climate N, with respective strains of 4.09 mm/m and 5 mm/m. The initial settlement is also influenced by the evaporation rate, as high evaporations can lead to drying of the concrete matrix before its actual initial setting time, which is known as the time settlement ceases. As the time of initial settlement is reduced by a high evaporation rate (early drying) the time where settlement occurs due to capillary pressure forces, is earlier when compared to lower evaporation rates such as Climate N.

The pure plastic shrinkage crack for the HB-Mix exposed to Climate E, also showed the same formation characteristics as those described for the NB-Mix as shown in Figure 5.5. The crack formed at 165 minutes compared to 122 minutes for the NB-Mix in Climate E. The final crack width of the HB-Mix (0.85 mm) was smaller when compared to the NB-Mix (1.54 mm) when exposed to Climate E. This was as expected since the HB-Mix could delay the capillary pressure build-up for a longer period of time with a higher rate of settlement which results in more bleeding. As the initial crack occurred at a later stage, the severity of the initial plastic cracking phase as shown in Figure 5.2 and the time where it could further widen the crack before the final setting time, was reduced.

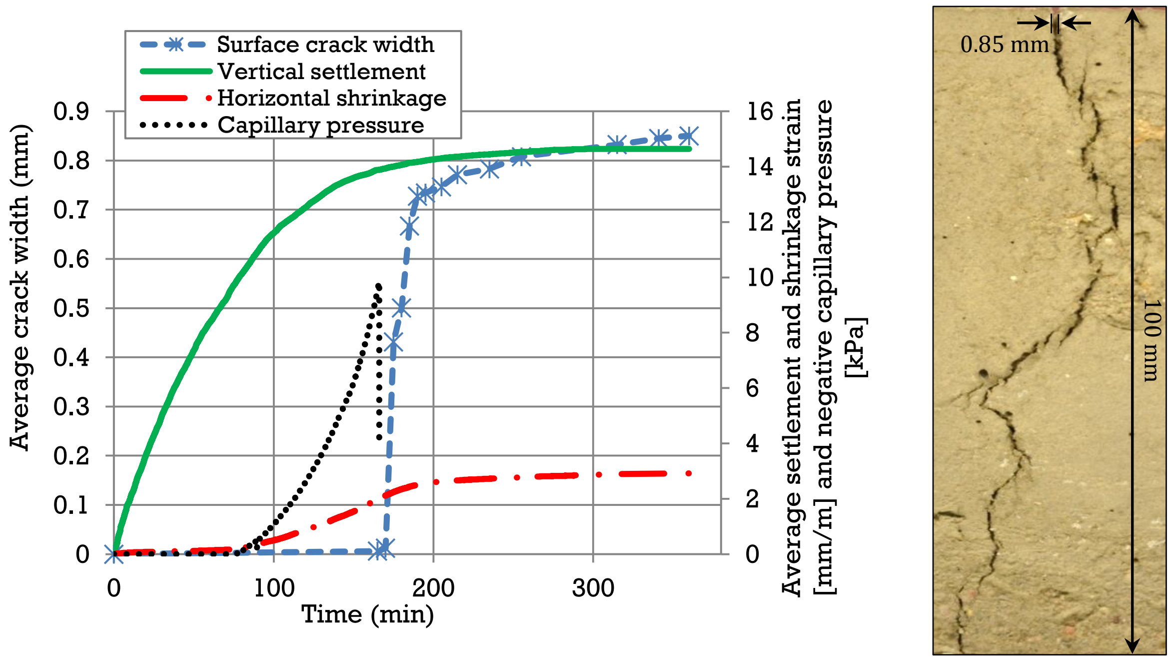

Figure 5.5: Plastic shrinkage cracking results for the HB-Mix in Climate E along with a digital image of the final crack width as seen from the side.

5.1.2. Setting times

Setting times has generally been used to indicate the phase concrete finds itself in. In this study, setting times were measured in two ways: covering and exposing the sample to only temperature (no evaporation) and a combination of temperature, wind and relative humidity. It was clear that there is a difference between drying and hydration. Hydration is responsible for the strength of concrete. Drying occurs as water evaporates from the surface which influences the penetration resistance measured with the Vicat apparatus. This leads to earlier setting times which do not necessarily mean hydration occurred earlier. Measuring the difference between drying and hydration, using setting times, proves difficult and investigating it, forms part of the recommendations of this study.

5.1.3. Effect of depth

This section does not only investigate the effect of depth on the average crack width, but also its effect on settlement, shrinkage and capillary pressure. The same pure plastic shrinkage cracking mould as discussed in Chapter 3 was used, where the only variable in its geometry was the mould depth. Varying depth proved to be invaluable in observing the formation of the pure plastic shrinkage cracks.

Figure 5.6 shows the progressive formation (average surface crack width) of a pure plastic shrinkage crack with concrete depths of 100, 150 and 200 mm for the NB-Mix at Climate E. It is apparent from Figure 5.6 that an increase in depth influenced both the time of formation and severity of the crack. The deeper the concrete section the longer it took for the crack to initiate. For the 100 mm deep concrete section, it took 122 minutes for the initial crack to form where for the 200 mm deep concrete section it took 220 minutes. Not only does an increase in concrete depth delay the formation of the crack and reduce the severity, but it also reduced the formation rate of the initial crack as shown in Figure 5.6. The initial gradient changes from 0.044 millimetres per minute for the 100 mm deep mould to 0.018 millimetres per minute for the 200 mm deep mould.

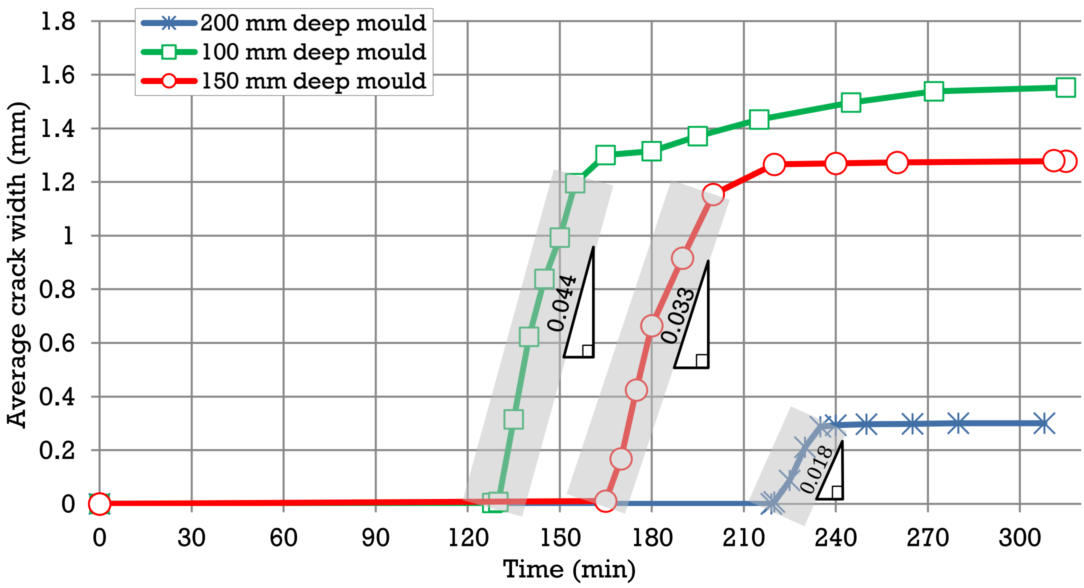

Figure 5.6: Results of the average surface crack width for 100, 150 and 200 mm cracking moulds for the NB-Mix at Climate E.

Figure 5.7 shows the progressive formation of the pure plastic shrinkage crack observed from the side for the 200 mm mould, containing the NB-Mix exposed to Climate E. As for the 100 mm deep concrete section described in Section 5.1.1, the fundamental formation characteristics of the crack in the 200 mm deep concrete section are similar but more distinct. The initial hairline cracks indicated in Figure 5.7 verify that the crack does not form from the top to the bottom, but rather suddenly and uniformly through the depth of the section. As for the 100 mm deep mould, the initial hairline cracks form randomly over the height of the section on the path of the final crack, as seen at 303 minutes after placing the sample in the climate chamber.

The influence of depth on plastic shrinkage and capillary pressure and its effect on the crack formation, is further discussed in the following sections which could assist in predicting these cracks.

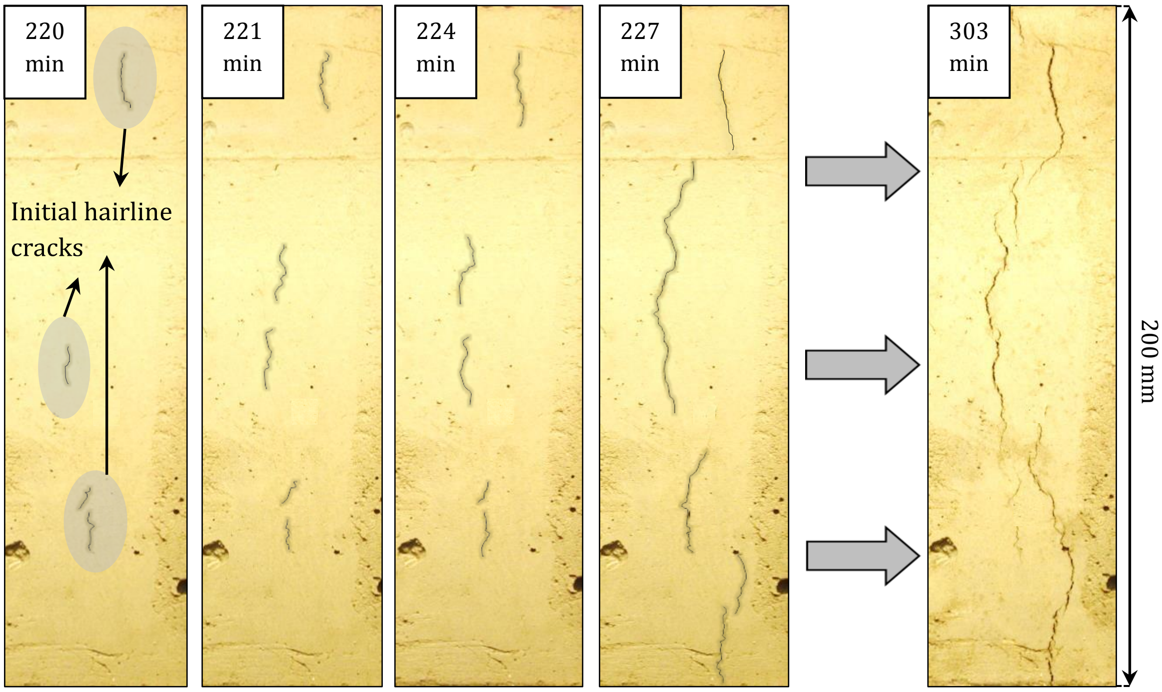

Figure 5.7: Plastic shrinkage crack propagation observed from the side for the NB-Mix at Climate E.

Capillary pressure

The capillary pressure build-up was measured at different depths in the 200 mm deep mould as shown in Figure 5.8. The average peak value for the capillary pressure measured at a 50 mm depth, was the highest followed by the capillary pressure peaks at depths of 100 mm and then 150 mm respectively. As the menisci become too small to bridge the gap between the solid particles, air enters the concrete matrix and the capillary pressure reaches its peak and drops locally.

The capillary pressure results were not as expected, as the peak capillary pressure values occurred long before the plastic shrinkage crack appeared in the 200 mm deep mould. This is different to the results of the 100 mm deep mould as the crack formed as the capillary pressure reached its peak and air entered the mix. In the 100 mm deep mould the capillary pressure build-up, settlement, shrinkage and crack formation occur in a short period of time. However, in the 200 mm deep mould all these parameters take longer to initiate and form which makes identifying them easier.

For the 200 mm mould the capillary pressure build-up reached its peak at around 150 minutes where the pure plastic shrinkage crack only initiated at 220 minutes. This happens because even when air enters the concrete matrix, the lower part of the concrete section prevents the entire section from separating. The concrete section only cracks once the horizontal shrinkage reaches or nears the bottom part of the concrete section. This is of critical importance when estimating the time when a pure plastic shrinkage crack would form. This is explained further in the next section.

Plastic shrinkage

As underlined in the experimental framework, the shrinkage was measured in the 200 mm deep shrinkage mould at depths of 50, 100 and 150 mm. Figure 5.8 shows the shrinkage results of the shrinkage for the NB-Mix exposed to Climate E. The shrinkage at a depth of 50 mm started around the time the initial settlement ceased and capillary pressure started to rise. The shrinkage at a depth of 100 and 150 mm started at 90 and 180 minutes respectively. The results from Figure 5.8 show that the shrinkage started at the surface and propagated downwards.

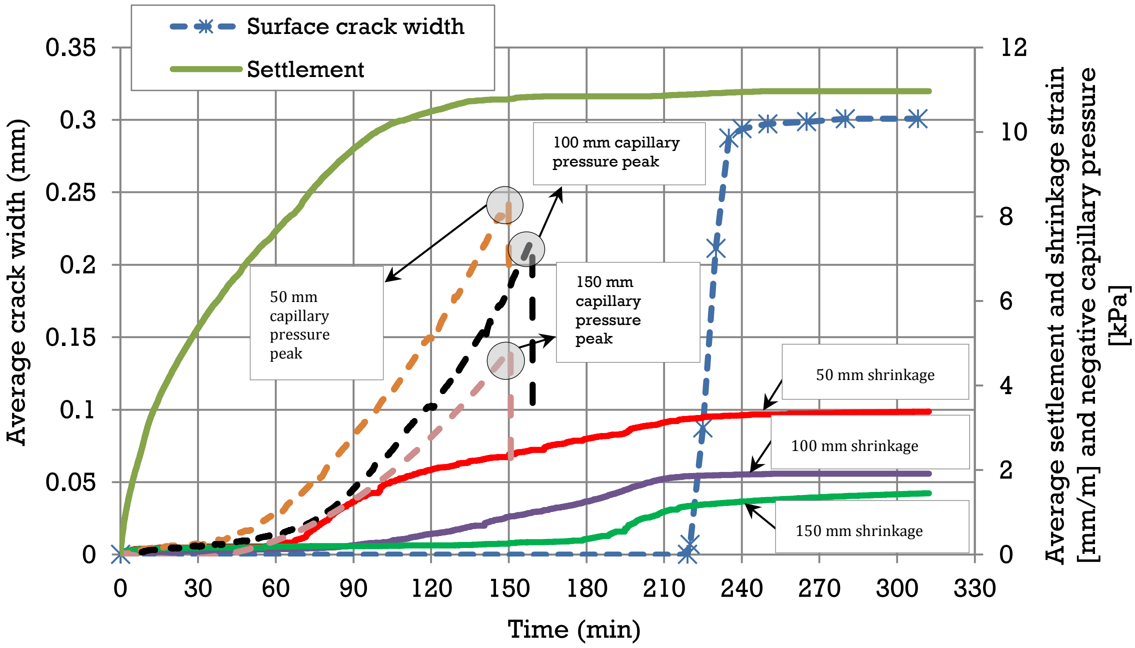

Figure 5.8: Plastic shrinkage cracking results and mix properties in 200 mm deep mould for the NB-Mix at Climate E.

The differences in the shrinkage trends over the depth become even more comprehensible when considering shrinkage over the depth as a function of time as seen in Figure 5.9. Figure 5.9 shows the shrinkage results measured in the 200 mm mould at Climate E over the depth at selected time intervals. The shrinkage was also measured on the surface of the mould for the purpose of this figure. This was done by taking digital images at selected times and then measuring the shrinkage displacement using a Digital Image Processing Program (DIPP). The DIPP used was ImageJ IJ 1.46r (2012) as discussed in Chapter 4.

The shrinkage trend from the surface to the bottom is not linear but rather exponential as shown in Figure 5.9. This trend can be explained by considering the movement of water in the interconnected pore system.

As the evaporation amount exceeds the accumulated amount of bleed water that rises to the surface, the capillary pressure starts to build-up. This leads to menisci forming between the solid particles right at the very top of the concrete matrix. The menisci induce an attractive force between the solid particles and the concrete matrix starts to shrink horizontally and vertically. For the NB-Mix at Climate E this occurs somewhere between 0 and 50 minutes as shown in Figure

5.9. The initial shrinkage on the surface is rapid, especially at Climate E. As the menisci become too small to bridge the gap between the solid particles, the system becomes unstable and relocation of water in the interconnected pore system takes place. At this point, air enters the concrete matrix locally near the surface.

However, water sleeves still connect these particles when the menisci become too small to bridge the gap (Wittmann, 1975). After this critical point in time, the negative capillary pressure still rises in the global concretes interconnected pore system. The water sleeves still result in contracting forces between the solid particles. However, these forces are prominently smaller than the forces due to the formation of menisci between the solid particles (Slowik et al., 2008).

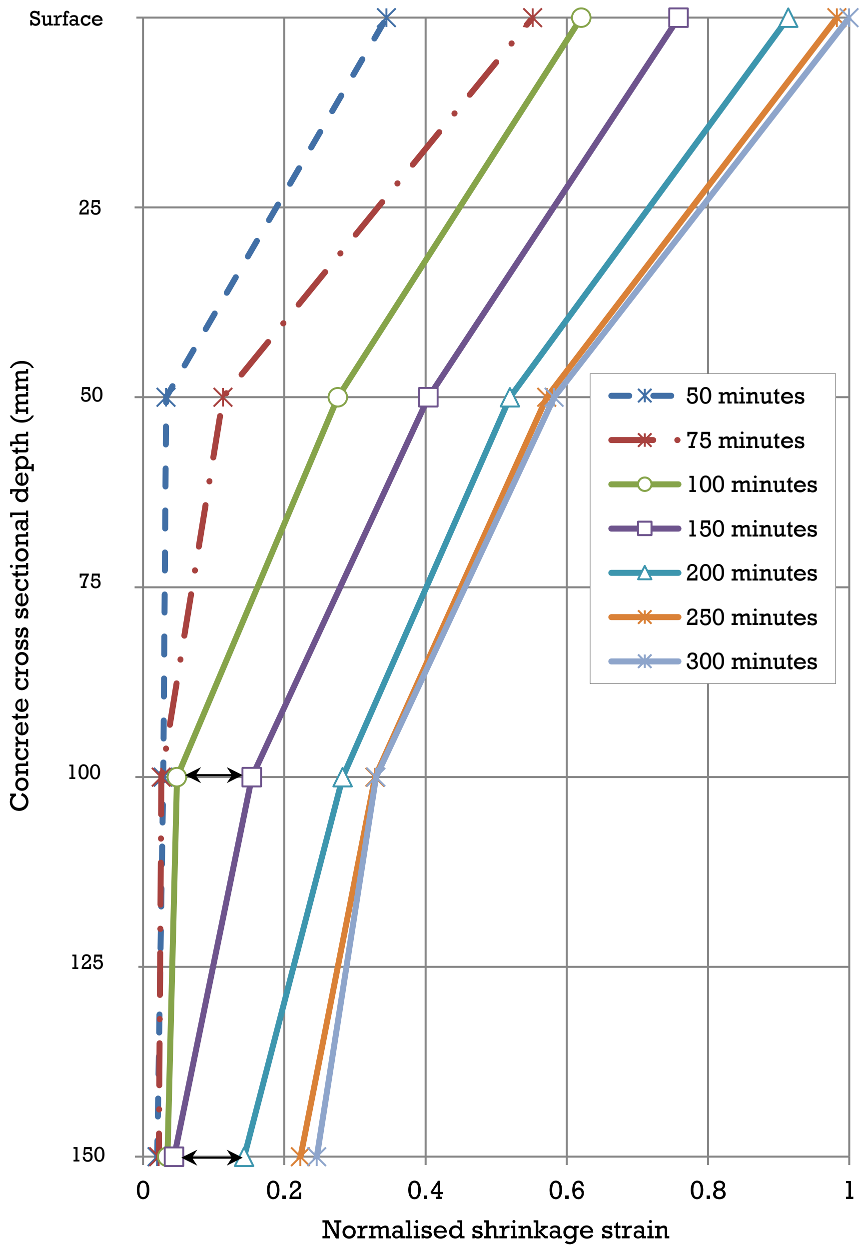

Figure 5.9: Shrinkage results measured in the 200 mm mould over the depth at selected time periods for the NB-Mix at Climate E.

This discussion of the principal behaviour is further substantiated by considering the data lines between the surface and 50 mm as shown in Figure 5.9. The rate of shrinkage stabilises between 100 and 150 minutes at this depth but still moves horizontally relative to the side of the mould. The left-hand axis on Figure 5.9 can be seen as representing the side of the mould. Water sleeve forces still exist between the particles at this depth but the negative capillary forces beneath this depth dominates the horizontal shrinkage values and it appears that shrinkage in the top section completely stops relative to the underlying concrete.

Effective depth/ false bottom

Concrete slabs without embedded reinforcing steel, rarely exist and are mostly present in the form of a steel mesh. If internal steel bars are present and the initial settlement cracks are prevented, firstly with a proper concrete mix design and finally by placing and consolidating the concrete correctly, the initial crack that forms is still pure plastic shrinkage of nature. However, with the use of internal steel bars the effective concrete area resisting the shrinkage strains, reduces.

Through numerous tests, with an embedded steel bar at different depths (presented in Chapter 5), it was found that the effective depth that initial plastic shrinkage crack forms, is near the steel bar insert. It is not the entire concrete section as one would expect. The concrete section resisting the shrinkage is reduced due to the rigid steel bar forming a false bottom.

The plastic cracking mould used in this study only had one steel bar placed at the centre of the mould. However, structural floor slabs usually have multiple steel bars placed at certain spacing throughout the entire floor. This creates a horizontal rigid steel mesh in the concrete slab. It is believed that the steel mesh will reduce the effective depth, resisting the initial shrinkage crack to the top of the steel mesh and not beneath it. This however needs further testing and verification.

If initial settlement cracks are present before shrinkage occurs, the behaviour of cracking completely changes. However, if shear cracks are present without tension cracks, the effective depth is further reduced and an initial pure plastic shrinkage crack can still form. Shear cracks form from the reinforcing steel upwards. This means that after these initial settlement shear cracks had been formed, the concrete above the crack did not split. The top section that was not split, still resisted shrinkage until the shrinkage reached the top of the shear crack. At this point in time, a plastic shrinkage crack could form between the surface and the top of the shear crack.

Figure 5.10 shows the average surface crack width for the NB-Mix at Climate E for a concrete section with and without a steel bar embedded at a depth of 45 mm. Mixture properties such as shrinkage and negative capillary pressure for the 100 mm deep section are also shown, all as a function of time. This mould had no initial settlement cracks as shown on a digital image taken from the side and shown in Figure 5.10, just after the side door was removed.

A second digital image showing the final crack is also shown in Figure 5.10. As discussed in Section 5.1.2, a pure plastic shrinkage crack only forms once the concrete starts to shrink at the bottom. In this case, the effective depth reduced to 45 mm with the addition of embedded reinforcing steel placed at 45 mm. Figure 5.10 shows that the crack forms at 73 minutes just before the shrinkage at a depth of 50 mm starts.

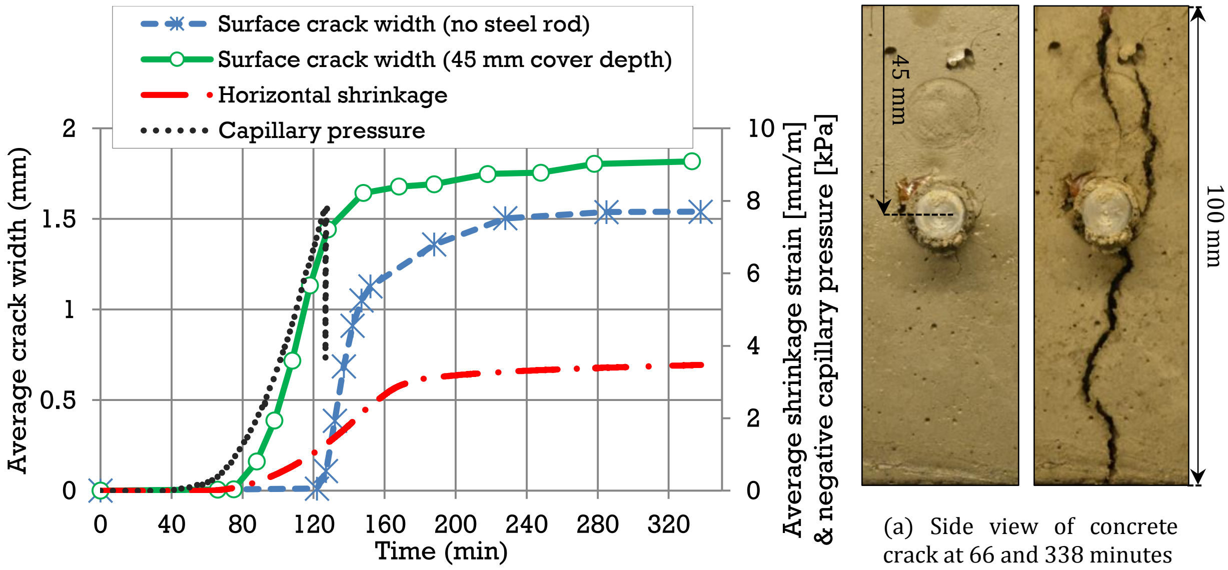

(a) Side view of concrete crack at 66 and 338 minutes

Figure 5.10: Results of the NB-Mix in Climate E in the 100 mm deep mould without a steel bar and with 45 mm embedded steel bar with no settlement cracks, along with digital images of the section as seen from the side.

5.1.4. Conclusions

This section firstly evaluated pure plastic shrinkage cracking at a depth of 100 mm together with measurements such as settlement, shrinkage and capillary pressure. Varying climate conditions and a depth up to 200 mm proved to be invaluable in describing the crack formation. The following conclusions can be made about pure plastic shrinkage cracking:

- Setting times cannot be used to indicate the phase concrete finds itself in for high evaporation rates. This is due to the complex interaction between drying and hydration and their respective influence on penetration resistance of plastic concrete.
- Pure plastic shrinkage cracking occurs suddenly without any warning signs. The crack formation is not from the top to the bottom but the initial cracks form randomly on the path of the final crack when monitored from the side.
- The time of formation and severity of the crack changed when varying the climate and concrete mix design. However, the principal formation of the pure plastic shrinkage crack remained the same.
- The time of formation of a pure plastic shrinkage crack takes longer in deeper sections, while the severity of the crack is also reduced.
- Horizontal shrinkage starts at the surface of the concrete and gradually moves down the concrete section. The final horizontal trend is exponential from the bottom to the surface.
- If internal reinforcing steel is present and initial settlement cracks are prevented, the effective depth resisting the shrinkage, reduces to the depth of the steel reinforcing. This however needs further testing. Internal shear cracks can further reduce the effective depth of concrete resisting the shrinkage, and they could further reduce the initial surface crack and increase the severity of the final crack.

5.2. Interaction between plastic settlement and shrinkage cracking

Pure plastic shrinkage cracking rarely occurs on its own without the influence of initial plastic settlement cracks. Cracking in slabs mostly map the underlying steel bars, as a result of initial settlement cracks that are further widened by plastic shrinkage. These cracks can still map the underlying steel bars even if initial settlement cracks are not present. This is attributed to the reduction in effective depth over the reinforcing steel, as discussed in the previous section.

The objective of these tests was to observe the formation and interaction between plastic settlement and shrinkage cracking. The moulds used in these tests included the pure plastic cracking mould (with and without embedded steel bars), shrinkage and settlement mould, as well as the capillary pressure mould.

Figure 5.11 shows the surface crack width (with and without a steel bar), shrinkage, settlement and capillary pressure results for the NB-Mix exposed to Climate E. The pure plastic cracking mould was modified to contain a rigid 10 mm diameter steel bar. This steel bar creates an initial weak spot through the differential settlement which can split the concrete section before horizontal shrinkage starts. The interaction between plastic settlement cracks and shrinkage cracks is evident when examining Figure 5.11. From the results obtained, the interaction between plastic settlement and shrinkage cracking can be split up into three distinct phases as shown in Figure 5.11.

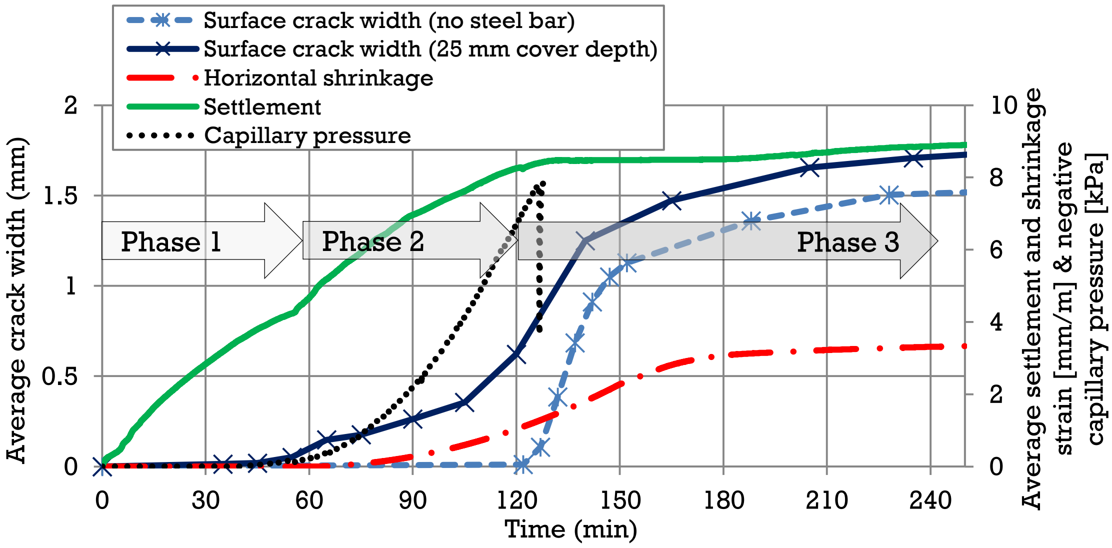

Figure 5.11: Interaction results for the NB-Mix at Climate E with and without embedding a steel bar in the 100 mm mould.

Phase 1

Phase 1 is characterised by cracking as a result of differential settlement and it forms before shrinkage (capillary pressure build-up) occurs. These settlement cracks can be categorised and split up into either tension and/or shear cracks (Combrinck, 2016). These settlement cracks can act in combination with one another or separately. Tension cracks generally appear as multiple cracks (extremely fine cracks) on the surface of the concrete directly above the embedded reinforcing steel, as shown in Figure 5.12 (a). Tension cracks form from the top to the bottom.

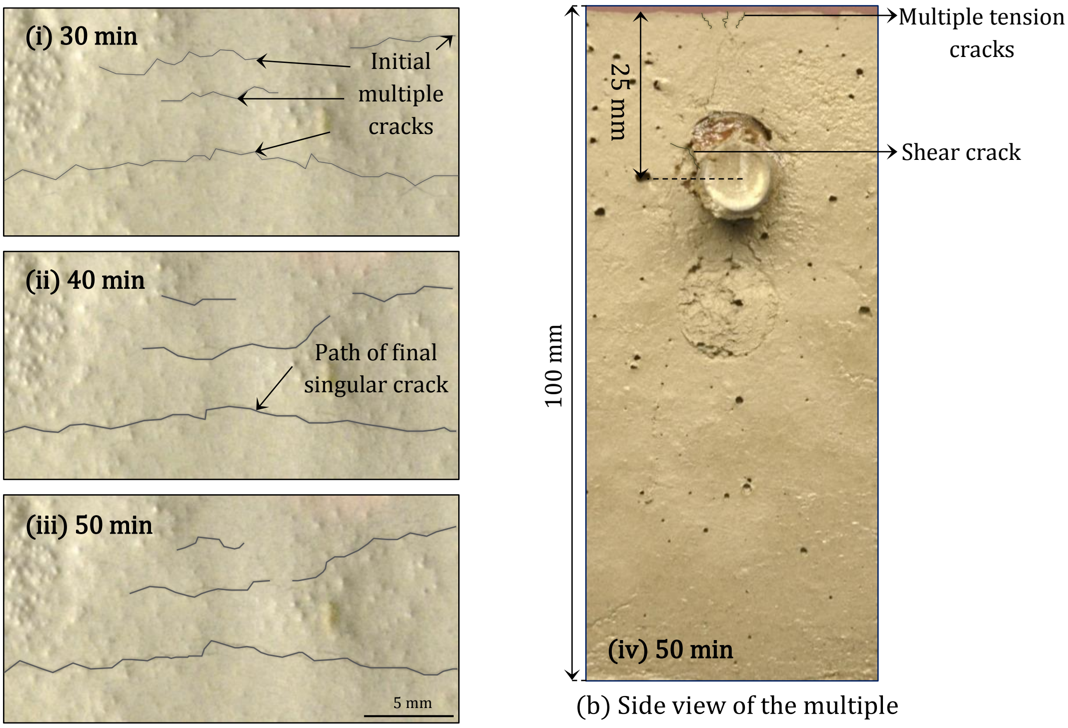

(a) Top view of the multiple surface tension cracks at different times

(b) Side view of the multiple surface tension cracks and a shear crack

Figure 5.12: Example of typical tension and shear cracks in Phase 1 obtained from the NB-Mix at Climate

For sufficient cover depths, tension cracks can be prevented and do not form. Shear cracks are the second type of crack that forms in Phase 1 and is illustrated in Figure 5.12 (b). Shear cracks form on the most left- and right-hand side of the embedded reinforcing steel and they usually form before the tensile cracks. These cracks form from the side of the steel upwards. The latter means that the cracks can be present beneath the surface without being visible on the surface. Decreasing the cover depth increases the angle of the shear crack.

In the case where shear cracks are present without tension cracks and do not split the entire concrete section, the initial surface crack that forms, are pure plastic shrinkage of nature. In this case, the effective concrete depth resisting the shrinkage, is reduced as discussed in Section 5.1.3. Phase 1 ends once the capillary pressure starts to rise.

Phase 2

Phase 2 follows where the small hairline tension cracks are further widened due to additional settlement and shrinkage, as a result of capillary pressure build-up. Not all the hairline cracks widen as some of these cracks open up further. Other cracks close, to ultimately form one crack over the concrete surface as indicated in Figure 5.12 a. The start of Phase 2 coincides with the rise in capillary pressure where the capillary pressure forces the solid particles on the surface downwards, due to the negative pressure build-up as discussed in Chapter 3. This is also verified through the change in the rate of settlement as seen in Figure 5.11 at around 60 minutes. The change in the rate of settlement is not always distinct as for the HB-Mix at Climate E as shown in Figure 5.13. Phase 2 ends once the settlement finally ceases and the capillary pressure reaches its peak, where air enters the concrete matrix locally.

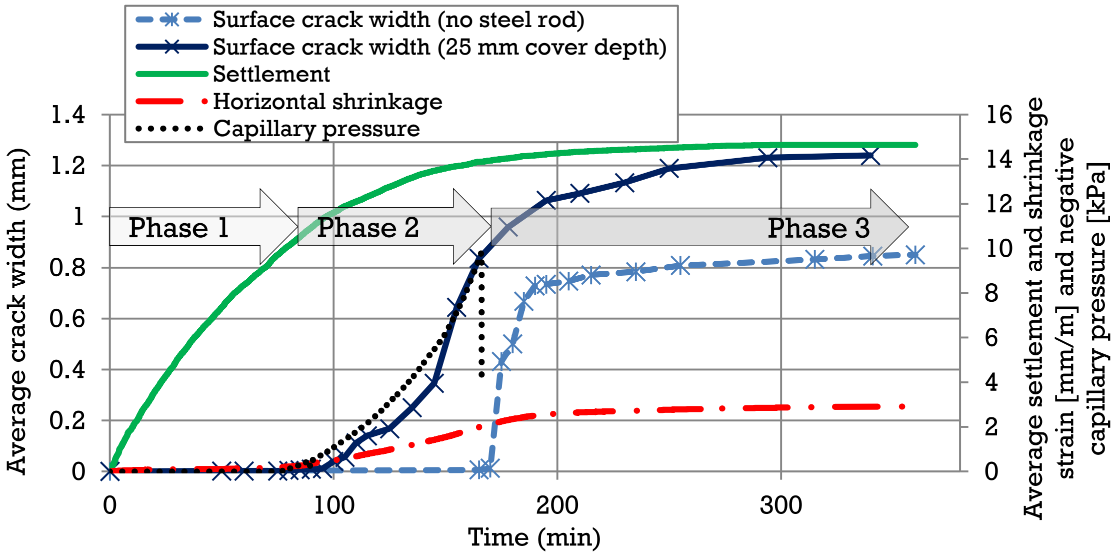

Figure 5.13: Interaction results for the HB-Mix in Climate E with and without an embedded steel bar (100 mm mould).

Phase 3

The majority of the crack widening occurs in Phase 3, especially for mixtures prone to plastic shrinkage. The crack is widened by horizontal shrinkage and occurs around the same time the crack would appear if no steel bar was present, as shown on Figure 5.11. However, this is not always the case as seen in Figure 5.13, and when investigating deeper concrete sections in Section 5.2.2. The formation of the crack from Phase 3 and onward is different to that of a pure plastic shrinkage crack. As the top part of the concrete section was split in Phases 1 and 2, the horizontal shrinkage steadily widens the crack from the bottom of the steel bar downwards as the horizontal shrinkage propagates down in Phase 3. The overall crack propagation is from the top downwards over a longer period of time which is different to that of a pure plastic shrinkage crack.

Monitoring the crack from the side gives even more insight with regard to the behaviour and propagation of the crack, especially for Phase 2 and 3 as indicated in Figure 5.14. Figure 5.14 shows the cracking width results measured on the surface and from the side together with selected high quality digital images at selected times taken from the side. The average crack width measured from the side was split up into the top quarter and the bottom three quarters. It should be noted that initial settlement cracks could have been present beneath the surface before the side door was removed. This is shown in Figure 5.14. Phase 2 and 3 become more apparent when investigating the crack behaviour from the side as shown in Figure 5.14. The crack development in Phase 1 could not have been measured from the side as the concrete was not stiff enough for the side door to be removed.

The side door could only be removed in Phase 2 at 90 minutes (Image A in Figure 5.14) from placing the specimen in the climate chamber. From this point onwards up to the beginning of Phase 3 the top quarter of the side crack width rapidly increased as the capillary pressure build-up increased.

In Phase 3 the crack penetrates the full depth of the concrete section (from the bottom of the steel bar and downwards) and the biggest part of the final crack formation occurs. The two halves of the concrete section at the steel bar are no longer in contact with each other and they are moved further apart due to the horizontal shrinkage up until the concrete finally hardens. The formation of this plastic crack is different to that of a pure plastic shrinkage crack.

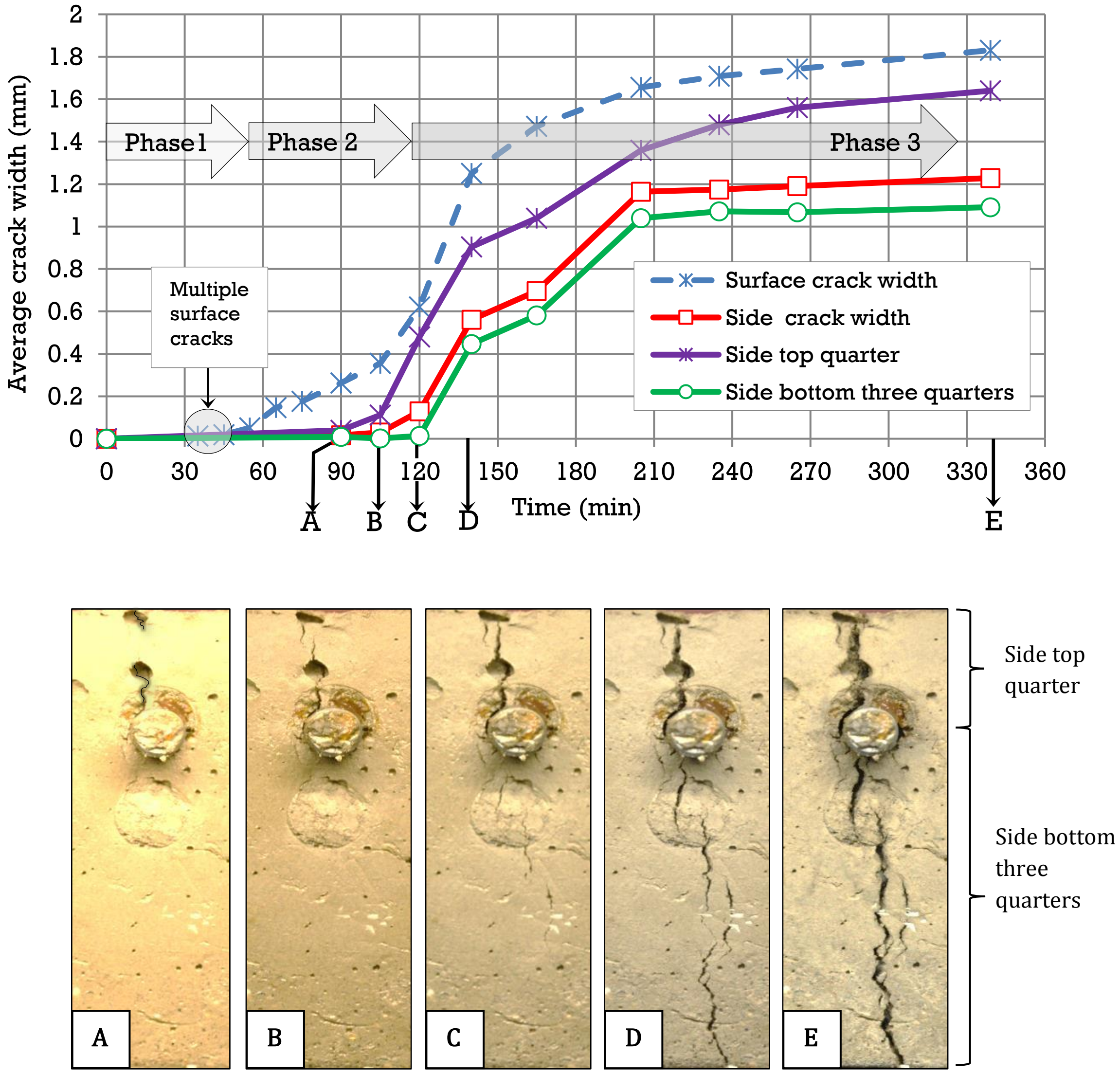

Figure 5.14: Side surface cracking results (25 mm steel bar in 100 mm deep mould) for the NB-Mix exposed to the Climate E.

When an initial weak spot is created through differential settlement, the concrete section is split and no longer resists horizontal shrinkage. By the time the section shrinks at a depth of 30 mm, the crack was widened in Phase 1 and 2. Horizontal shrinkage causes the crack to widen gradually through the concrete depth. This is different to that of a pure plastic shrinkage crack without an initial weak spot where the crack only appears, and appears suddenly, when the concrete shrinks near the bottom part of the section, as discussed in Section 5.1.3.

Figure 5.15 shows the average surface crack width results for the HB-Mix exposed to Climate E, with and without embedded reinforcing steel. The high bleeding amount and rate of the HB-Mix makes it less prone to plastic shrinkage cracking when compared to the NB-Mix. However, the HB-Mix is more prone to settlement cracking, due to its increased settlement and therefore differential settlement as a result of the high bleeding rate. The pure plastic shrinkage crack for the HB-Mix occurs at 165 minutes compared to 122 minutes for the NB-Mix.

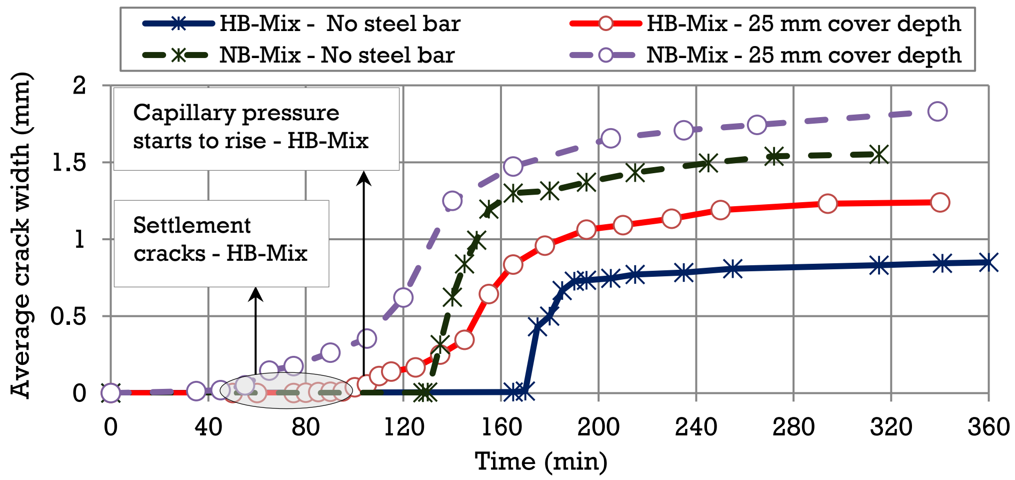

Figure 5.15: Average surface crack width results for the HB-Mix and NB-Mix in Climate E with and without a steel bar.

Even though the rate that bleeds water is removed from the surface is the same for both the NB-Mix and HB-Mix at Climate E, the pure plastic shrinkage crack formation is delayed for the HB-Mix. The higher bleeding rate of the HB-Mix compared to the NB-Mix, continually replaces the evaporated water with bleed water for a longer period of time. This causes a delay in the capillary pressure build-up and shrinkage, which results in a delay in the formation of the pure plastic shrinkage crack.

Figure 5.15 shows this delay with the grey circle between 40 and 100 minutes. The initial settlement cracks do not widen as the shrinkage is delayed. It is only around 110 minutes that these cracks widen as the capillary pressure starts to rise.

5.2.1. Effect of depth

Deeper concrete sections have more settlement which directly increases the risk of plastic settlement cracking. However, deeper sections result in more bleeding which delays and thus decreases the severity of the plastic shrinkage.

The 200 mm deep mould displayed the same fundamental behaviour as the 100 mm deep section. The formation period of the crack took longer in the deeper mould and therefore gave more distinct information on the interaction between plastic settlement and shrinkage cracking. As for the 100 mm deep mould discussed in Section 5.2, the formation characteristics of the 200 mm deep mould can be split up into three distinct phases. The fundamental behaviour for the deeper 200 mm mould is the same as for the 100 mm deep mould. Nevertheless, the three phases become clearer when investigating for a deeper mould.

Phase 1

The tension and shear cracks in the 200 mm deep mould are more severe than in the 100 mm mould. Settlement increases as the height of a section increase. Furthermore, as the settlement increases so do the differential settlement, due to the rigid inclusion of an embedded reinforcing steel bar. The increase in the differential settlement is directly proportional to an increase in the widening of the tension and shear cracks. Phase 1 ends once the capillary pressure starts to rise as shown in Figure 5.16 which is the same for the shallower 100 mm deep mould.

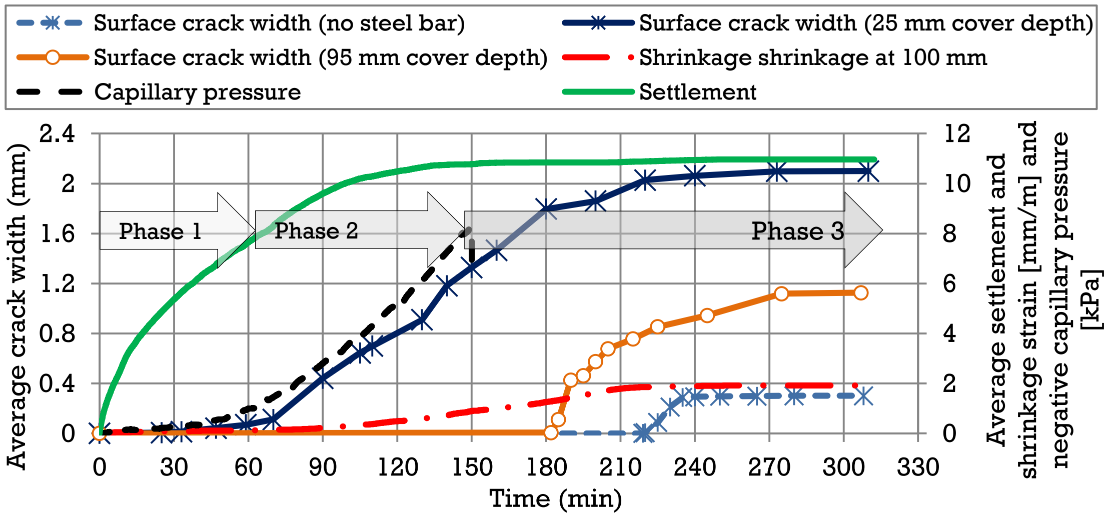

Figure 5.16: Crack interaction results for NB-Mix at Climate E with and without an embedded steel bar in the 200 mm deep mould.

Phase 2

The average peak capillary pressure in the deeper 200 mm is reached later than in the 100 mm section. For deeper moulds, more bleed water is available to relieve this capillary pressure build-up and therefore air entry is reached at a later stage. Therefore, in the deeper 200 mm concrete mould the settlement is greater and takes longer before ceasing. Phase 2 is therefore, longer in the deeper mould compared to the 100 mm deep mould. Phase 2 ends as the settlement ceases and air entry has occurred which is the same in the shallower 100 mm deep mould.

Phase 3

In Phase 3 the crack is further widened (primarily) by horizontal shrinkage and does not necessarily occur around the same time the crack would appear if no steel bar was present as shown in Figure 5.16 and stated for the 100 mm deep mould. Figure 5.16 shows that the majority of crack widening in Phase 3 starts long before the pure plastic shrinkage crack would have formed. The formation of the plastic crack in Phase 3 becomes exceedingly distinct in deeper sections and the difference to that of a pure plastic shrinkage crack is more apparent than first realised in the 100 mm deep mould.

As the top part of the concrete section has been split in Phase 1 and 2, the horizontal shrinkage steadily widens the crack as the horizontal shrinkage propagates down the concrete section. Considering the formation of the crack from the side is now further investigated.

For concrete sections with larger cover depths, the effect of settlement cracking (Phase 1) still has a large effect on plastic cracking, even when no tensile cracks form on the surface. Shear cracks can form without the presence of tensile cracks. These shear cracks form from the embedded steel bar upwards and can be present without being visible from the surface. Consider the average surface crack width for a concrete mould with embedded steel bar at 95 mm deep shown in Figure 5.16. No tensile cracks formed on the surface in Phase 1. There did however form a shear crack that could be seen once the side door was removed, as shown in Figure 5.17. The shear crack formed in Phase 1. The shear crack was deep enough and the surface cracking only became visible in Phase 3.

This crack that formed in Phase 3 at 180 minutes behaved similarly to that of a pure plastic shrinkage crack. The crack that formed between the surface and shear crack was instant and hairline cracks formed randomly on the path of the final crack when monitored from the side. This crack formation is the same as a pure plastic shrinkage crack as discussed in Section 5.1. After the pure plastic shrinkage crack split the concrete section above the steel bar, the crack gradually propagated from the steel bar to the bottom of the mould.

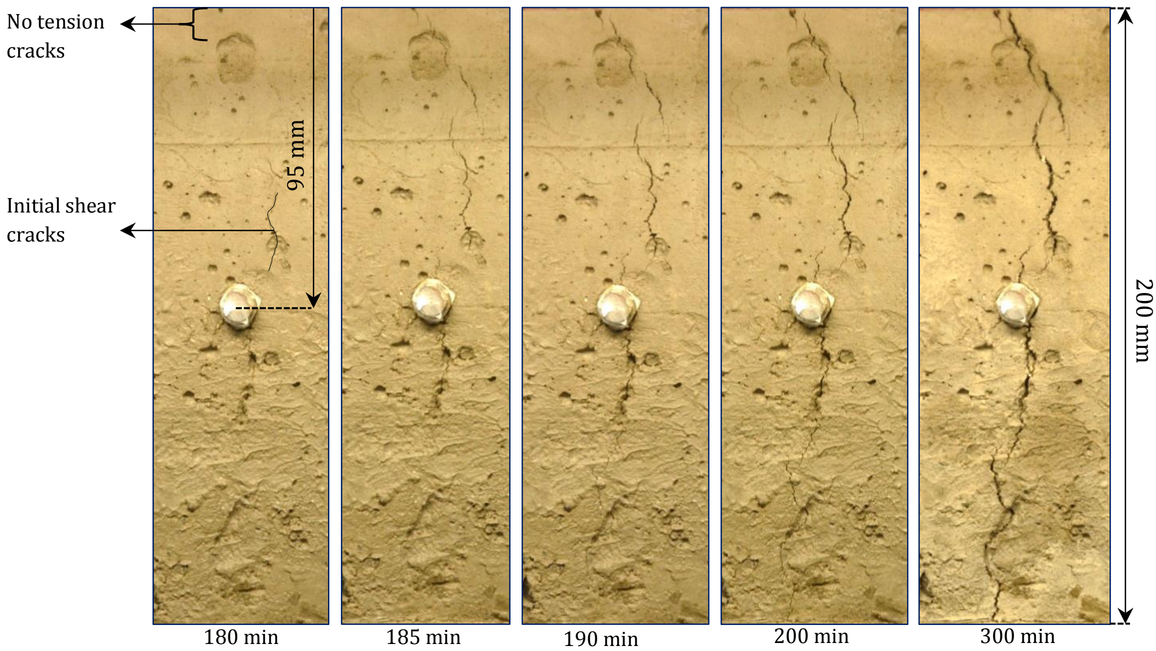

Figure 5.17: Crack development for the NB-Mix at Climate E with an embedded steel bar at 95 mm as seen from the side.

Figure 5.18 shows the behaviour of the crack as seen from the side in the 200 mm deep mould containing a piece of embedded steel bar at a depth of 25 mm. As for the 100 mm deep mould the side crack width measurements for the 200 deep sections was split into the top quarter and bottom three quarters. Figure 5.18 also shows selected high-quality digital images of the crack from the side over a period of time.

The side door could only be removed once the concrete was stiff enough. The side door was removed after 120 minutes and is represented by Point A as shown in Figure 5.18. The settlement cracks in Phase 1 formed before the side door was removed. Unknown data points is the reason for the straight line between the time of zero and 120 minutes for the average crack width of the side top quarter.

As discussed in Section 5.2, the widening action is even more evident when considering deeper sections as the formation of the crack occurs over a longer period of time. As the shrinkage propagates from the surface downwards, the crack steadily widens. This further verifies that the shrinkage steadily moves downwards and in turn widens the already split concrete section.

The crack in this section took around 45 minutes to form from the steel bar to the bottom of the concrete section. After the concrete section had been entirely split, further widening only occurred for 30 minutes before the crack stabilised.

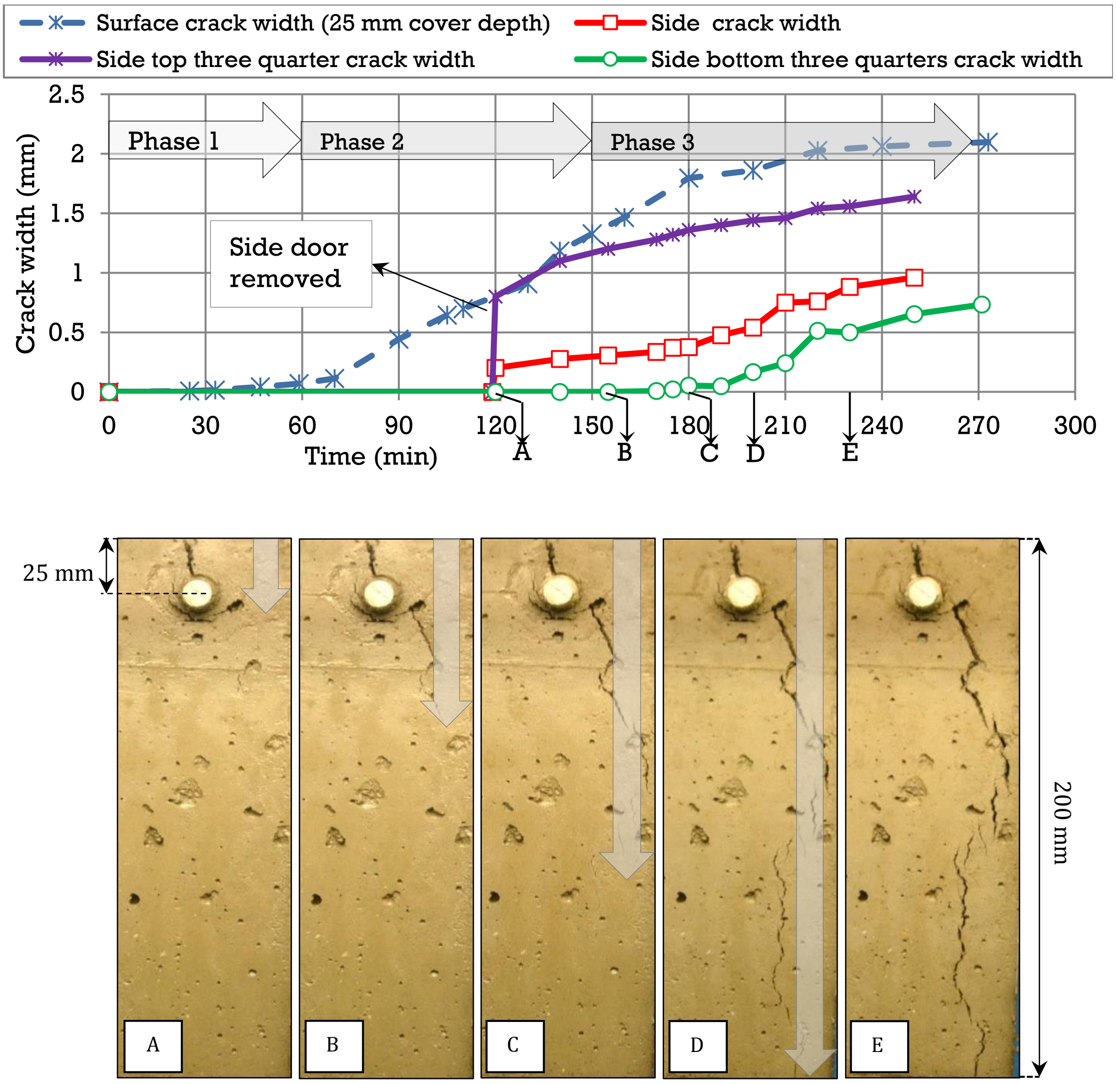

Figure 5.18: Side surface cracking results (25 mm embedded steel bar in 200 mm deep mould) for the NB-Mix exposed to Climate E along with selected digital images.

5.2.2. Conclusions

This section first evaluated plastic cracking at a depth of 100 mm together with the settlement, shrinkage and capillary pressure. Varying climate conditions, the degree of settlement and depth from 100 to 200 mm proved to be invaluable in describing the plastic crack interaction. The following conclusions can be made about plastic cracking interaction:

- Plastic cracking can be split up into three distinct phases. Phase 1 is characterised by settlement cracking without the influence of any horizontal shrinkage. Phase 1 ends once the capillary pressure starts to rise and horizontal shrinkage starts. In Phase 2 the crack further widens due to the capillary pressure build-up which causes additional vertical settlement and initiates horizontal shrinkage. Phase 2 ends once the capillary pressure drops and settlement reaches its maximum value. The majority of crack widening occurs in Phase 3 for pure plastic shrinkage cracking, but not necessarily when interacting with settlement cracking. The crack in this phase is only widened by horizontal shrinkage and ends once the concrete hardens and plastic shrinkage stops.

- The driving force behind the crack that forms in Phase 2 and Phase 3 is horizontal shrinkage. This is the same driving force behind a pure plastic shrinkage crack. However, the formation characteristics completely change. A pure plastic shrinkage crack appears suddenly and the initial formation is uniform through the entire section. As the top part of the concrete section has been split in Phase 1, the crack formation in Phases 2 and 3 gradually forms from the steel bar downwards at the same rate the shrinkage propagates downwards.
- The formation of the plastic cracks is much more apparent in deeper sections as they take longer to form. This proves to be invaluable when observing the formation characteristics.
- Deeper sections are more prone to plastic settlement cracking but less prone to shrinkage cracking. However, combining plastic settlement and shrinkage cracking in deep sections, rapidly increases the severity of cracking.
- Shear cracks can stay dormant in concrete sections and can drastically reduce the effective depth of concrete resisting shrinkage. The crack that forms between the surface and embedded steel bar is similar to that of a pure plastic shrinkage crack. After the formation of this crack, the concrete above the steel bar splits and the crack then gradually propagates down to the bottom.

5.3. Summary of cracking types

The fundamental cracking mechanisms that dominate cracking in the plastic phase are differential settlement and restrained shrinkage. The driving forces behind differential settlement and restrained shrinkage is settlement and capillary pressure build-up (shrinkage). The interaction between the two driving forces has not entirely been understood until now, due to the lack of research on their interaction. Varying the depth while changing the climate conditions and concrete mixture, proved to be invaluable in observing plastic cracking. Plastic cracking as a result of settlement and shrinkage can be classified into three distinct types:

1. Settlement cracking
2. Pure plastic shrinkage cracking
3. Settlement induced plastic shrinkage cracking

Plastic cracking can be split into three distinct phases as discussed in Sections 5.2 and 5.3. Each phase is characterised by a driving force which is either settlement and shrinkage or a combination of both, and is shown in Figure 5.19. Figure 5.19 also shows the different types of cracking in the respective Phases as a function of time.

Settlement cracking

Settlement cracking is arguably the earliest form of cracking in concrete. Settlement cracking occurs when vertical settlement is restrained, which is then referred to as differential settlement. The driving force behind differential settlement is settlement. The differential settlement can be due to rigid inclusions such as embedded reinforcing steel or non-uniform section depths. The principal factors influencing settlement cracking are the rate and amount of settlement and the degree of differential settlement. Pure plastic settlement cracking only occurs in Phase 1 before any shrinkage starts, which is indicated by a rise in capillary pressure as shown in Figure 5.19. However, there is some degree of settlement in Phase 2, due to the capillary pressure build-up, but this does not exist without the influence of horizontal shrinkage.

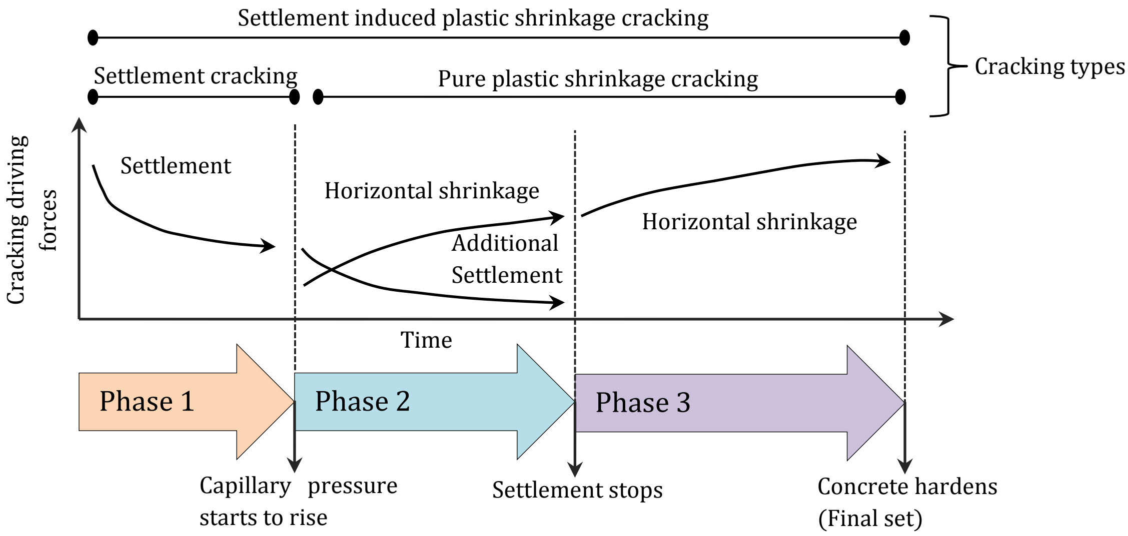

Figure 5.19: Plastic cracking diagram with respective driving forces.

Pure plastic shrinkage cracking

Pure plastic shrinkage cracking can occur either in Phase 2 or 3 if initial settlement cracking is prevented. The mechanism behind pure plastic shrinkage cracking is restrained shrinkage. Shrinkage starts on the surface of the concrete as the capillary pressure starts to rise, which is the primary driving force behind shrinkage cracking. This shrinkage gradient propagates downwards and if it reaches the bottom of the concrete section or the embedded reinforcing steel (if present), a pure plastic shrinkage crack forms. If reinforcing steel is present, only the initial formation between the steel bar and surface is pure plastic shrinkage of nature. The crack can then further propagate down towards the bottom but this formation is not the same as the initial pure plastic shrinkage crack. The initial formation of a pure plastic shrinkage crack is uniform through its section and not from the top to the bottom.

Settlement induced plastic shrinkage cracking

Settlement induced plastic shrinkage cracking is a combination of settlement and shrinkage cracking and can occur in all the phases shown in Figure 5.19. Initial settlement cracks create a weak spot and can even split the concrete section. If the initial settlement cracks split the concrete section above the embedded steel bar, shrinkage then further widen these cracks. The crack widening is then from the top to the bottom. In the case where the initial settlement cracks only consist of shear cracks that do not penetrate the entire concrete section above the steel bar, a pure plastic shrinkage crack could still form between the top of the shear crack and the surface. Nevertheless, generally settlement cracks penetrate the entire concrete depth above the embedded reinforcing steel. The crack is then further widened from the top to the bottom as the shrinkage propagates downwards.

5.4. Finishing operations

Finishing operations are applied to a concrete's surface to make it aesthetically acceptable and can improve its mechanical properties. Finishing operations are almost always used and its effect on plastic cracking is not fully understood. This section aims to exploit its effect on plastic cracking, using standard finishing operations. The moulds that were used include the 100 mm plastic cracking mould with and without an embedded steel bar.

The surface of the concrete was finished using a steel trowel for a period of one minute at specific times. The concrete was either finished when the bleeding stopped or after the formation of the crack. The finishing operations cannot begin while bleed water is still rising to the surface of the concrete. The strength of the surface is reduced if bleed water is reworked back into the top surface as the strength of concrete is directly related to the water-cement ratio. If the surface is sealed before bleeding stops, trapped bleed water can further cause weak sport and delaminations.

The effect of finishing operations on pure plastic shrinkage cracking is considered first. As mentioned in Section 5.3, restrained shrinkage is the mechanism behind pure plastic shrinkage cracking. For the NB-Mix exposed to Climate E the formation of the pure plastic shrinkage crack occurs at 120 minutes. However, the bleed water stopped rising to the surface at 60 minutes where after the finishing operations were applied to the concrete surface. Figure 5.20 shows digital images from the top and side before and after finishing operations were applied.

The finishing operations had no significant influence on the initial formation of the pure plastic shrinkage crack. However, after the crack appeared at 120 minutes, finishing operations were applied for a second time at 130 minutes. The crack on the top surface was easily closed. Nonetheless, the finishing operations had little to no effect on the crack formation through the concrete section. Images are taken from the side and Figure 5.20 (b) indicates that the crack is still present from the side even when closed on top.

These results were as expected. The driving force that is responsible for the formation of a pure plastic shrinkage crack is shrinkage. The application of finishing operations has no significant effect on the propagation of shrinkage through the section and the crack still forms as it would without finishing operations. However, finishing operations can close the crack on the surface and hide its true severity as seen in Figure 5.20 (c). At 200 minutes an image of the final surface crack was taken as illustrated in Figure 5.20 (a). The crack appears small on the surface but Figure 5.20 (b) shows that the entire concrete section is split.

Figure 5.21 shows the effect of finishing operations on plastic settlement cracking. The finishing operations were applied as the bleed water stopped rising to the surface after 60 minutes. The finishing operations closed the majority of the tension settlement crack as seen in Figure 5.21. However, the formation of additional shear cracks was evident after the finishing operations were applied. Finishing operations apply an additional force (apart from gravity) on the surface of the concrete. The concrete matrix is not stiff enough to resist this force and some degree of settlement occurs due to the downwards force of the finishing operation tool. This additional settlement leads to differential settlement over rigid inclusions and shear cracks can form.

It would appear that finishing operations can increase the effective depth resisting shrinkage by closing the tension settlement crack. This leads to the conclusion that finishing operations reduce the severity of settlement induced plastic shrinkage cracking.

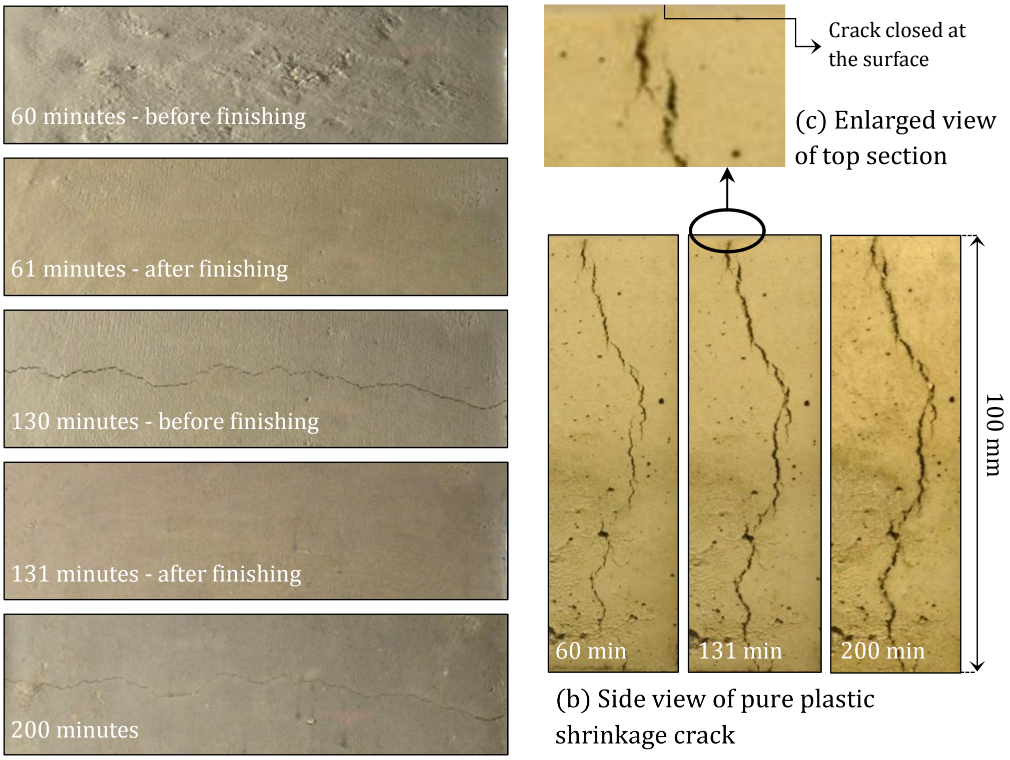

(a) Top view of pure plastic shrinkage crack at different times before and after finishing

(b) Side view of pure plastic shrinkage crack

(c) Enlarged view of top section

Figure 5.20: Effect of finishing operations on pure plastic shrinkage cracking for the NB-Mix at Climate E.

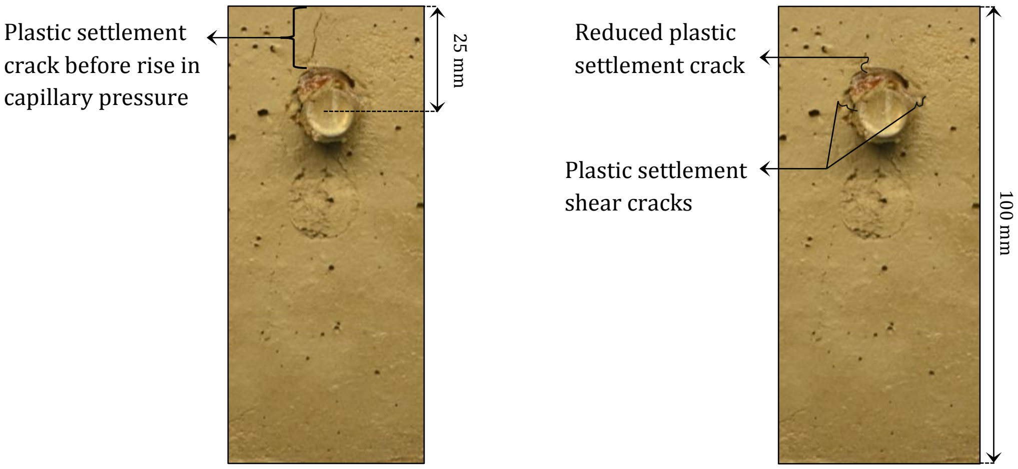

(a) Plastic settlement cracking with no finishing operations applied

(b) Plastic settlement cracking with finishing operations applied

Figure 5.21: The effect of finishing operations on plastic settlement cracking for the NB-Mix at Climate E with an embedded steel bar at a depth of 25 mm.

5.4.1. Conclusions

The aim of this section was to investigate the effect of finishing operations on the plastic cracking of concrete. The finishing operations were applied not only as the bleed water stopped rising to the surface, but they were also used to close the surface crack. The following conclusions can be drawn:

- Finishing operations do not have an effect on pure plastic shrinkage cracking. However, it can be used to close and hide the true severity of the crack when monitored from the surface.
- Finishing operations close initial tension settlement cracks but can induce shear settlement cracks on the sides of rigid inclusions.

5.5. Concluding summary

This chapter consists of the presentation and discussion on all the test results. In the first place focus is given to the formation of a pure plastic shrinkage crack, together with the effect of the depth. A discussion on the interaction between plastic shrinkage and settlement cracking then follows where after the different cracking types are presented as a summary. Finally, the influence of finishing operations on plastic cracking are discussed.

Chapter 6 : Plastic cracking risk model and prevention guidelines

This chapter aims to assist contractors and engineers to predict the risk of plastic cracking and to provide general guidelines to prevent the plastic cracking of concrete. Firstly, the procedure that was followed in creating a risk model for plastic shrinkage cracking is presented. Two unique cracking types dominate the plastic phase namely, plastic shrinkage cracking and plastic settlement cracking. Estimating the risk of these two plastic cracking types separately is considered first, followed by estimating the increase in risk, due to their interaction. Lastly, an outline of preventative measures to minimise these cracks, as well as an example of the risk model is given. The plastic cracking model need much improvement and is only presented as a framework to assist future studies.

6.1. Introduction

The accurate prediction of plastic cracking in terms of time and crack width for a specific mix and application is currently not possible, except through experimental testing. No model exists which can predict these cracks. This is mainly due to the large number of interdependent variables which influence cracking. These factors can generally be split into either internal or external factors. The internal factors include mixture properties such as aggregate characteristics, paste content, water cement ratio, mix constituent ratios, setting time, cement type, admixtures, fibres and depth, just to mention a few. External factors mainly include evaporation rates, restraint, finishing operations and curing practices.

The internal and external factors which influence plastic cracking must be simplified to increase the effectiveness of models while maintaining reasonable accuracy. Boshoff & Combrinck (2013) published a guideline on the prediction of plastic shrinkage cracking risk of concrete, which entailed estimating the risk of plastic shrinkage cracking by using a basic formula. The internal and external factors were simplified to setting times, evaporation amount, and bleeding volume and it was assumed to be sufficient. The formula basically estimated the severity of plastic shrinkage cracking as the difference between the evaporation rate and the accumulated amount of bleeding at the initial setting time. The use of fibres was also incorporated in this formula as a crack reducing agent.

From the experiments conducted in the study and discussed in the previous chapters, it became clear that plastic settlement and shrinkage cracking, rarely occur isolated from each other and they generally interact to some degree. The aim of the proposed risk model is to include the effect of both plastic settlement and shrinkage cracking to assist engineers and contractors alike in more accurate risk estimations of plastic cracking.

Only the driving forces and selected influencing factors, effecting each cracking mechanism are considered for this risk model. This is to reduce the number of variables (factors) and ensures an effective and non- time-consuming risk model. These selected dominant influencing factors are deemed sufficient. Settlement cracking is caused by the mechanism differential settlement where settlement is the primary driving force. Differential settlement is influenced by internal and external factors. The internal factors include settlement, depth and setting time, while the external factors include the degree of restraint and finishing operations. Shrinkage cracking is caused by the mechanism restrained shrinkage where shrinkage is the primary driving force. The internal factors influencing this include bleeding, depth and setting time, while the external factors include the degree of restraint and the evaporation rate. Capillary pressure build-up (shrinkage) is a direct result of evaporation. It is assumed that all the dominant influencing factors that were considered, include the majority of interdependent variables which influence plastic cracking. The factors influencing the mechanisms and driving force behind plastic cracking is now considered along with their respective risk estimations.

6.2. Plastic settlement cracking risk

Figure 6.1 shows the plastic settlement risk estimation plotted with the differential settlement while considering dominant influencing factors on plastic settlement cracking. The influencing factors shown in Figure 6.1 are displayed in relative terms to one another with regard to the impact that each factor has on the differential settlement. The driving force and dominant influencing factors are further discussed in Section 6.4 together with their effect on plastic shrinkage cracking.

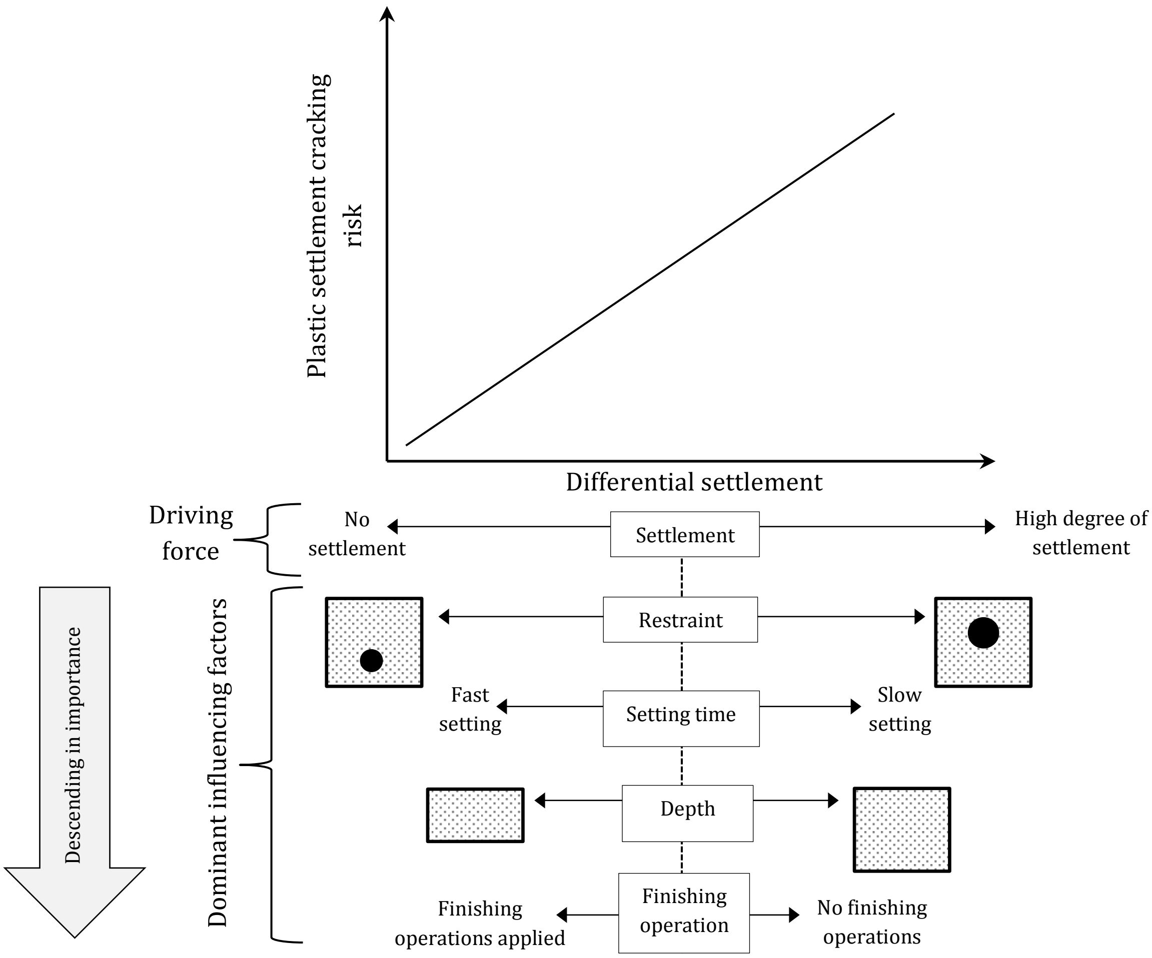

Figure 6.1: Plastic settlement cracking risk estimation.

It is assumed that there is a linear increase in the plastic settlement cracking risk and differential settlement as shown in Figure 6.1. The same assumption is made for the plastic shrinkage cracking risk compared to the restrained shrinkage as discussed in the next section. This assumption was confirmed through the tests done in this study.

6.3. Plastic shrinkage cracking

Figure 6.2 shows the plastic shrinkage risk estimation plotted over the shrinkage while considering the driving force and dominant influencing factors on plastic shrinkage cracking. The driving force behind plastic shrinkage cracking is evaporation. Some dominant influencing factors shown in Figure 6.1, for settlement cracking also have an influence on plastic shrinkage cracking. These factors include restraint, depth, setting time and settlement, which result in bleeding. These dominant influencing factors are discussed in the following sections.

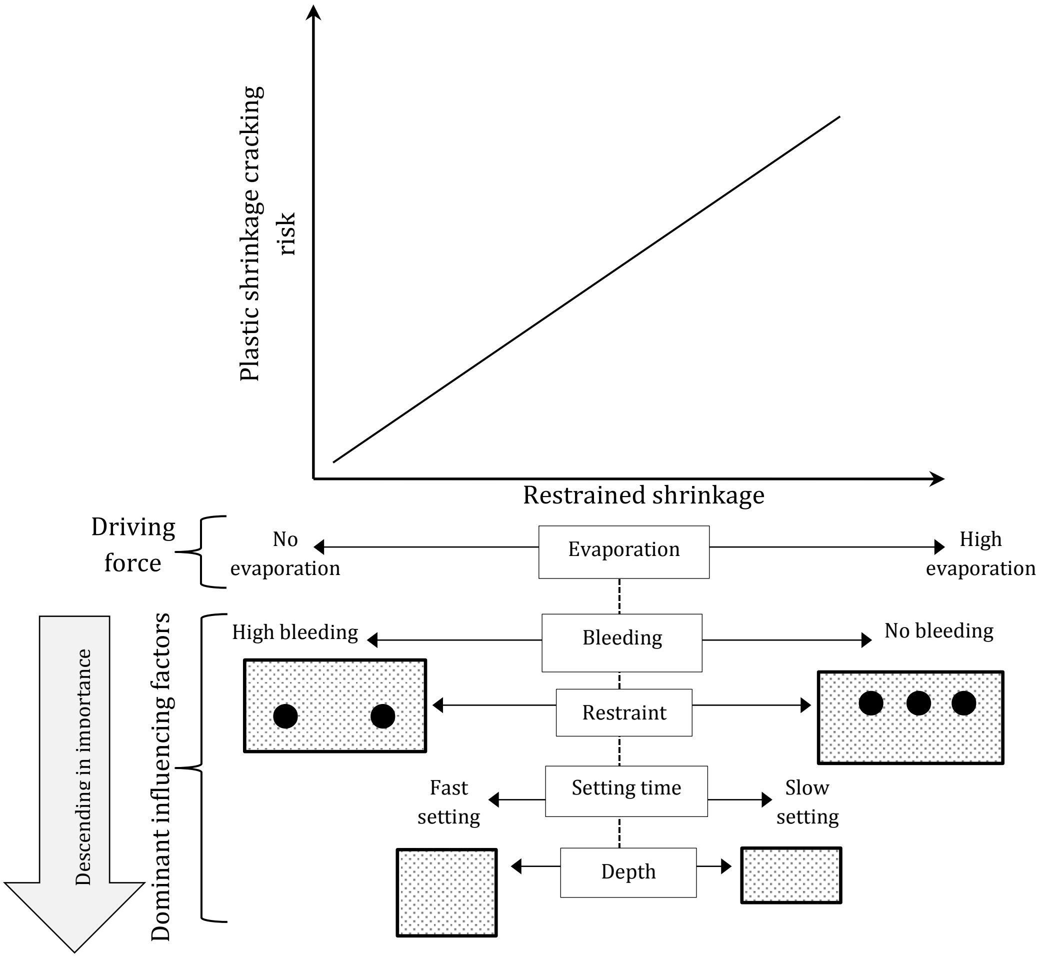

Figure 6.2: Plastic shrinkage cracking risk estimation.

6.4. Factors influencing plastic settlement and shrinkage cracking

This section discusses the primary factors which influence plastic cracking. There exist many interdependent variables which have an effect on plastic cracking, but it is believed that the dominant factors considered in this risk model is sufficient and include most of the interdependent variables. Their exact degree of influence should be determined in future studies and forms part of the recommendations of this study.

6.4.1. Settlement

Settlement in fresh concrete occurs due to the difference in densities of water, cement and aggregates. The solid heavier particles settle in the concrete matrix and in turn displace water upwards. Initial settlement as a result of gravity occurs from the time of placing up to the initial setting time where the concrete matrix is stiff enough to resist gravity. Capillary pressure build-up can cause a second phase of settlement if the evaporation rate exceeds the cumulative bleeding amount, but this is not currently considered in the settlement risk model. The degree of settlement can be estimated by measuring the accumulative amount of bleeding.

Bleeding is the processes where water in the concrete mixture displaces upwards due to the downward displacement of solid particles. Mixtures with higher bleeding values settle more than mixtures with lower bleeding values. Mixtures with higher bleeding rates are more susceptible to plastic settlement cracking. Typical bleeding values are given in Table 6.1.

Table 6.1: Typical bleeding rates after an hour.

Degree of settlement/bleeding	Bleeding volume (kg/m^2/h)
Low	0 - 0.5
Medium	0.5 – 1
High	1 – 1.5

In literature bleeding rate values range from 0.5 kg/m^2/h to 1.5 kg/m^2/h (Uno, 1998). The bleeding rate is influenced by the reabsorption of bleed water which is a complex process and which has a big influence on bleeding as recent studies show (Combrinck, 2016). It is believed that if bleed water is extracted an hour after mixing, the effect of reabsorption is sufficiently accounted for.

The bleeding rate can be calculated using basic tools and it should be measured an hour after mixing. The bleeding rate should be measured in a cylindrical container with a diameter between 100 and 150 mm with the same depth (plus 20 mm) of the specific concrete member. The concrete container should be filled, consolidated and then covered for a period of one hour. To further increase the accuracy of the bleeding rate, the container should be exposed to the ambient temperature of the evaporation rate. However, the container should be closed to prevent drying due to the wind and relative humidity.

The container should then be tilted and the accumulated bleed water can be extracted from the top using a syringe. The weight of the bleed water removed from the surface should be recorded ($m_{bleedwater}$). The bleeding rate can then be calculated by dividing the mass of the bleed water by the area of the container ($A_{container}$). This is shown in Equation 6-1.

$$\text{Bleeding volume} = \frac{m_{bleedwater}}{A_{container}} \qquad \text{Eq. 6-1}$$

6.4.2. Restraint

To quantify the degree of restraint proves to be difficult and no standard exists which could assist in this. Common types of restraint include embedded reinforcing steel, sudden change in sectional dimensions or the formwork and/or underlying surface, which are shown in Table 6.2. The main factors which influence the degree of restraint (especially for slabs) include the cover depth and spacing of the embedded reinforcing steel. The cover depth and spacing is generally specified by the design engineer.

Table 6.2: Typical restraint types.

Degree of restraint	Cover depth to embedded steel (mm)	Spacing between the embedded steel (mm)	Change in cross sectional depth	Underlying surface/formwork
High	0-15	100 - 200	Sudden	Rough
Medium	15-45	200 - 300	Gradual	Moderate
Low	40-60	300 - 400	None	Smooth

The values in Table 6.2 are only approximate values which need further confirmation and they form part of the recommendations of this study.

6.4.3. Setting time

Setting times measure the penetration resistance of concrete and are used as indications to the state that concrete finds itself in. Initial set indicate the end of the stiffening phase and beginning of the setting phase. The final set indicates the end of the setting phase and the beginning of the hardening phase. Table 6.3 shows different setting times as based on values obtained from literature (Boshoff & Combrinck, 2013).

Table 6.3: Typical initial setting times.

	Initial setting time (h)
Fast setting	1-2
Normal setting	2-3
Slow setting	3+

Setting times are commonly determined by measuring the penetration resistance of a concrete mixture. Generally, two types of methods are used to calculate the setting times namely the ASTM C403 (2008) which uses a penetrometer and EN 196-3 (2005) that uses a Vicat apparatus. Both these methods include sieving the freshly mixed concrete and then filling their respective moulds. Combrinck (2016), recently compared these two methods and found that the ASTM C403 (2008) is impractical and rather advised the use of the Vicat apparatus.

Setting times can also be measured using a simple pencil test or complex ultrasound spectroscopy. Either way, setting times do not indicate an exact value or change in the concrete matrix but serve as an indication to the state that concrete finds itself in. Any method which proves to be consistent and similar to that of other methods can be used.

6.4.4. Depth

The depth of concrete sections varies depending on their structural application. Table 6.4 contains typical slab depths ranging from 75 mm to 200+ mm. This study indicated and discussed in Chapter 5 that the depth of a section has a large influence on plastic cracking. For deeper concrete sections the degree of plastic shrinkage cracking is generally reduced while increasing the severity of plastic settlement cracking. However, the severity of the final crack can rapidly increase if plastic settlement and shrinkage interact.

Table 6.4: Typical slab depths.

	Slab depth (mm)
Shallow	75 - 125
Standard	125 - 200
Deep	200 +

6.4.5. Finishing operations

Finishing operations are applied to a concrete's surface to make it aesthetically acceptable and they can improve its mechanical properties. Finishing operations do not have an effect on plastic shrinkage cracking. The existing plastic shrinkage cracks can be closed on the surface but this only hides the true severity of the actual crack. However, finishing operations close initial tension settlement cracks which do reduce the risk of plastic settlement cracks.

6.4.6. Evaporation

Evaporation is the process where water changes from a liquid to a gas or a vapour. High evaporation rates are characterised by high wind speeds, low relative humidity and high air temperatures. High concrete temperature in combination with lower air temperatures also promote high evaporation rates.

Equation 6-2 developed by Uno (1998), is used for calculating evaporation rate in terms of kilograms per square meter per hour.

$$ER = 5 \times 10^{-6} \times [(T_c + 18)^{2.5} - r \times (T_a + 18)^{2.5}] \times (V + 4) \quad \text{Eq. 6-2}$$

where:

ER = Evaporation rate [kg/m²/h]
T_c = Concrete temperature [°C]
T_a = Air temperature [°C]
V = Wind velocity [km/h]
r = Relative humidity [%]

The evaporation rate values in Table 6.5 were obtained from a plastic shrinkage cracking guideline published by Boshoff and Combrinck (2013). These values match other literature values where most researchers state that care must be taken in evaporation rates that exceed 1 kg/m²/h. Each environment is characterised by different evaporation rates and should be considered individually.

Table 6.5: Typical evaporation rates.

Degree of evaporation	Evaporation rate (kg/m²/h)
Low	0 - 0.5
Medium	0.5 - 1
High	1 +

There exist other methods to calculate evaporation rates. It is generally assumed that the use of Equation 6-2 is sufficient.

6.5. Interaction between plastic settlement and shrinkage cracking

One of the main objectives of this risk model was to consider the effect of interaction between plastic settlement and shrinkage cracking. This study proved that this interaction plays an extremely important role in plastic cracking. Figure 6.3 shows the increase in risk over the interaction between differential settlement and restrained shrinkage. An increase in interaction between these two dominant plastic cracking types exponentially increases the plastic cracking risk. This was confirmed through the experimental tests done in this study and discussed in Chapter 5. The degree of differential settlement and shrinkage is also shown in relative terms in Figure 6.3. The exact degree of differential settlement and restrained shrinkage should be studied further and it forms part of the recommendations of this study.

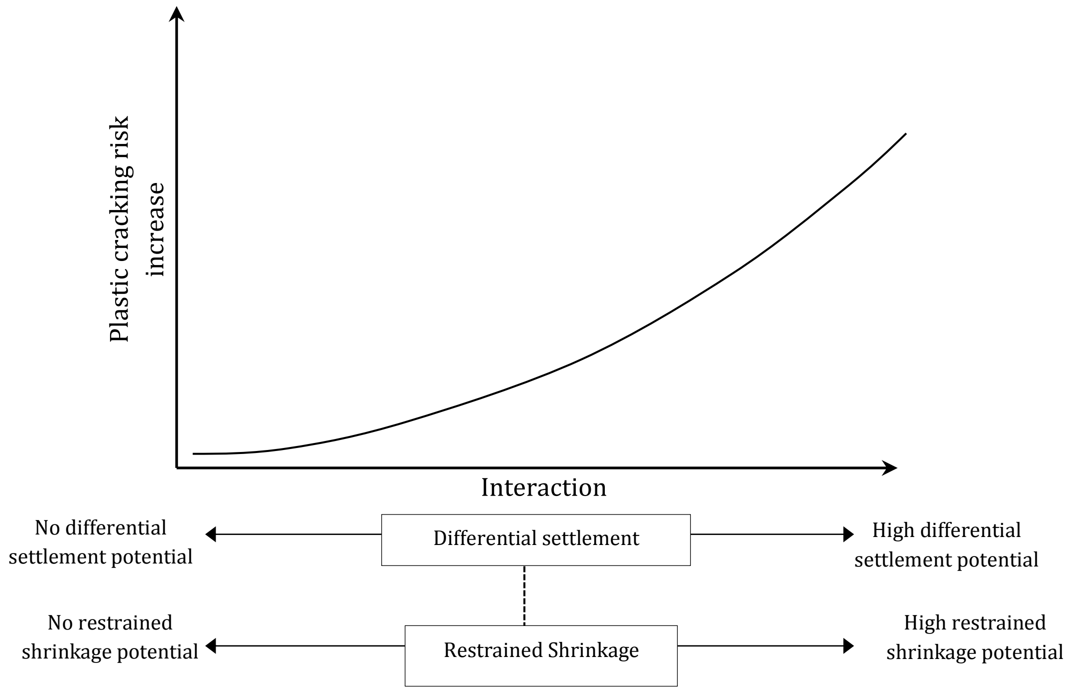

Figure 6.3: Interaction risk between plastic settlement and shrinkage cracking.

6.6. Preventative measures

Precautionary measures should be taken to minimise and even prevent plastic cracking. This can be achieved by controlling the driving forces and dominant influencing factors. The driving forces and dominant influencing factors include restraint, depth, setting time, evaporation, finishing operations and settlement which result in bleeding. It is important to consider that some of these factors could increase settlement cracking while they decrease shrinkage cracking and vice versa. The two driving forces that dominate plastic cracking are settlement and shrinkage.

The amount and rate of differential settlement which causes cracking, can be controlled through settlement, setting time, depth, restraint and finishing operations. Settlement cracking would be most significant for a deep concrete section with a high settlement concrete mixture and long setting time, accompanied by a high degree of restraint without any application of finishing operations. The degree of settlement cracking can be controlled and reduced by the following:

- Increase the paste content.
- Using admixtures (air-entraining admixtures are generally used to reduce settlement).
- Reduce the amount of water in the mixture.
- Increase the number of fine particles in a mixture (particles smaller than 300 μm).
- Add micro synthetic fibres to the mixture.
- Increase the cover depth.
- Avoid sudden changes in the height of concrete sections.
- Sequential placing of concrete for concrete members with different depths.
- Reduce the depth of the concrete section.
- Application of finishing operations at the correct time.

The amount and rate of restrained shrinkage which causes cracking can be controlled through bleeding, setting time, restraint, depth and evaporation. Plastic shrinkage cracking would be the worst for a shallow concrete section with a low bleeding concrete mixture and long setting time, accompanied by a high degree of restraint and exposed to high evaporation rates. The degree of shrinkage cracking can be controlled and reduced by the following:

- Reduce the evaporation rate with wind breaks, fog sprays, providing sunshades, scheduling concrete placement late afternoons or early mornings, dampening subgrade and using moisture-retaining coverings.
- High bleeding concrete mixtures. Care must be taken as the bleeding greatly influences settlement cracking.
- Increase the depth of the concrete section.
- Using construction joints to control cracking.
- The use of synthetic micro fibres.

6.7. Practical risk model example

For the purpose of the following two risk model examples or applications, it is assumed that the relative weights of the influencing factors are known. The dominant influencing factors and their respective values are indicated in Figure 6.4 and are given a value between 1 and 5. Furthermore, the vertical axes in Figure 6.4 have been modified with crack width values. The axis was scaled with the use of the experimental results (actual crack width) obtained in this study and presented in Chapter 5 together with literature values. This was done with minimal tests and should be improved in future studies. It is believed that an increase in differential settlement leads to a linear increase in the average crack width. The horizontal axis (differential settlement) has a minimum value of 0 and maximum value of 15.

The examples chosen for this section were used as actual mixes in this study. This was done to compare the actual results with the results obtained from the model. The examples were chosen as follows:

Example 1:

- NB-Mix
- 200 mm deep mould
- 25 mm deep embedded steel bar
- Climate E

Example 2:

- HB-Mix
- 100 mm deep mould
- 45 mm deep embedded steel bar
- Climate M

These two examples cover a broad range of mixes and conditions and should prove the effectiveness of the model presented. The actual final crack width of Examples 1 and 2 was 2.01 mm and 1.2 mm respectively.

Table 6.6 contains all the information for the determinations of the various weights of Examples 1 and 2 for settlement cracking. The dominant influencing factors for Example 1 have a combined weight of 9.5. The combined weight of the influencing factors for Example 2 is 6. This indicates that Example 1 has higher differential settlement which increases the average plastic settlement cracking risk, as illustrated in Figure 6.4. The weight for the respective influencing factors was given according to the information presented in the sections above. The weight is assumed and further large scale tests are needed to allocate weight values more accurately as well as the degree of weight values for each influencing factor.

The average plastic settlement crack width for Examples 1 and 2 can be seen in Figure 6.4 and is 0.25 and 0.55 mm. The purpose of this model is to account for the interaction between plastic settlement and shrinkage cracking. Plastic shrinkage cracking is now considered, followed by the interaction between plastic settlement and shrinkage cracking.

Figure 6.5 illustrates the shrinkage cracking risk model. Again, it is assumed that the relative weights of the influencing factors are known. The dominant influencing factors are given a value between 1 and 5. The vertical axis is scaled according to estimated crack widths calibrated with the experimental tests done in this study. It is important to recognise that all the values in Figure 6.4 and 6.5 are approximate values and further tests should be done to estimate the influence of the driving force, dominant factors as well as their combined effect on the crack width. Table 6.6 contains all the information for the determination of the various weights for Examples 1 and 2. The dominant influencing factors for Example 1 and Example 2 have a combined weight of 9 and 5.5 respectively as can be seen in Table 6.7.

The average shrinkage cracking width for Example 1 and 2 is 0.52 and 0.1 mm respectively. The interaction between plastic settlement and shrinkage cracking which calculates the final average crack width is now considered. Figure 6.6 shows the interaction cracking model used for the examples.

The vertical axis is scaled according to estimated crack widths and the horizontal axis is scaled according to an interaction factor. The interaction factor has a maximum value of 30 and minimum value of zero. The maximum value of 30 consist of a combination of 15 for differential settlement and 15 for restrained shrinkage.

Example 1 has a combined differential settlement and restrained shrinkage value of 18.5 where Example 2 has a combined value of 11.5. The latter leads to a final crack width of 1.75 mm for Example 1 and 1.1 mm for Example 2 as seen in Figure 6.6. The actual average cracking width for Example 1 and 2 is 2.01 and 1.2 mm. It can be concluded that the model adequately accounts for the interaction between settlement and shrinkage cracking.

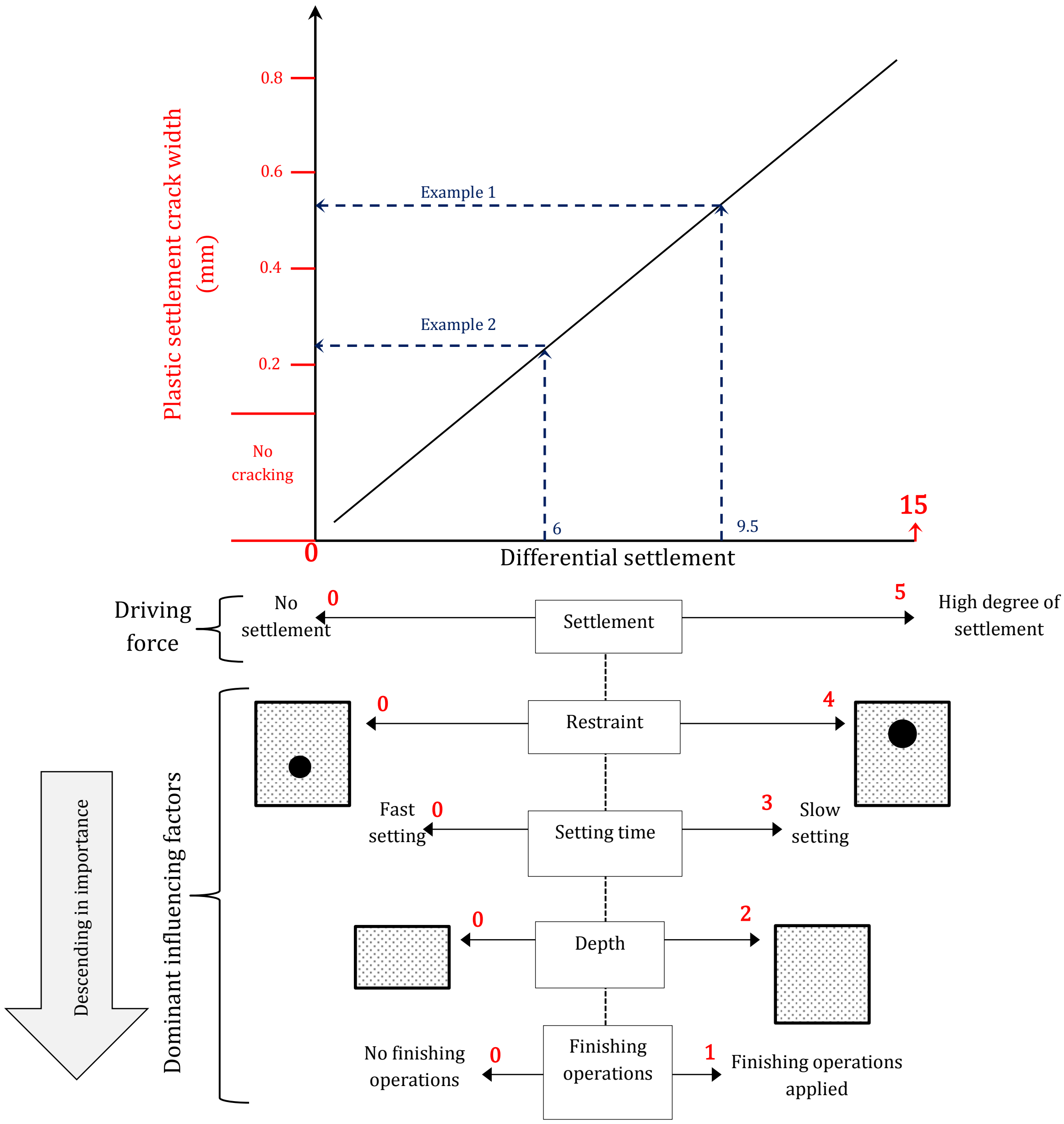

Figure 6.4: Example of the settlement cracking model with values.

Table 6.6: Example of settlement cracking influencing factors.

	Example 1		**Example 2**	
Influencing factor	Value	Model factor	Value	Model factor
Settlement	0.67 kg/m²/h	3	1.23 kg/m²/h	4
Restraint	Medium	3	Low	1
Setting time	1 h	0.5	1.2 h	0.5
Depth	200 mm	2	100 mm	0.5
Finishing operations	No	1	Yes	0
Total		**9.5**		**6**

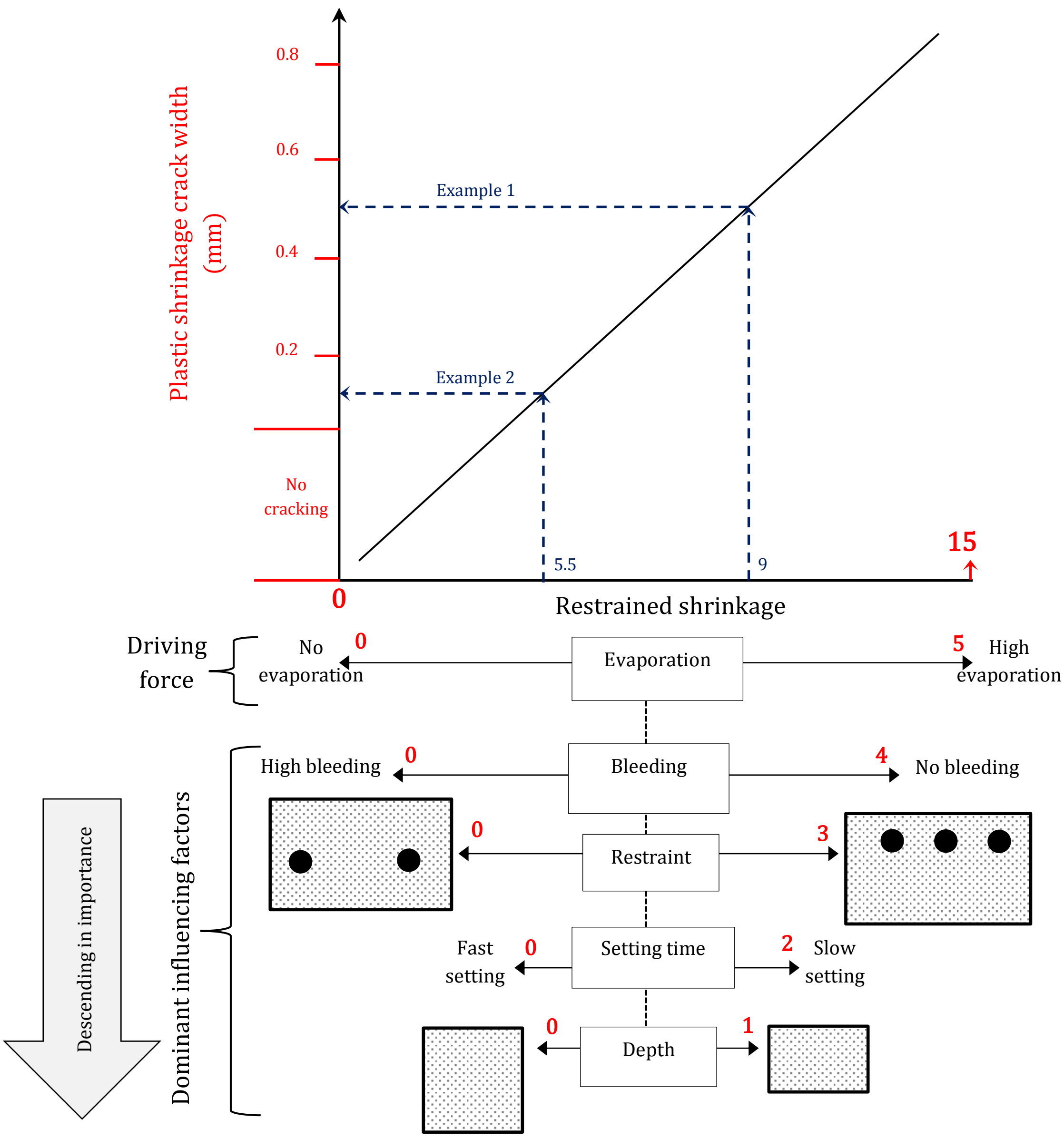

Figure 6.5: Example of the shrinkage cracking model with values.

Table 6.7: Example of shrinkage cracking model.

	Example 1		**Example 2**	
Influencing factor	Value	Model factor	Value	Model factor
Evaporation	climate E	4	climate M	2
Bleeding	0.67 kg/m²/h	3	1.23 kg/m²/h	1
Restraint	Medium	1.5	Low	1
Setting	1.5 h	0.5	1.5 h	0.5
Depth	200 mm	0	100 mm	1
Total		**9**		**5.5**

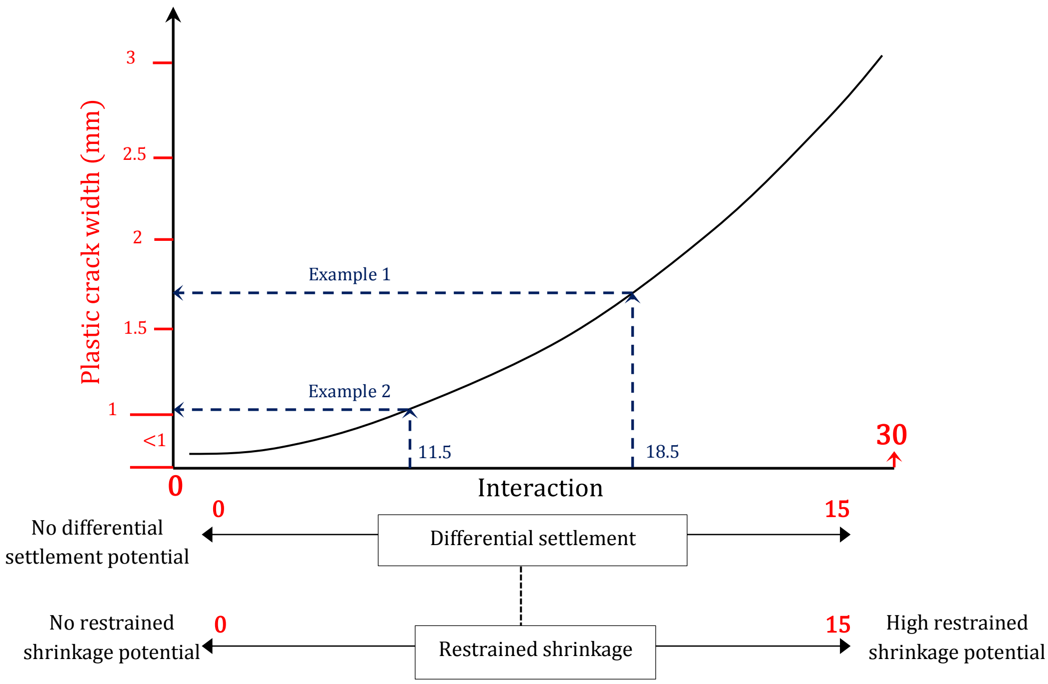

Figure 6.6: Example of the interaction cracking model with values.

6.8. Concluding summary

This chapter consists of presenting plastic cracking risk models for individual cracking types as well as the interaction between these cracking types. To conclude the study, basic guidelines to prevent plastic cracking are given along with two examples where this model was used. The following conclusions can be drawn from this chapter:

- Plastic cracking types generally interact and should not only be considered separately but in combination with one another.
- It is believed that the presented driving forces and dominant influencing factors are comprehensive. However, further studies must determine the degree of influence that each of these factors has relative to one another.

- The examples prove that the model adequately accounts for the interaction between the cracking types. This model can further be improved by future studies which can calculate more accurate weights of the driving forces and dominant factors, as well as calibrate the model.

Chapter 7 : Conclusions and recommendations

This study focused on plastic settlement and shrinkage cracking which dominate cracking in the plastic phase for conventional concrete. The objectives of this study were to design a standard pure plastic cracking mould for studying plastic shrinkage cracking, investigate the interaction between plastic settlement and shrinkage cracking, study the effect of depth on plastic cracking, determine the effect of surface finishing operations and ultimately provide a fundamental understanding as well as a model which could assist in the prediction of plastic cracking.

The following significant conclusions were made in this study:

- The plastic shrinkage cracking mould proposed in this study, can be used to investigate pure plastic shrinkage cracking from the surface as well as internally, with or without the influence of plastic settlement cracking.
- Restrained settlement and shrinkage are the two dominant mechanisms responsible for cracking in the plastic phase. Cracking can either occur as a result of one or a combination of both restrained settlement and shrinkage. This leads to three cracking types namely, settlement cracking, pure plastic shrinkage cracking and settlement induced plastic shrinkage cracking.
- Settlement cracking is arguably the earliest form of cracking in concrete. Initial settlement cracking occurs before any shrinkage starts and its severity is a combination of the rate and amount of settlement and the degree of differential settlement.
- Pure plastic shrinkage cracking occurs suddenly without any warning signs. The crack formation is not from the top to the bottom, but the initial cracks form randomly on the path of the final crack when monitored from the side. A drop in capillary pressure does not necessarily indicate the time a pure plastic shrinkage crack would form. Cracking occurs once the concrete shrinks nears the bottom of the section.
- Settlement induced plastic shrinkage cracking is a combination of settlement and shrinkage cracking and generally results in the most severe cracks. Initial settlement cracks create a weak spot which can even split the concrete section. As shrinkage starts and moves through the concrete sections, the crack is gradually widened from the top to the bottom.
- Three distinct cracking phases were identified in the plastic phase. Phase 1 starts once the concrete is placed, and ends once the capillary pressure starts to rise. Pure settlement cracking occurs only in this phase and can be accompanied by the start of settlement induced plastic shrinkage cracking. Phase 2 starts once the capillary pressure starts to rise, and ends once settlement reaches its maximum. Pure plastic shrinkage cracking can start in this phase, as well as further widening of a settlement induced plastic shrinkage crack. Phase 3 starts once the settlement stops, and ends once the concrete hardens and reaches the final setting time. This end of Phase 3 is characterised by the stabilisation of plastic cracking.
- An increase in concrete depth decreases the risk of pure plastic settlement cracking, while increasing the risk of settlement cracking and settlement induced plastic shrinkage cracking. If these two cracking types interact in deeper sections, the cracking severity drastically increases.

- Finishing operations can close initial settlement cracks which mean the severity of settlement induced plastic shrinkage cracks also reduces. However, finishing operations have no effect on pure plastic shrinkage cracking, but they can be used wrongfully to close plastic cracking on the surface to hide the true severity of the cracking.
- The framework for the risk model that is presented is believed to be sufficient, and it accounts for the interaction between plastic settlement and shrinkage cracking.

From all the knowledge gained in this study the following recommendations are given for future studies:

- The plastic cracking mould designed in this study was practical for experimental tests. However, further studies need to determine the comparison between this mould and large scale tests to better understand actual on-site cracking, especially regarding the effect of restraint.
- The need for a test apparatus and method is required to determine the effect of drying versus the effect of hydration. This can lead to the estimation of more accurate setting times.
- Investigate the effect of different types of finishing operations on plastic shrinkage cracking.
- The influence of admixtures and fibres on pure plastic shrinkage cracking should be explored.
- The weights of the driving forces and influencing factors used for the plastic cracking risk model should be determined and calibrated. This includes understanding the link between large scale tests and experimental tests to determine the values of the influencing factors in the model. The crack width values of the model can further be calibrated by testing different ranges of the influencing factors.

References

ACI 231R, 2010. *Early-Age Cracking: Causes, Measurement, and Mitigation,* Farmington Hills: American Concrete Institute.

ACI 308R, 2001. *Guide to Curing Concrete,* American Concrete Institute: Farmington Hills.

ACI Committee 224, 2008. *Control of Cracking in Concrete Structures,* Michigan: American Concrete Institute.

Aïtcin, P. C., 2016. Supplementary cementitious materials and blended cements. *Science and Technology of Concrete Admixtures,* Issue 2nd, p. 53–73.

Aïtcin, P. C. & Eberhardt, A. B., 2016. Historical background of the development of concrete admixtures. *Science and technology of concrete admixtures,* Issue 2nd, p. xli–lii.

ASTM C 1579, 2004. *Standard Test Method for Evaluating Plastic Shrinkage Cracking of Restrained Fiber Reinforced Concrete,* West Conshohocken: ASTM International.

ASTM C 403/C 403M, 2008. *Standard Test Method for Time of Setting of Concrete Mixtures by Penetration Resistance,* West Conshohocken: ASTM International.

Basham, K., 2000. *Finishing-Tool Primer,* Washington: Hanley-Wood.

Bentz, D. P. & Weiss, J. W., 2008. *REACT: Reducing Early-Age Cracking Today,* Gaithersburg: National Institute of Standards and Technology.

Boshoff, W. P., 2012. *Plastic Shrinkage Cracking of Concrete Part 1: Guideline,* Stellenbosch: University of stellenbosch.

Boshoff, W. P. & Combrinck, R., 2013. Modelling the severity of plastic shrinkage cracking in concrete. *Cement and Concrete Research,* Issue 48, pp. 34-39.

Chengqing, Q., 2003. *Quantitave assesment of plastic shrinkage cracking and its impact on the corrotion of steel reinforcement,* Indiana: Purdue University.

Combrinck, R., 2011. *Plastic shrinkage cracking in conventional and low volume fibre reinforced concrete,* Stellenbosch: The University of Stellenbosch.

Combrinck, R., 2016. *Cracking of Plastic Concrete in Slab-Like Elements,* Stellenbosch: University of Stellenbosch.

Combrinck, R. & Boshoff, W. P., 2014. *Fundamentals of plastic settlement cracking in concrete,* Stellenbosch University: Department of Civil Engineering.

Dakhil, F. H., Cady, P. D. & Carrier, R. E., 1975. Cracking of fresh concrete as related to reinforcement. *ACI Matetial journal,* pp. 421-428.

EN 196-3, 2005. *Methods for testing cement - Part 3: Determination of setting times and soundness,* Brussels: European Committee for Standardization.

Hammer, A., 2007. *Deformations, strain capacity and cracking of concrete in plastic and early hardening phases,* Trondheim: Norwegian University of Science and Technology.

Hassan , S., Arnaud , P. & Sofiane, A., 2010. A new look at the measurement of cementitious paste setting by Vicat test. *Cement and Concrete Research,* 5(40), p. 681–686.

Holt, E. E., 2000. Where did these cracks come from?. *Concrete International,* pp. 57-60.

Illstron, J. & Domone, P., 2010. *Construction materials Their nature and behaviour.* 4th ed. Abingdon: Spons Press.

Josserand, L., Coussy, O. & de Larrard, F., 2006. Bleeding of concrete as an ageing consolidation process. *Cement and Concrete Research,* Issue 36, p. 1603– 1608.

Kraai, P. P., 1985. Proposed test to determine the cracking potential due to drying shrinkage of concrete. *Concrete Construction,* pp. 775-778.

Kronlöf, A., Markku, L. & Sipari, P., 1995. Experimental study on the basic phenomena of shrinkage. *Cement and Concrete Research,* Issue 25, pp. 1747-1754.

Kwak , H. G. & Ha, S. A., 2006. Plastic shrinkage cracking in concrete slabs. Part II: numerical experiment and prediction of occurrence. *Magazine of Concrete Research,* 8(58), p. 517–532.

Kwak, H., Ha, S., Weiss, W. J. & M.ASCE, 2010. Experimental and Numerical Quantification of Plastic Settlement in Fresh Cementitious Systems. *JOURNAL OF MATERIALS IN CIVIL ENGINEERING,* Issue 22, pp. 951-966.

Maritz, J., 2012. *An investigation on the use of low volume-fibre reinforced concrete for controlling plastic shrinkage cracking,* Stellenbosch: The University of Stellenbosch.

Mehta, P. K. & Monteiro, P. J. M., 2006. *Concrete: microstructure, properties, and materials,* New York: McGraw-Hill.

Mora, J. et al., 2000. *Effect of the incorporation of fibers on the plastic shrinkage of concrete.* Lyon, Fifth International RILEM Symposium on Fibre-Reinforced Concrete (FRC).

Nachbaur, L., Mutin, J. C., Nonat, A. & Choplin, L., 2001. Dynamic mode rheology of cement and tricalcium silicate pastes from mixing to setting. *Cement and Concrete,* Issue 31, p. 183–192.

Neville, A. M., 2011. *Properties of Concrete..* 5th ed. London: Pearson.

NT Build 433, 1995. *Nordtest method,* Tekniikantie: NORDTEST.

Owens, G., 2009. *Fulton's concrete technology.* 9th ed. Midrand: Cement and concrete institute.

Powers, T. C., 1968. *The Properties of Fresh Concrete,* New York: John Wiley & Sons.

Qi, C., Weiss, J. & Olek, J., 2003. Characterization of plastic shrinkage cracking in fiber reinforced concrete using image analysis and a modified Weibull function. *Materials and Structures,* Volume 36, pp. 386-395.

Sanjuan, M. A. & Moragues, A., 1997. Polypropylene fiber reinforced mortar mixes: optimization to control plastic shrinkage. *Composite science and technology,* Volume 57, pp. 655-660.

SANS 1083, 2002. *Aggregates from natural sources - Aggregates for concrete,* Pretoria: Standards South Africa.

SANS 2001-CC1, 2007. *Concrete works (structural) ,* Pretoria: Standards South Africa.

Sant, G. et al., 2009. Detecting the Fluid-to-Solid Transition in Cement Pastes. *Concrete International.*

Schaeles, C. A. & Hover, K. C., 1988. Influence of mix proportions and construction operations on plastic shrinkage cracking in thin slabs. *ACI Material Journal,* Volume 85, pp. 495-504.

Shah, H. R. & Weiss, J., 2006. Quantifying shrinkage cracking in fiber reinforced concrete using the ring test. *RILEM,* Issue 39, p. 887–899.

Slowik, V., Schmidt, M. & Fritzsch, R., 2008. Capillary pressure in fresh cement-based materials and identification of the air entry value. *Cement & Concrete Composites,* Issue 30, p. 557–565.

Suprenant, B. A. & Malisch, W. R., 1999. *Sealing effects of finishing tools,* Whasington: Aberdeen Group,.

Uno, P. J., 1998. Plastic shrinkage cracking and evaporation formulas. *ACI material journal,* Issue 95, pp. 365-375.

Van Dijk, J. & Boardman, V. R., 1971. Plastic Shrinkage Cracking of concrete. *RILEM international symposium on Concrete and Reinforced Concrete in hot countries,* pp. 225-239.

Weyers, R. E., Conway, J. C. & Cady, P. D., 1982. Photoelastic analysis of rigid inclusions in fresh concrete. *Cement and Concrete Research,* Volume 12, pp. 475-484.

Witteman, F. H., 1975. Zur Ursache der so genannten Schrumpfrisse. *Zement und Beton,* Issue 85/86, pp. 6-10.

Wittmann, F. H., 1975. The action of capillary pressure in fresh concrete. *Cement and Concrete,* 1(6), pp. 49-56.